1994

Photophysics of a novel optical probe-7-azatryptophan and its application in the study of protein-protein interactions

Yu Chen
Iowa State University

Order Number 9424203

Photophysics of a novel optical probe-7-azatryptophan and its application in the study of protein-protein interactions

Chen, Yu, Ph.D.

Iowa State University, 1994

U·M·I
300 N. Zeeb Rd.
Ann Arbor, MI 48106

Photophysics of a novel optical probe-7-azatryptophan and its application in the study of protein-protein interactions

by

Yu Chen

A Dissertation Submitted to the

Graduate Faculty in Partial Fulfillment of the

Requirements for the Degree of

DOCTOR OF PHILOSOPHY

Department: Chemistry
Major: Physical Chemistry

Approved:

Signature was redacted for privacy.

In Charge of Major Work

Signature was redacted for privacy.

For the Major Department

Signature was redacted for privacy.

For the Graduate College

Iowa State University
Ames, Iowa

1994

TABLE OF CONTENTS

CHAPTER I INTRODUCTION

In order to study experimentally the ultrafast molecular dynamics of protein-protein interactions, an optical probe is required. Tryptophan has been the most widely used intrinsic optical probe of protein structure and dynamics. There are, however, two major problems in using tryptophan, especially in fluorescence measurements. First, there are often several tryptophan in a protein molecule whose emission must be distinguished so one can related the experiments results with the function of a specific position of the protein. Second, the fluorescence decay of tryptophan itself in aqueous solution is nonexponential [1-3].

The nonexponential fluorescence decay of tryptophan, tryptophan-containing peptides, and most proteins containing tryptophan is a problem because it is difficult to interpret. Environmental effects owing to the role of adjacent peptide bonds on the rate of charge transfer from the indole moiety in tryptophan itself have given rise to interesting but elaborate explanations for nonexponential decay based on the presence of conformational isomers [3-7]. The extreme logical extension of this line of thought has been to postulate not three (or six) conformational isomers about the β_{C-C} (and the γ_{C-C}) bond [5], but distribution of conformational isomers.

There is one well known exception to nonexponential decay in small tryptophan-containing molecules, N-acetyltryptophanamide (NATA).Clearly that NATA cannot serve as a model for tryptophan in proteins. Naturally-occurring single-tryptophan-containing globular proteins are rare [8-16]. There are only two well documented case of single-exponential decay

of tryptophyl fluorescence in proteins: Pseudomonas aeruginosa azurin (5ns) [9-12], and Aspergillus oryzae RNase T1 [13, 14] (pH<6.5 4ns; pH>6.5 10% 1ns, 90% 4ns).

Thus there are several limitations of the use of tryptophan as an optical probe. Recently, we have proposed 7-azatryptophan as an alternative to tryptophan as an optical probe of protein structure and dynamics [17-19]. 7-Azatryptophan can be incorporated into synthetic peptides and bacterial protein [17, 20]. Its steady-state absorption and emission are sufficiently different from those of tryptophan that selective excitation and detection may be effected. Most important for it use as an optical probe is that the fluorescence decay is single exponential over most pH range when collecting the entire band. The greatest value of 7-azatryptophan is to probe the interaction of a smaller peptide or protein containing it with another protein that may contain several tryptophan [20].

The potential utility of 7-azatryptophan as an probe suggests a thorough investigation of the photophysics of it and its chromophore, 7-azaindole. Much of the chemistry that we shall discuss are about the excited-state proton transfer (ESPT) and charge transfer reaction that are ubiquitous in biology. ESPT are much less popular than ground-state proton transfer reaction which are one of the simplest and most important process formed in chemistry. But unquestionably, they are indispensable in fundamental and applied photochemistry. They have been employed as mechanistic tools and in technological applications in pH [21] and pOH [22] jump experiments aimed at the study of proton hydration dynamics [23, 24], photolithography [25], and as probes of the environment around proteins [26], micelles [27], reversed micelles [28], β-cyclodextrin [29], and films [30], also applied in chemical lasers,

energy storage systems and information storage device [31].

In 1931, Weber [32] reported for the first time that the shift of an acid-base equilibrium of some organic molecules occurred at a different pH depending on whether it was observed by absorption or emission. In 1949, Förster [33] provided the correct explanation for their observation and proposed a valuable method to estimate the pK of excited-state, which became known as the Förster cycle.

In 1955, Weller [34] found that methyl salicylate presented an unusually large Stokes-shifted fluorescence emission. When the acidic proton of the phenol group was methylated, the fluorescence became the common mirror image of the absorption. He proposed that the red-shifted fluorescence corresponded to an excited state isomer, formed via a proton transfer (PT) in the excited state. Since then excited-state proton transfers have been intensively studied.

Until the 80's, the kinetics of PT step in singlet state was mainly assessed through the steady-state method initially proposed by Weller. In this method, the pH dependence of the fluorescence efficiencies of the conjugate acids and bases in the lowest excited singlet state are related to the competition between PT and photophysical deactivation. This method enables one to measure protonation and deprotonation rate and therefore pK^* and is still very useful today.

Because many singlet state have relatively short lifetime, the real time determination of many rate had to wait with fast time resolution. In the 80's dynamic analysis with nanosecond and picosecond resolution became popular. Fast spectroscopic techniques have

been applied to the study of ESPT, and opened a new window in this field. Some work was reviewed by Huppet [35, 36], including inter- and intramolecular ESPT. More recently, some data with femtosecond time-resolution has become available.

Charge transfer processes play an important role in many areas, such as photosynthesis, energy conversion and storage systems, nonlinear optics and the photostability of media exposed to high-intensity optical irradiation. The study of it is the key in the molecular level to understand chemical reactions.

Many central problems in charge-transfer process such as the role of the solvent, the involvement of vibrational degrees of freedom, the pathway and mechanism of electronics interactions, including long-range electron transfer, the excited state quenching by charge transfer have been studied and brought into progress. Excellent reviews have been given by Newton and Sutin [37], Marcus [38]. Most theories of electron transfer reactions in solution are formulated in terms of a model in which the transferring electron is localized at a donor molecular site in the reactant and at a different acceptor molecular site in the product.

Rehm and Weller [39], and Closs and coworkers provide an early study of excited state quenching by electron transfer. Time-resolved spectroscopy provide new insights into this areas. Hopfield [40] presents an appealing model to calculate quenching rate (charge transfer rate) in terms of donor and acceptor. In his model, the charge transfer rate is the function of "electron removal" and "electron insertion" spectra of the donor and acceptor. It is this property and ESPT responsible for the single exponential decay of 7-azatryptophan while try is very complicated.

This thesis is organized as following: in Chapter II we describe the instruments and method used to study fluorescence decay. Chapter III discuss the fluorescence species of 7-azaindole and 7-azatryptophan in water trying to understand why these molecules have one emission band in water while two band in alcohols. In Chapter IV, proton inventory technique is employed to study the mechanism and dynamics of PT of 7-azaindole in alcohols and water. In Chapter V, we presents a general understanding of solvation and dynamics of 7-azaindole in water and alcohols. In Chapter VI, the reason of single exponential decay of 7-azatryptophan in water has been discussed and the potential utility of it as an optical probe been addressed.

CHAPTER II INSTRUMENTS

A. Time-Correlated Single-Photon Counting

There are a variety of techniques that can be used to measure the time evolution of fluorescence on a time-scale from nanosecond to tens of picosecond. But over the last ten years, the most popular one is time-correlated single-photon counting. Our system was built by Michelle Négrerie. A Coherent 701 rhodamine 6G dye laser is pumped with about 1 W of 532 nm radiation from an Antares 76-s CW mode-locked Nd:YAG laser. (The remaining 1 W of second harmonic pumps a dye laser whose pulses are amplified to 1-2 mJ at 30 Hz by a regenerative amplifier. This branch of the experiment is used to perform pump-probe transient absorption spectroscopy.) The 701 dye laser is cavity-dumped at 3.8 MHz. The pulses have an autocorrelation of about 7 ps full width at half-maximum (fwhm). Excitation of 7-azaindole from 282 to 305 nm is effected by focusing the dye laser pulses with a 5 cm lens into a crystal of $LiIO_3$ or KDP. Fluorescence is collected at right angles through a polarizer mounted at 54.7° to the excitation polarization and then passed through an ISA H-10 monochromator with a 16 nm band-pass or through cutoff filters. A Hamamatsu 2809u microchannel plate, amplified by a Minicircuits ZHL-1042J, and an FFD 100 EG&G photodiode provide the start and stop signals, respectively. Constant-fraction discrimination of these signals is performed by a Tennelec TC 455, and time-to-amplitude conversion, by an ORTEC 457. Data are stored in a Norland 5500 multichannel analyzer before transfer to

and analysis with a IBM personal computer. The instrument function of this system has a fwhm of 50-65 ps and a full width at tenth maximum of 160-170 ps.

Sample temperature was controlled with a M9000 Fisher refrigerated circulator connected to a brass cell holder and monitored directly at the sample by an HH-99A-T2 Omega thermocouple.

B. Time-Resolved Measurements

The time-dependent anisotropy, r(t), is constructed in a manner similar to that of its steady-state counterpart. It is related to the correlation function of the transition dipole moment for absorption to state i at time zero, $\hat{\mu}^i_{abs}(0)$, with the transition dipole moment for emission from state i at subsequent times, t, $\hat{\mu}^i_{em}(t)$. For a sphere undergoing rotational diffusion by Brownian motion [41]:

$$r(t) = \frac{I_{\parallel}(t) - I_{\perp}(t)}{I_{\parallel}(t) + 2I_{\perp}(t)} = \frac{2}{5} \langle P_2 \left[\hat{\mu}^i_{abs}(0) \bullet \hat{\mu}^i_{em}(t) \right] \rangle = \frac{2}{5} P_2(\cos\theta) e^{-t/\tau_r} \quad (1)$$

$I_{\parallel}(t)$ and $I_{\perp}(t)$ are the time dependent fluorescence intensities parallel and perpendicular to the excitation polarization. P_2 is the second Legendre polynomial, θ is the angle formed by $\hat{\mu}^i_{abs}(0)$ and $\hat{\mu}^i_{em}(0)$, and τ_r is the diffusion relaxation time for a sphere (i.e., τ_r = 1/6 D, D being the diffusion coefficient). Accurate construction of the fluorescence anisotropy decay function demands that the sample be exposed to equivalent excitation intensity during the

collection of the parallel and perpendicular emission profiles. Numerous methods have been proposed for the normalized collection of $I_{\parallel}(t)$ and $I_{\perp}(t)$. They have been summarized by Cross and Fleming [41]. In general, these methods fall into two categories: genuine simultaneous collection or alternate sampling procedures. If these methods are not adequate, the two curves must be scaled, "tail-matched", to have equal intensity at times where the fluorescence emission is expected to be depolarized. In the following, we present a method for acquiring fluorescence depolarization data without recourse to scaling procedures. This technique is based upon alternate detection of $I_{\parallel}(t)$ and $I_{\perp}(t)$, obviates the need for scaling procedures, and permits very precise measurements of fast reorientation times.

Automation of both polarizer movement and multichannel analyzer (MCA) operation provides our apparatus with the capability of sampling fluorescence at multiple orientations of the analyzer polarizer. A polarizer (Polaroid, HNP,B) is mounted on a modified motorized rotation stage (RSA-1TM, Newport, Corp.) and is synchronously controlled in conjunction with the MCA (Norland 5500), making possible alternate readings of $I_{\parallel}(t)$ and $I_{\perp}(t)$. Polarization bias in our system is negligible. By alternately acquiring $I_{\parallel}(t)$ and $I_{\perp}(t)$, one may compensate for drift in the laser system over long periods of time, at least up to seven hours, thereby allowing for the collection of fluorescence depolarization data without recourse to scaling procedures. (Long-term drift in electronic components may still present a problem that is more difficult to compensate for.) Such compensation is crucial if the sample is weakly fluorescent and many hours of data accumulation are required.

An IBM 386 clone controls both the rotation stage and the MCA under the direction

of Asyst software, an advanced fourth-generation data acquisition and analysis language. Data transfer and MCA control are achieved over an RS-232 serial link connecting the computer to the MCA. The motorized rotation stage is interfaced to the computer via a parallel port connection to a manual-stage controller (Newport 860 SC-C).

The computer presents the operator with a windowing user interface to input experimental parameters and to monitor the progress of the experiment. The operator specifies the data names in which to store the $I_{\parallel}(t)$ and $I_{\perp}(t)$ data, the maximum count of any channel that will terminate the experiment, the length of the $I_{\parallel}(t)$ and $I_{\perp}(t)$ acquisition times (usually 1-5 minutes), and the present orientation of the analyzer polarizer. At the end of each recording interval, the computer instructs the MCA to stop recording, downloads the data recorded in the MCA for analysis, and commands the rotation stage to move to a new position. If the maximum channel value was not exceeded, the MCA begins recording the decay for the alternate angle of polarization. Currently, 90° rotation is effected in approximately twelve seconds. Taking into account the time for data transfer, 36 seconds are required between the termination of one acquisition and the beginning of another.

Above, we have only discussed the collection of fluorescence emission separated by 90°. Our software, however, is designed for collecting data at several angles, thus making possible the utilization of global techniques for anisotropy analysis developed by Flom and Fendler [43] and originally introduced by Brand and coworkers [44].

Approaches similar to ours have been presented [45-52]. For example, Fayer and coworkers use a Pockels cell to rotate the polarization of their excitation beam by 90° every

; [50, 51]. Millar et al. [52] describe an apparatus for sampling parallel and perpendicular emission intensities; but they do not discuss the long-term reliability of their system, nor are the results calibrated against a standard.

One of the most thoroughly investigated dye molecules is the fluorescein derivative, rose bengal [53, 54]. Figure 1 presents the data obtained for rose bengal in methanol at 20°C using an acquisition time of one minute for the $I_{\parallel}(t)$ and $I_{\perp}(t)$ curves. The experiments were performed with an excitation wavelength at 570nm and a power of about 60mw. These data yield results that are in excellent agreement with literature values: ten measurements of $I_{\parallel}(t)$ and ten measurements of $I_{\perp}(t)$ yield a limiting anisotropy, $r(0) = 0.360$

Figure 1. Fluorescence depolarization data for rose bengal in methanol at 20 ± 0.5°C using 1-minute accumulations: the upper trace corresponds to raw data for $I_{\parallel}(t)$; the lower, to $I_{\perp}(t)$. λ_{ex} = 570 nm, $\lambda_{em} \geq$ 650 nm. Residuals obtained by fitting rose bengal anisotropy decays to one exponential are displayed above. The different sets of residuals correspond to different accumulation times for the rose bengal experiment. In descending order, we have: 15-minute accumulations (2.5-hour total acquisition time), r(t) = 0.361 exp(-t/166 ps), χ^2 = 1.60; 2-minute accumulations (3.0-hour total acquisition time), r(t) = 0.360 exp(-t/172 ps), χ^2 = 1.26; 1-minute accumulations (3.5-hour total acquisition time), r(t) = 0.360 exp(-t/179 ps), χ^2 = 1.05. In all cases, the data were collected to 16,000 counts in the maximum channel. The excited-state decay was well-described by a single exponential with a 532-ps time constant.

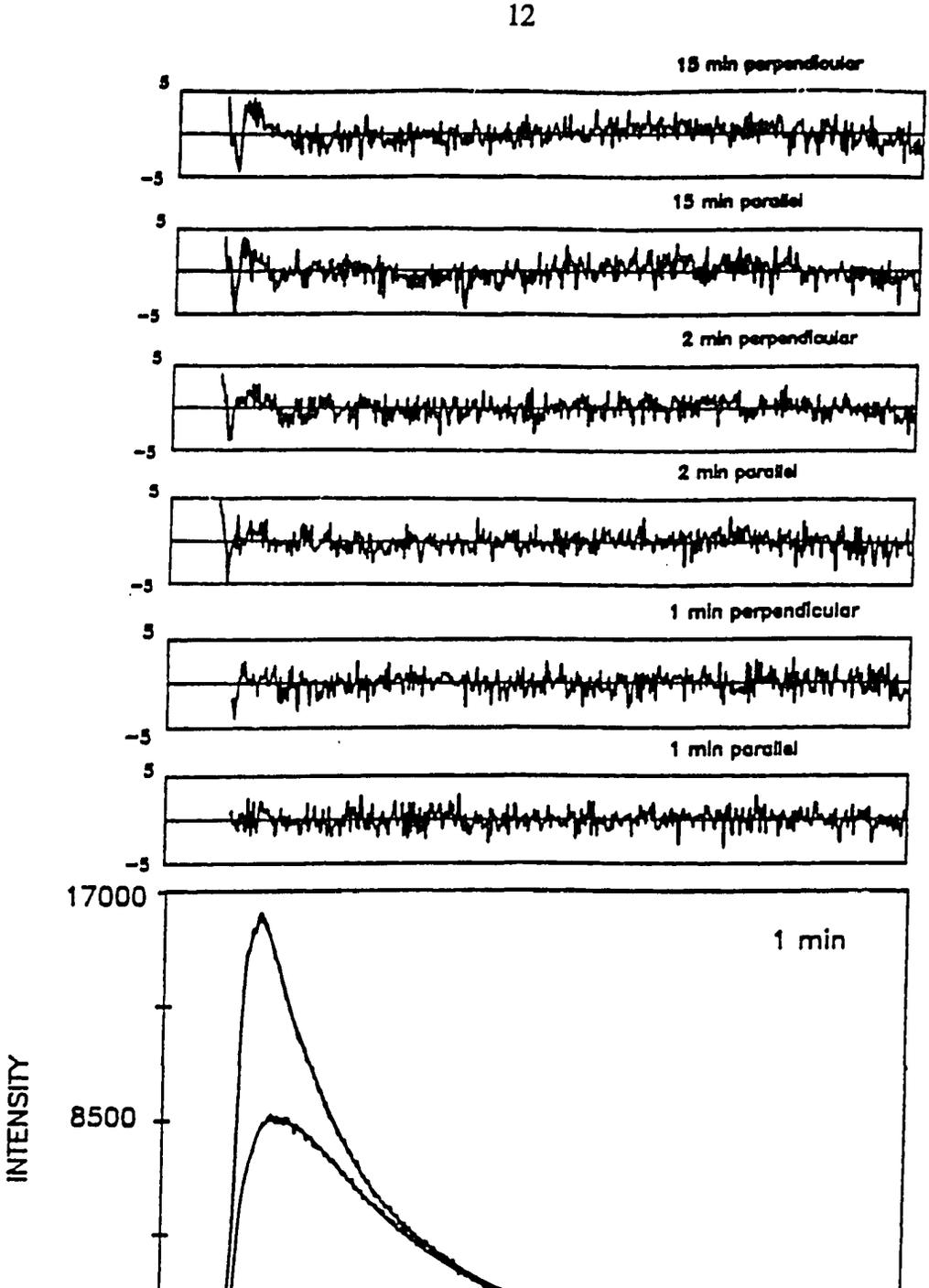
15 min perpendicular
15 min parallel
2 min perpendicular
2 min parallel
1 min perpendicular
1 min parallel
5
-5
17000
8500
0
1 min
INTENSITY
0.0
1.0
2.0
3.0
TIME (NANOSECONDS)

depolarization data may confidently be acquired on a time scale where depolarization is not complete (which is not possible if "tail-matching" were to be employed). This is particularly important for applications to protein dynamics. Here, the local motion of the probe molecule with respect to the larger body is of primary concern. This corresponds to the particular case of studying the behavior of a probe molecule attached to globular proteins. In this case, one may evaluate the reorientational motion by fitting the anisotropy decay to a sum of two exponentials. The underlying assumption here is that each exponential has physical significance: the one more rapidly decaying at τ_1 corresponds to the localized motion of the probe; the other more slowly decaying at τ_2 corresponds to the overall reorientational motion, the "tumbling," of the entire molecule in the solvent [38]. We thus have, $r(t) = r_1(0)\exp(-t/\tau_1) + r_2(0)\exp(-t/\tau_2)$. When tail matching is not mandatory, the time scale may be made finer so as to focus on the region of rapidly depolarizing phenomena. Information contained in this region may be lost or obscured when a coarser time scale is required to observe the fully depolarized fluorescence that facilitates tail matching.

CHAPTER III FLUORESCENCE SPECIES OF 7-AZAINDOLE IN WATER

A. Introduction

Recently, we have proposed 7-azatryptophan as an alternative to tryptophan as an optical probe of protein structure and dynamics [18-20]. Figure 2 shows the structure of the molecules. There are several advantages to use 7-azatryptophan as an probe. The basic factor is the absorption and emission spectrum are different (Figure 3). Most important for its use as an optical probe is that its fluorescence decay over most of the pH range, when emission is collected over the entire band, is single exponential while tryptophan is nonexponential. In order to characterize its fluorescence properties and to elucidate its pathways of nonradiative decay, first we should understand its chromophore, 7-azaindole (Figure 2).

The photophysics of 7-azaindole were originally studied by Kasha and coworkers [56] in nonpolar hydrocarbon solvents where it was suggested to dimerize by forming two $N_1H\cdots N_7$ hydrogen bonds [56-59]. The major nonradiative decay pathway of these dimers was shown to be a very rapid excited-state tautomerization producing two $N_1\cdots HN_7$ hydrogen bonds. Recently Hochstrasser and coworkers have shown that in nonpolar solvents at room temperature this tautomerization occurs in 1.4 ps [60].

A similar reaction occurs for 7-azaindole in alcohols. The fluorescence emission of 7-azaindole is characterized by two bands with distinct and widely separated maxima as well as different fluorescence lifetimes (Figure 4) [18,61-64]. The redder of the two bands

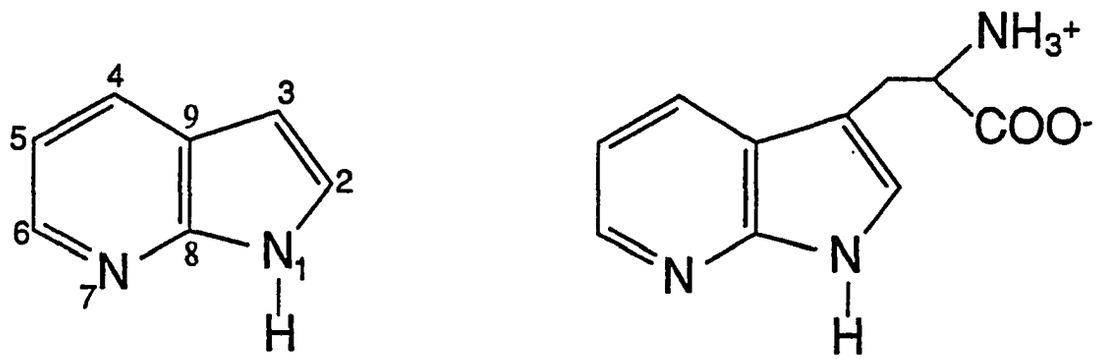

A

B

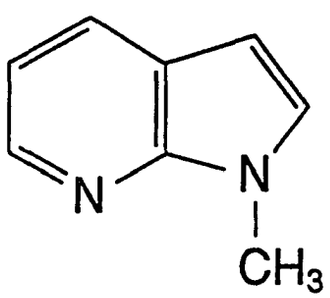

C

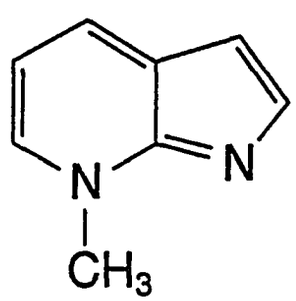

D

Figure 2. Structures of (a) 7-azaindole, (b) zwitterionic 7-azatryptophan, (c) N_1-methyl-7-azaindole (1M7AI), and (d) 7-methyl-7H-pyrrole [2,3-b]pyridine (7M7AI).

Figure 3. Comparison of the absorption and fluorescence spectra of (a) tryptophan and (b) 7-azatryptophan. For tryptophan, $\varepsilon_{280} \approx 5400\ M^{-1}\ cm^{-1}$ [45], for 7-azatryptophan, $\varepsilon_{288} \approx 6200\ M^{-1}\ cm^{-1}$. Absorbance and fluorescence spectra are normalized to the same peak intensity. (Taken by Négrerie, M.)

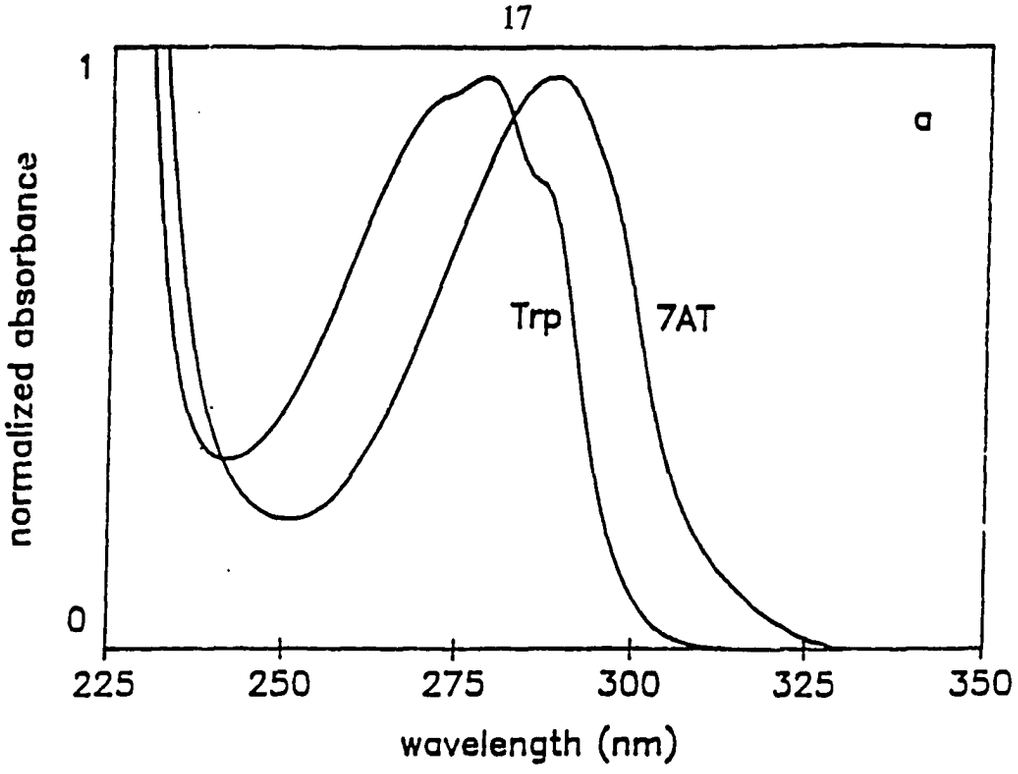
1
0
normalized absorbance
a
Trp
7AT
225
250
275
300
325
350
wavelength (nm)

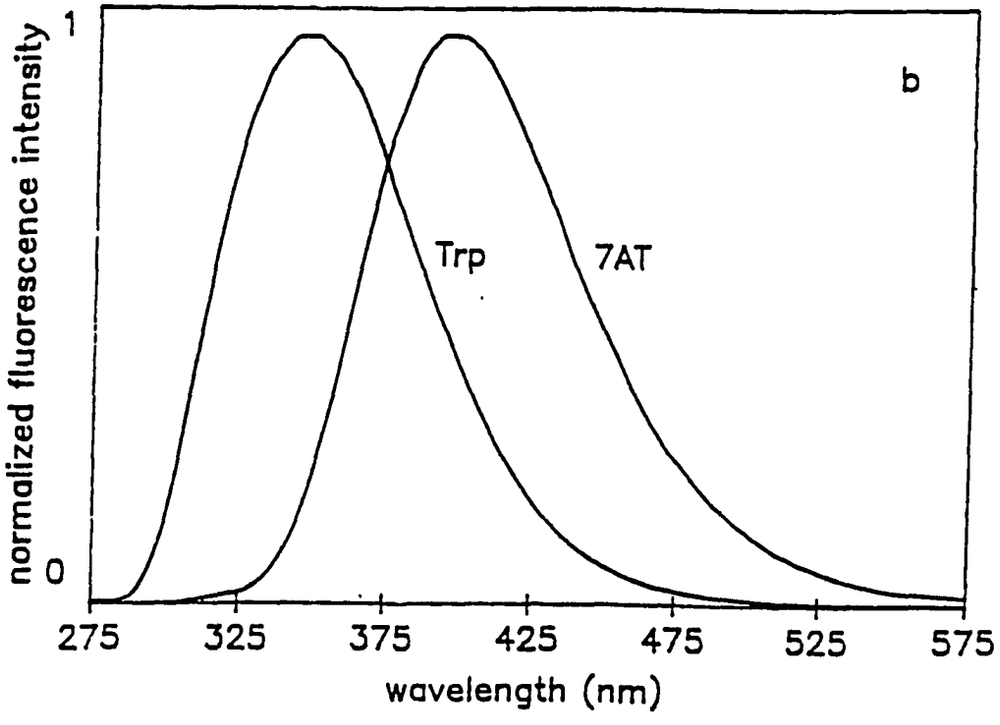
1
0
normalized fluorescence intensity
b
Trp
7AT
275
325
375
425
475
525
575
wavelength (nm)

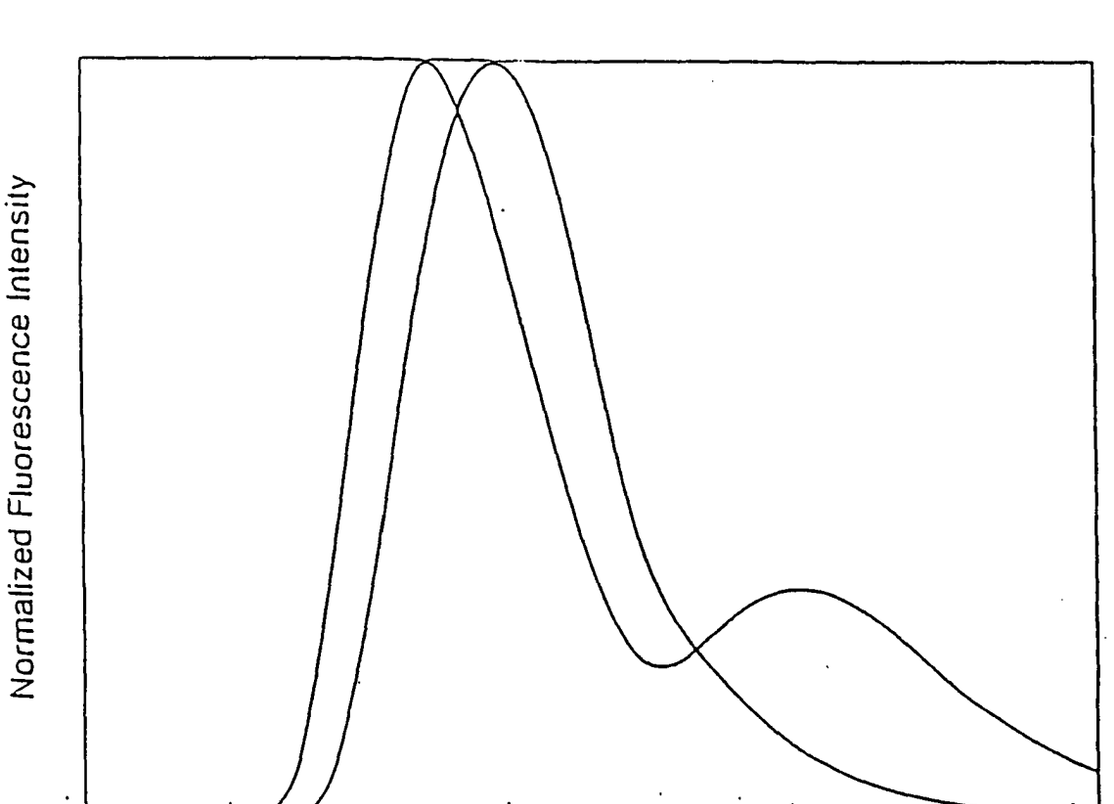

Figure 4. Comparison of the fluorescence spectra of 7-azaindole in water and methanol.

observed in alcohols is attributed to an excited-state tautomer that is formed by one solute molecule with one solvent molecule vs DPT reaction. Consequently, the bluer of the two bands is attributed to a "normal" species. Because of the interest in using 7-azaindole as a probe of protein structure and dynamics, we began time-resolved studies of 7-azaindole in water [18] to complement the existing steady-state work, carried out predominately in mixed water/alcohol solvents [61, 65]. An intriguing characteristic of the emission of 7-azaindole in water is that only a smooth band is detected (Figure 4) and the fluorescence lifetime is single exponential when emission is collected over the entire band over most of the pH range.

People have argued the nature of the one smooth band. Two different suggestions have been proposed [18, 125]. In this chapter we will present new data to clarify the nature of the fluorescent state of 7-azaindole in water and broadens the understanding of this chromophore in general. Three types of experiments are considered. The fluorescence decay of 7-azaindole is measured as a function of emission wavelength with adequate time resolution to resolve various excited-states. The temperature dependence and the deuterium isotope effect of the lifetimes of these excited states are investigated. And a detailed study is made of the protonated and unprotonated forms of 7-azaindole as well as of its methylated derivatives that mimic untautomerized and tautomerized 7-azaindole (Figure 3): N_1-methyl-7-azaindole (1M7AI), and 7-methyl-7H-pyrrolo[2,3-b]pyridine (7M7AI). The synthesis of these derivatives were performed by my colleague R. L. Rich.

Comparing the emission wavelength dependence study with the transient absorption measurements, we propose that the percentage of 7-azaindole molecules capable of

undergoing this reaction is small (~20%) and the fluorescence lifetime and spectrum is dominated by solute molecules that are inappropriately solvated. These molecules are "blocked" from executing an excited-state tautomerization. The coexistence of these two types of solute molecules suggests a time scale for their interconversion. It is argued that $\geq$ 10 ns are required for solvent to rearrange about the "blocked" species, converting it to a form that can undergo tautomerization during the excited-state lifetime.

B. Materials and methods

1. Spectroscopic Measurements

Fluorescence lifetime measurement were performed by time-correlated single photon counting that has been described previously. Time-resolved fluorescence data were fit to a single exponential or to a sum of exponentials by iteratively convoluting trial decay curves with the instrument response function and employing a least-squares fitting procedure. A good fit was determined largely by the χ^2 criterion: $0.8 \leq \chi^2 \leq 1.2$. Steady-state, corrected fluorescence emission and excitation spectra were obtained with a Spex Fluoromax with emission and excitation bandpasses of 4nm.

2. Purification of 7-Azaindole

Commercial preparations of 7-azaindole contain < 1% impurity (Sigma, personal communication). Thin-layer chromatography (TLC) with silica gel plates and ethyl acetate indicates that commercial 7-azaindole has an R_f ~ 0.60 and resolves two fluorescent contaminants having R_f ~ 0.15 (impurity 1) and 0.00 (impurity 2). To remove the impurities, flash chromatography [60] was performed using ethyl acetate. Fractions containing 7-azaindole were concentrated and run through the flash column four times to ensure isolation. The 7-azaindole crystals were uniformly white and appeared as a single spot on TLC plates. (Purification of 7-azaindole was done by R. L. Rich.) The two impurities have nonexponential fluorescence lifetimes in water at neutral pH: impurity 1, $F(t) = 0.38 \exp(-t/607 \text{ ps}) + 0.25 \exp(-t/2035 \text{ ps}) + 0.37 \exp(-t/8895 \text{ ps})$; and impurity 2, $F(t) = 0.18 \exp(-t/383 \text{ ps}) + 0.37 \exp(-t/1087 \text{ ps}) + 0.45 \exp(-t/7414 \text{ ps})$. Samples were changed regularly. Subsequent to light exposure they were analyzed by TLC to monitor their integrity.

Several groups have recently commented on the difficulty of obtaining pure 7-azaindole and the problems that impurities may present in the interpretation of high resolution spectra [67], dynamic solvation [64], and the assignment of spectral features in the condensed phase [18]. It is thus important to characterize the spectral characteristics of purified 7-azaindole and of the other products that are contained in commercial 7-azaindole. Figure 5 presents the fluorescence emission spectra of purified 7-azaindole and the two isolated impurities in water. The significantly increased purity of our 7-azaindole preparation

Figure 5. Normalized fluorescence spectra in water at 20°C of (A) purified 7-azaindole, (B) isolated impurity 1, and (C) isolated impurity 2.

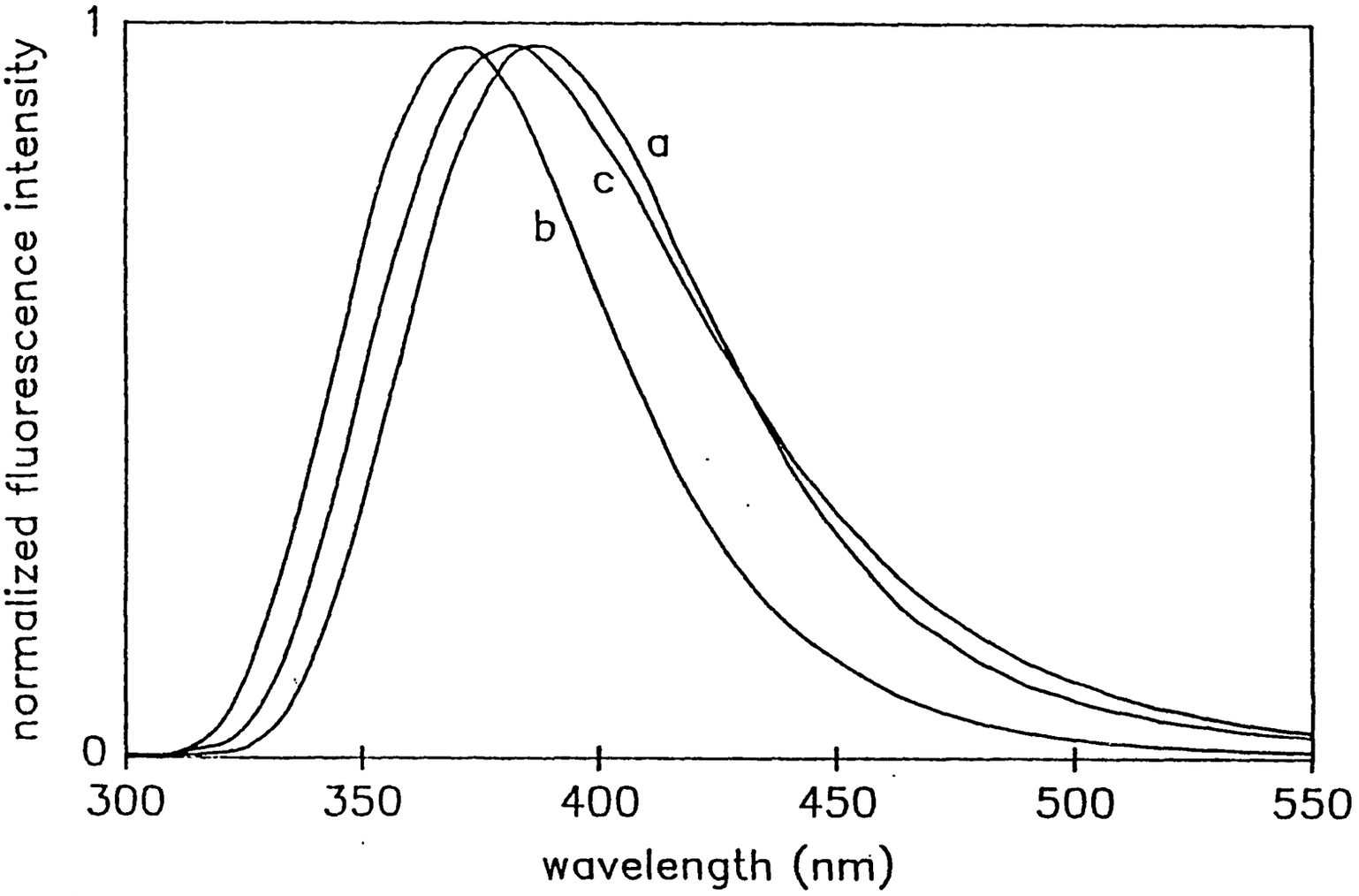
normalized fluorescence intensity
1
0
300
350
400
450
500
550
wavelength (nm)
a
b
c

is supported by the superimposability of the excitation spectra obtained at three different wavelengths (Figure 6). These data are to be contrasted with the excitation spectra of the two impurities (Figure 7).

Using such purified 7-azaindole give the identical results with the commercial one. Along with other experiments, such as temperature dependence of amplitude change of short component, attribution to impurity to explain the experiments results turns out to be wrong (see Chapter IV).

C. Results

1. Dependence of the Fluorescence Lifetime on Emission Wavelength

7-Azaindole exhibits a single-exponential fluorescence decay of 910 ± 10 ps in water at neutral pH and 20°C if emission from the entire band ($\lambda_{em} \geq 320$ nm) is collected [18,19]. The fluorescence decay, however, deviates from single exponential if emission is collected with a limited bandpass. For $\lambda_{em} \leq 450$ nm, a single exponential does not provide a satisfactory fit (Figure 8). An acceptable fit is obtained using two exponentially decaying components and indicates that about 20% of the fluorescent emission decays with a time constant between 40 to 100 ps (depending on the full-scale time base chosen for the experiment). Shorter lifetimes are obtained with a full-scale time base of 1.5 ns; longer lifetimes, with a full scale time base of 3.0 ns. The amplitude of this fast component did not

Figure 6. Normalized fluorescence excitation spectra in water at 20°C of 7-azaindole. The detection wavelengths are indicated in the Figure.

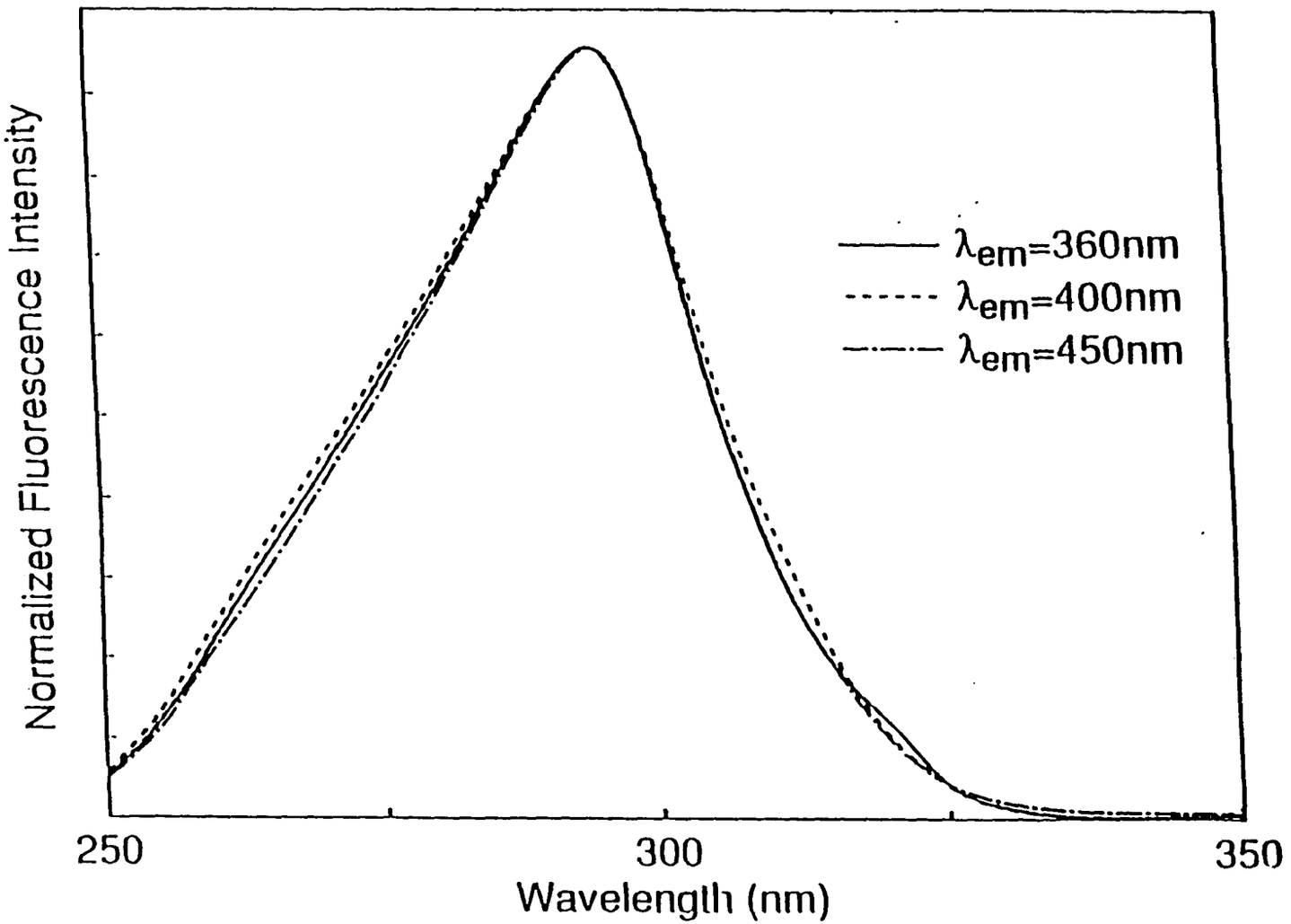
Normalized Fluorescence Intensity
λem=360nm
λem=400nm
λem=450nm
250
300
350
Wavelength (nm)

Figure 7. Normalized fluorescence excitation spectra in water at 20°C of the two impurities isolated from commercial preparations of 7-azaindole: (a) impurity 1; (b) impurity 2. The detection wavelengths are indicated in the Figure.

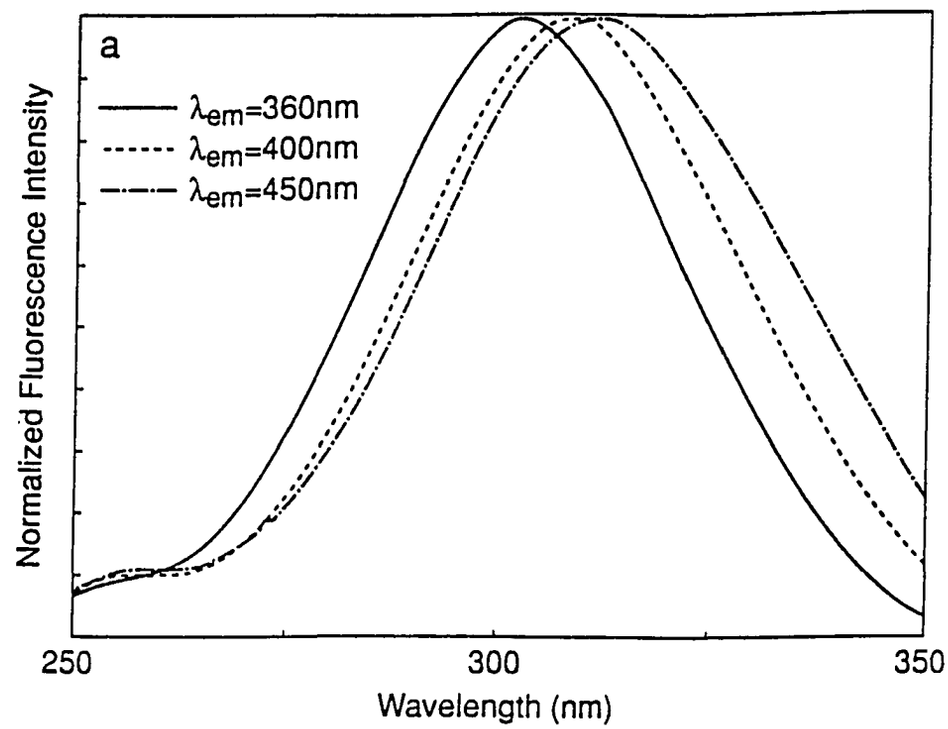
a
λem=360nm
λem=400nm
λem=450nm
Normalized Fluorescence Intensity
250
300
350
Wavelength (nm)

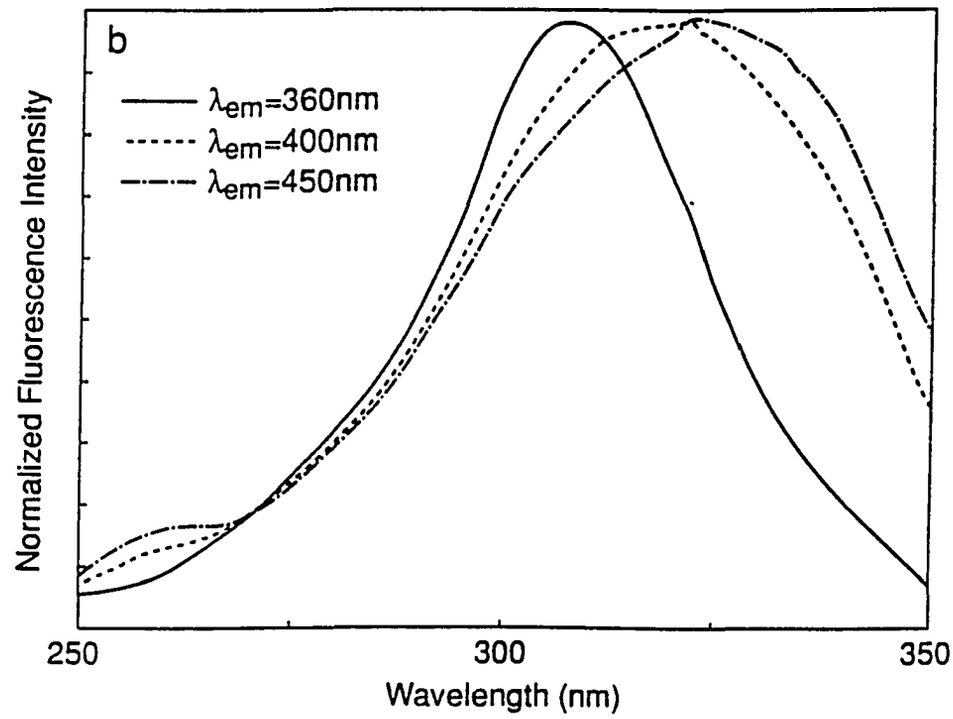
b
λem=360nm
λem=400nm
λem=450nm
Normalized Fluorescence Intensity
250
300
350
Wavelength (nm)

Figure 8. Fluorescence decay of 7AI in water, pH 6.1, 20°C, λ_{ex} = 288 nm, λ_{em} = 380 nm (16-nm bandpass). The upper set of residuals corresponds to a single-exponential fit to the data, which yields a decay time of 816 ps with χ^2 = 2.6. The lower set of residuals corresponds to a double-exponential fit yielding F(t) = 0.20 exp(-t/41 ps) + 0.80 exp(-t/835 ps), χ^2 = 1.2. 835 ps is obtained for the long-lived component instead of 910 ps because the 1.5-ns time base is too fine to provide enough dynamic range to measure accurately an ~ 1-ns decay. In preliminary work [2] we could not resolve the short component because experiments were performed on a 6-ns full-scale time base.

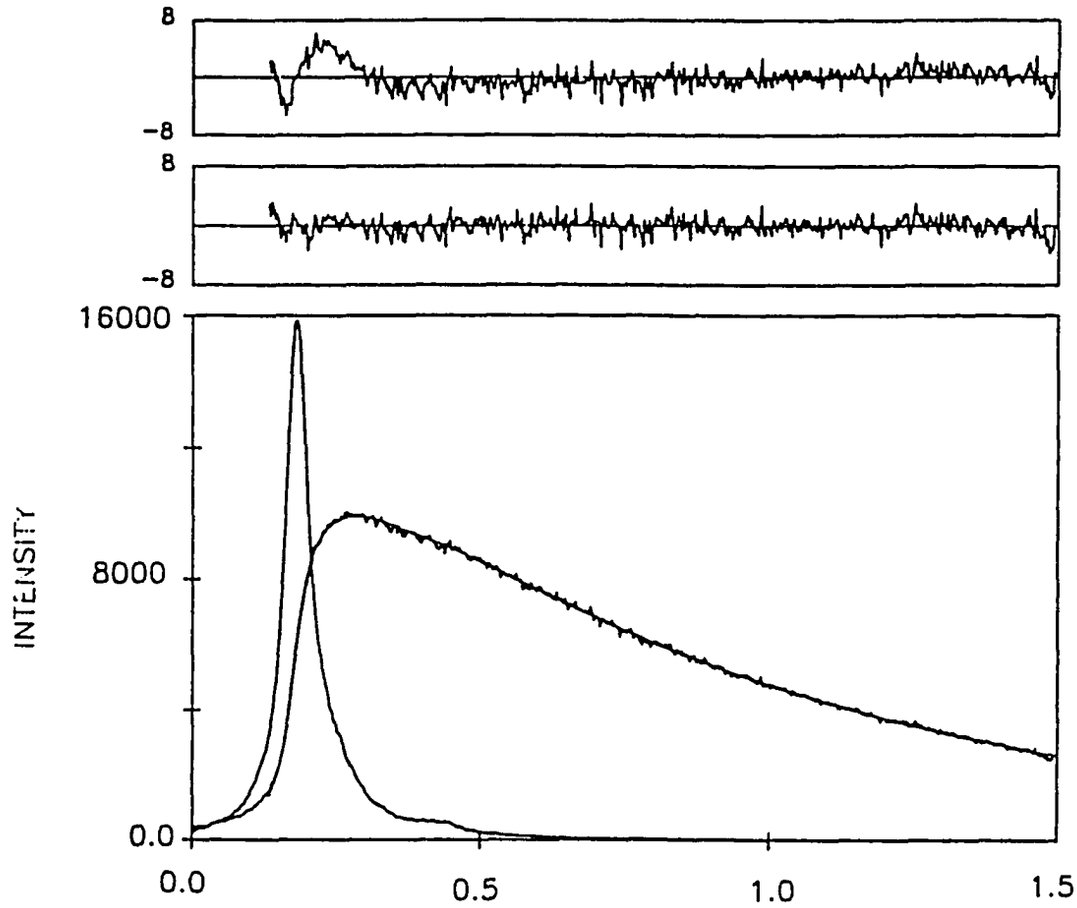
8
-8
8
-8
16000
8000
0.0
INTENSITY
0.0
0.5
1.0
1.5

depend on the time base chosen. A component with a 70-ps decay time is also detected in the transient absorbance of 7-azaindole in water [19]. There is no such rapid component in the fluorescence decay or the transient absorption of 7M7AI or 1M7AI. We have thus attributed this rapid component to a small population of 7-azaindole molecules that undergo excited-state tautomerization. For the duration of the discussion, we shall refer to this transient as the 70-ps component because it is more clearly resolved in the transient absorption measurements [19]. (A 40-100-ps decay is too long to be attributed to solvation dynamics in water, which occur on a time scale of $\leq$ 1 ps [69].)

The 910 ps component that is resolved for $\lambda_{em} \leq 450$ nm or when emission is collected over the entire band is attributed to the majority of the 7-azaindole molecules that are not capable of excited-state tautomerization. This assignment will be described in more detail below.

When $\lambda_{em} \geq 505$ nm, the fluorescence decay can be fit to the form F(t) = -0.69 exp(-t/70 ps) + 1.69 exp(-t/980 ps). The long-lived component is observed to lengthen from 910 to 980 ps. This lengthening of the lifetime at long emission wavelengths was reported earlier [18], but no significance was drawn to it. If the rise time of the fluorescence emission can be attributed to the appearance of tautomer, then for $\lambda_{em} \geq 505$ nm $|0.69/1.69| \sim 0.40$ is the fraction of tautomer present. The rest of the emission arises from 7-azaindole molecules incapable of tautomerization and characterized by a 910 ps lifetime. Thus, 980 ps represents the weighted average of 910 ps and a longer lifetime, namely ~ 1100 ps. This decay time is identical to that of protonated (pH < 3) 7-azaindole (Table I).

Table 1

Summary of Fluorescence Lifetimes and Quantum Yields

of 7-Azaindole (7AI) and Its Derivatives[a]

compound	pH	ϕ_F[b]	τ_F	k_{rad}[c] (10^7 s^{-1})	λ_{max}^{em} (nm)	λ_{max}^{abs} (nm)	ε[d] (M^{-1} cm^{-1})
7AI	7	1.0	910 ± 10 ps	----	386	288	8100 [41]
7AI (N_1H^+)[e]	7		~ 1100 ps[f]	~ 1.0	~ 440		
1M7AI	11	18.30	21.0 ± 0.5ns	2.6	395	287	8300[g]
7M7AI	13	0.02	480 ± 20 ps	0.14	510	303	8800 [22]
7AI (N_7H^+)	2	0.27	1.10 ± 0.03 ns	0.74	444	290	8700 [41]
1M7AI (N_7H^+)	1	0.10	2.80 ± 0.20 ns	0.11	456	291	8300[g]
7M7AI (N_1H^+)	3	0.26	780 ± 10 ps	1.0	442	294	8500 [22]

[a] Experiments are performed at 20°C.

[b] All ϕ_F reported are relative to 7AI at pH 7 and 20°C.

[c] Calculations of k_{rad} are based on a value of 0.03 for the quantum yield of 7AI neutral pH and ambient temperature [61].

[d] Decadic molar extinction coefficient at the reported maximum of the absorption band.

[e] The protonated tautomer species of 7AI at neutral pH. It is proposed that about 20% of the

Table 1 (continued)

solute population is converted to this species.

[f] This lifetime is recovered from the 980-ps component that is observed when emission is collected at wavelengths longer than 505 nm. It represents a weighted average of the lifetime of the blocked solute (910 ps) and that of the protonated tautomer at neutral pH.

[g] Estimated using the data of Robinson and Robinson for compounds dissolved in cyclohexane [86].

It is possible to construct time-resolved emission spectra for these species. The fluorescence intensity at a given emission wavelength and time, F(λ, t), is given by:

$$F(\lambda,t) = \frac{[A_1(\lambda)\ \exp(-t/\tau_1) + A_2(\lambda)\ \exp(-t/\tau_2)]}{A_1(\lambda)\tau_1 + A_2(\lambda)\tau_2} F_{ss}(\lambda) \qquad (2)$$

where $F_{ss}(\lambda)$ is the steady-state intensity of fluorescent emission. The quantity in square denbrackets is the fluorescence decay measured at a given emission wavelength. The ominator is the integrated emission at this wavelength. Because solvation in water is extremely rapid [69], this expression differs from those used to evaluate transient Stokes shifts [70] in that τ_1 and τ_2 do not change appreciably over the range of emission

wavelengths. Here, τ_1 and τ_2 are considered to have distinct and clear physical meaning, although there are other instances where this may not be the case (see Eqns 11 and 12). τ_1 is attributed to the decay of the normal species (or the rise of the tautomer). τ_2 is attributed to another species that does not undergo excited-state tautomerization on the time scale of the fluorescence lifetime. (Owing to the low fluorescence intensity at $\lambda_{em} \geq 505$ nm, not enough data could be collected to resolve the contribution of the ~ 1100-ps component and hence to distinguish its spectrum from that of the 910-ps component. In the spectral decompositions discussed here, τ_2 refers to either the 910- or the ~ 1100-ps component.)

Figure 9 presents spectra at t = 0 and t = 1 ns for 7-azaindole and 7-azatryptophan. For 7-azaindole, at 480 nm the t = 0 and t = 1 ns spectra are scaled to have the same intensity because no short-lived component is resolved at this wavelength. In order to facilitate observation of the spectral evolution between t = 0 and t = 1 ns, the spectra are subsequently normalized to the same intensity at 380 nm. At 1 ns, the spectra are not as broad because there is no contribution from the short-lived component.

The relative contributions of the short- and long-lived components to the steady-state fluorescence spectrum can be estimated as follows. For the short-lived component,

$$F_S(\lambda) = \frac{A_1(\lambda)\tau_1}{A_1(\lambda)\tau_1 + A_2(\lambda)\tau_2} F_{ss}(\lambda) \qquad (3)$$

and for the long-lived component,

$$F_L(\lambda) = \frac{A_2(\lambda)\tau_2}{A_1(\lambda)\tau_1 + A_2(\lambda)\tau_2} F_{ss}(\lambda) \qquad (4)$$

Figure 9. Time-resolved fluorescence spectra of (a) 7-azaindole and (b) 7-azatryptophan at pH 6.8 and 20°C. The empty circles represent the spectrum at t=0; the solid circles, at t=1 ns. The spectra are normalized to have the same intensity at 380 nm.

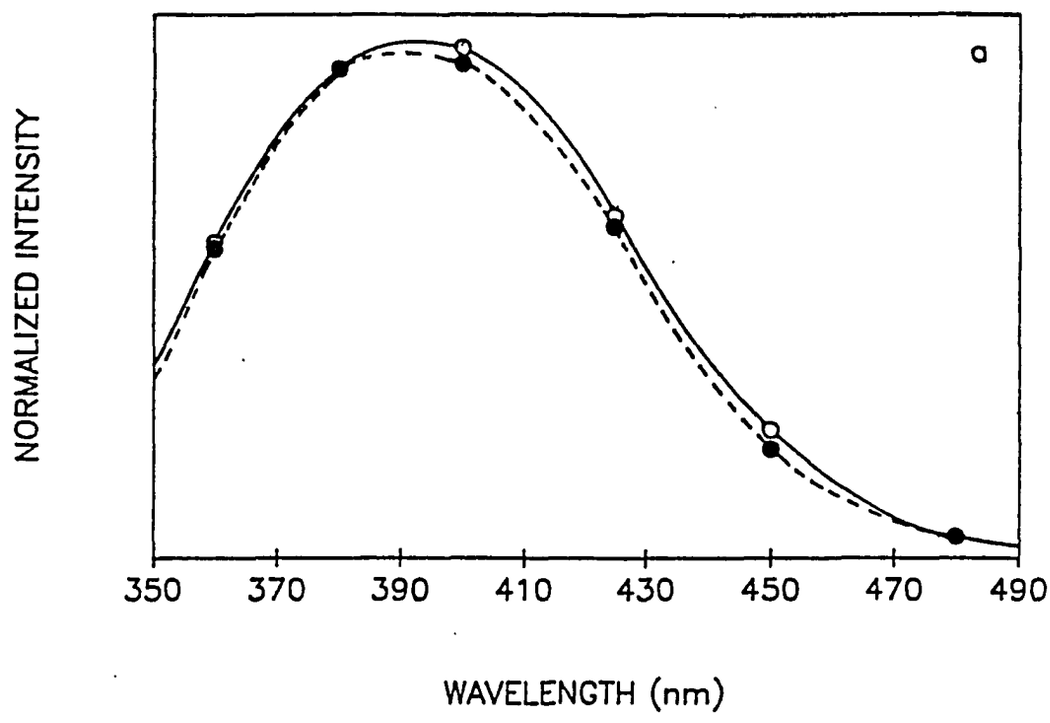
a
NORMALIZED INTENSITY
350
370
390
410
430
450
470
490
WAVELENGTH (nm)

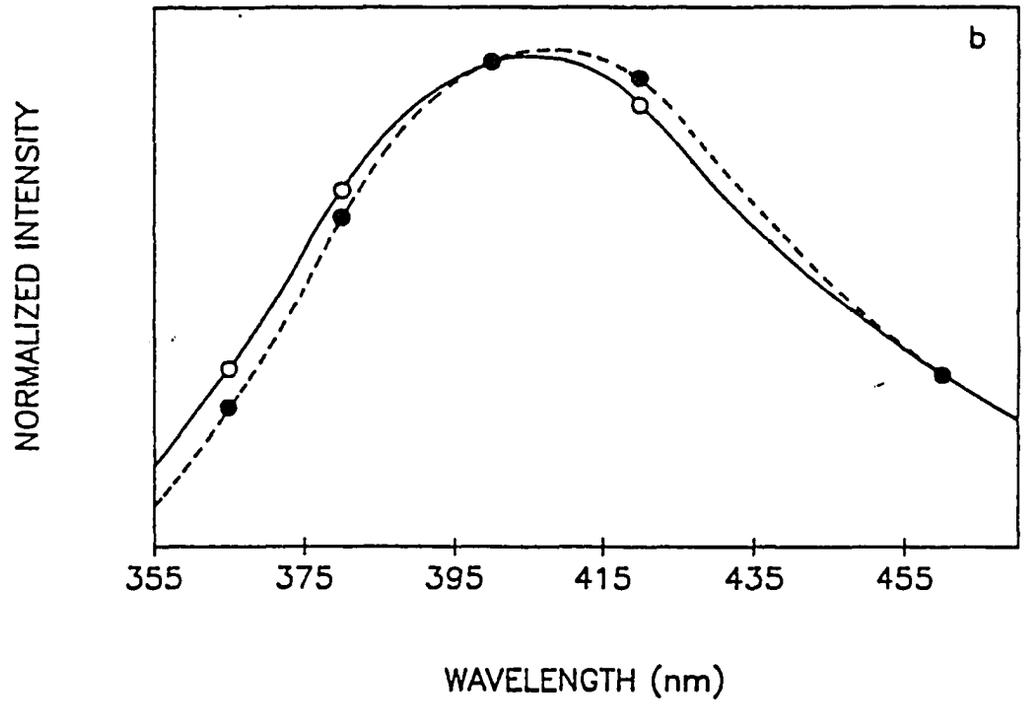
b
NORMALIZED INTENSITY
355
375
395
415
435
455
WAVELENGTH (nm)

The decompositions of the steady-state spectra for 7-azaindole and 7-azatryptophan using these relations are depicted in Figure 10. The contribution from the short-lived component is multiplied by a factor of 10 in order to facilitate viewing. It is evident that the short-lived component contributes negligibly to the total fluorescence spectrum. Note that the spectrum of the short-lived component is different in 7-azaindole than in 7-azatryptophan. In particular, it drops off more quickly to zero in 7-azatryptophan: at 460 nm instead of 480 nm.

2. Temperature Dependence and Deuterium Isotope Effect

The temperature dependence of the short-lived component in H_2O yields an Arrhenius activation energy of 2.7 ± 1.7 kcal/mol (Figure 11). Within the admittedly large experimental error, this result is comparable to the viscosity activation energy of H_2O [71], $E_\eta^{H_2O}$ = 3.71 kcal/mol. In D_2O the short-lived component yields an activation energy of 2.7 ± 1.3 kcal/mol. This result is in accord with the large viscosity activation for D_2O [71], $E_\eta^{D_2O}$ = 4.74 kcal/mol. (More precise measurements of the temperature dependence of the short-lived component are difficult owing to its small amplitude (Figure 8). This is especially true in D_2O where the lifetime of the short-lived component is lengthened and hence more difficult to extricate from the double exponential decay.)

At ambient temperature, the isotope effect on the 7-azaindole short-lived fluorescence lifetime is $\tau_F(D_2O)/\tau_F(H_2O) \sim 3.4$. Table II summarizes these data for the fluorescence

Figure 10. Steady-state spectral decomposition of (a) 7-azaindole and (b) 7-azatryptophan at pH 6.8 and 20°C. The empty circles represent the steady-state emission arising from the longer-lived lifetime component; the solid-circles, from the shorter-lived component. The spectrum of the short-lived component is multiplied by a factor of 10.

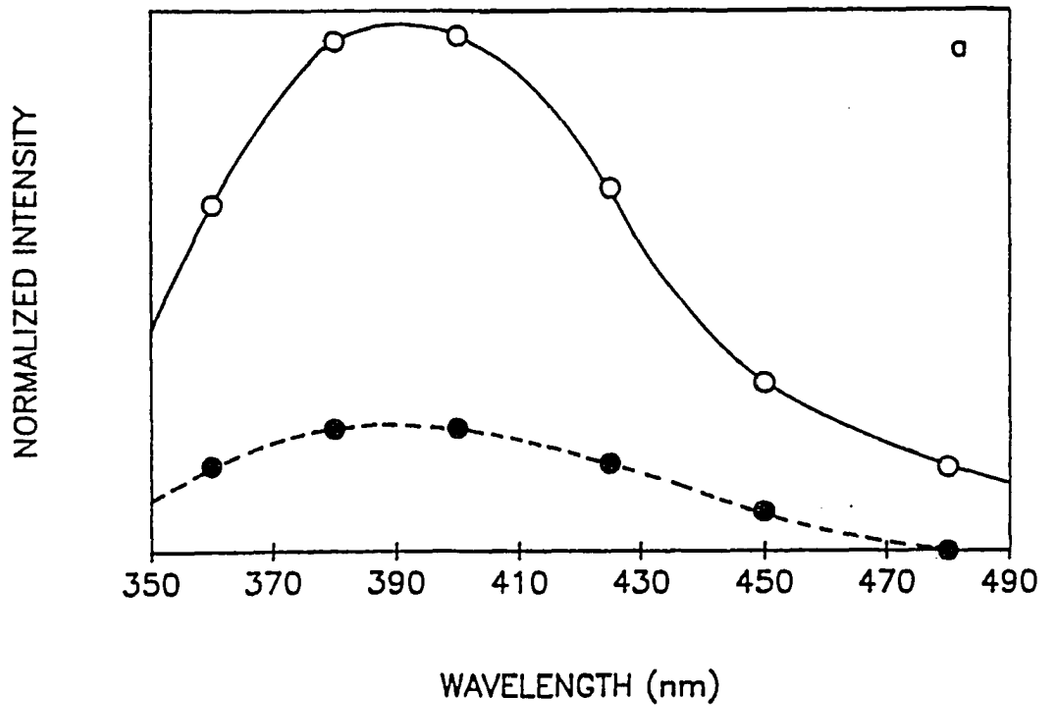
a
NORMALIZED INTENSITY
350
370
390
410
430
450
470
490
WAVELENGTH (nm)

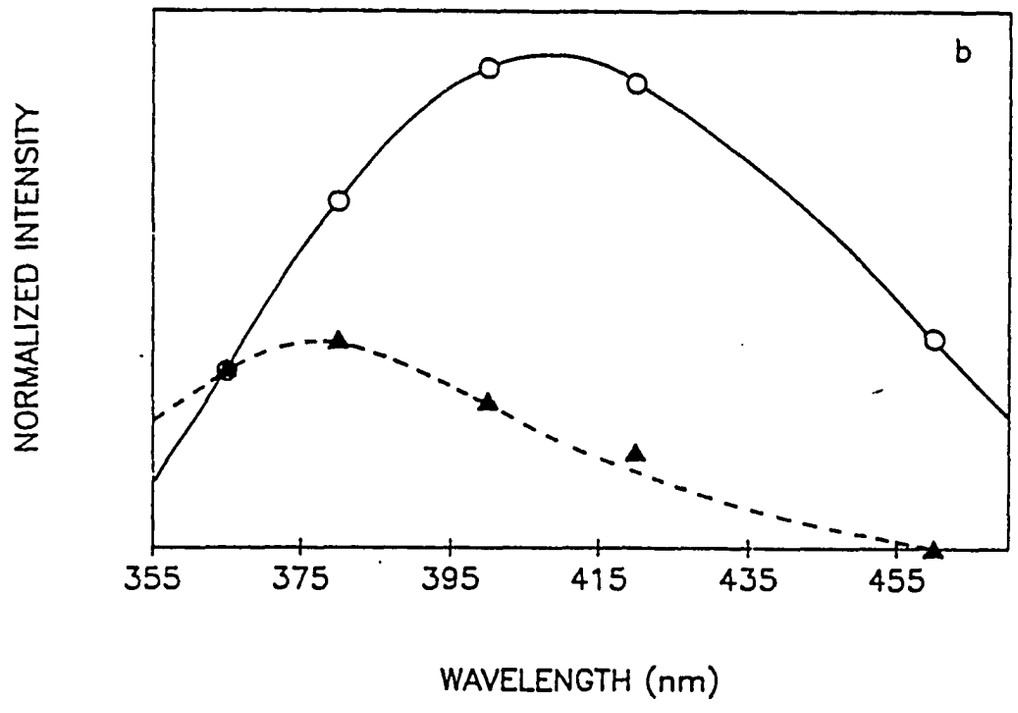
b
NORMALIZED INTENSITY
355
375
395
415
435
455
WAVELENGTH (nm)

quantum yields and lifetimes of 7-azaindole and indole derivatives. A clear trend is established. For 7-azaindole and its methylated derivatives the presence of a "full" N_1-H bond yields an isotope effect of ≥ 2.6. The fluorescence quantum yields and lifetimes presented in Table II were collected over the entire emission band. Hence, since only a small fraction of the 7-azaindole molecules undergo excited-state tautomerization, it is unlikely that the observed isotope effect arises from this process. Under these detection conditions, the decaying and rising contributions will cancel each other out. If we assume that isotopic substitution affects neither the rate of photoionization nor that of intersystem crossing [72], then another nonradiative process must be involved.

7M7AI is a special case in that its fluorescence lifetime and quantum yield are the smallest of all the compounds listed in Table I, yet it does not possess a covalent N_1H bond. Waluk et al. [75] have discussed the role of internal conversion in 7M7AI and two of its derivatives in butanol and 3-methylpentane. While a hydrogen-bonding interaction with the solvent may contribute to the short lifetime and low quantum yield of 7M7AI, it is likely that internal conversion is most significantly enhanced by its reduced S_1-S_0 energy gap relative to 7-azaindole: 25,900 as opposed to 19,600 cm^{-1}. For smaller energy gaps, the frequency of the acceptor vibrational mode is less crucial because fewer quanta are required in S_0 [73, 74].

Figure 11. Arrhenius plots formed from the inverse of the short-lived lifetime component obtained from 7-azaindole in H_2O (open circles) or D_2O (filled circles). For H_2O, the activation energy is 2.7 ± 1.7 Kcal and the Arrhenius prefactor is 2.3 ± 0.6 x 10^{12}. For D_2O, the activation energy is 2.7 ± 1.3 and the prefactor is 6.7 ± 1.2 x 10^{11}. Experiments were performed at pH 6.8 and pD 7.2.

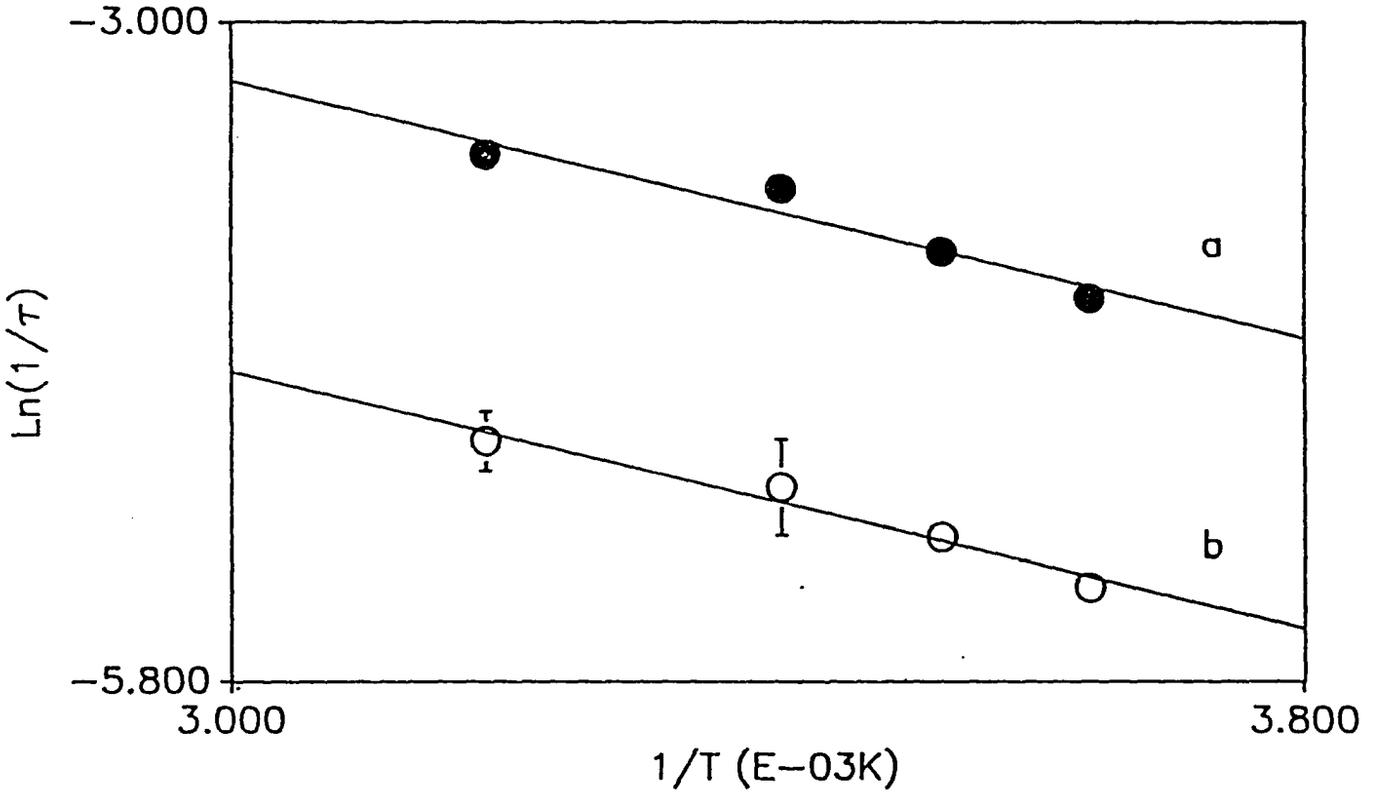
−3.000
−5.800
Ln(1/τ)
3.000
3.800
1/T (E−03K)
a
b

Table 2

Deuterium Isotope Effect on Fluorescence Lifetimes and Quantum Yields[a]

compound [b]	$\phi_F(D_2O)/\phi_F(H_2O)$[c]	$\tau_F(D_2O)/\tau_F(H_2O)$[c]
7AI (N_7, N_1H)	3.6	3.5
7AI (N_7H^+, N_1H)	2.7	2.6
1M7AI (N_7)	1.19 [61]	1.2
1M7AI (N_7H^+)	1.8	1.5
7M7AI (N_1)	1.6	1.4
7M7AI (N_1H^+)	2.6	3.1
indole (N_1H)	1.40 [61]	1.3
1-methyl-indole	1.19 [61]	1.1

[a] Experiments are performed at 20°C.

[b] The state of protonation of the relevant nitrogen atom is given by, for example, N_7 or N_7H^+. The pH regions in which N_7 and N_1 are protonated are presented in Figures 60 and 61.

[c] All data obtained in our laboratory were collected over the entire emission band.

3. pH Dependence of the Fluorescence Lifetimes and Quantum Yields of the Methylated Derivatives

In order to understand the nature of the fluorescent species of which the emission band of 7-azaindole at neutral—or any pH—is comprised, it is important to appreciate the pH dependence of the fluorescence lifetimes and quantum yields of the methylated analogies. Earlier we concluded that there was a negligible change in the excited-state pK_a of the N_7 of 7-azaindole owing to the similarity of the potentiometric and the fluorescence titration curves [18]. Figure 12 presents the fluorescence quantum yield of 7-azaindole as a function of pH. The form of this titration curve is qualitatively similar to that presented by Ingham and El-Bayoumi [57] except that we observe a more pronounced intensity change with pH. This change is a result of our accounting for the change in shape and position of the 7-azaindole spectrum with pH (Figure 12). The data yield an excited-state pK_a of 4.6 and ~ 13 for N_7H^+ and N_1H, respectively (Table III). These values are very near the ground-state values.

We have obtained titration curves based on fluorescence lifetimes for 1M7AI and 7M7AI in order to investigate in detail the excited-state, reversible proton-transfer equilibrium of N_7 and N_1. If, for example, the proton transfer equilibrium is not rapid on the time scale of the excited-state lifetimes, then titration curves based on fluorescence measurements, in particular those of quantum yields, will not accurately measure the excited-state pK_a. β-naphthol is a celebrated example of a molecule where the proton transfer equilibrium occurs on the same time scale as the excited-state lifetime [68, 76-78]. Fluorescence lifetimes

Table 3

Ground- and Excited-State pK_a Values of 7-Azaindole and Its Analogies

compound	$pK_a(S_0)$	pK_a (S_1)[a]
pyrrole	16.5 [80], 17.51 (25°C) [132]	
pyridine (H^+)	5.21 (18°C) [133]	
indole (N_1H)	16.97 (25°C) [132]	12.3 [77]
7AI (N_1H)	12.1 (26°C)	~ 13 (23°C)[b]
7AI (N_7H^+)	4.5 (26°C)[c], 4.59 (20°C) [134]	4.6 (23°C)[b]
7M7AI (N_1H^+)	8.9[d] [86]	10.3 (20°C)
1M7AI (N_7H^+)[e]		3.1 (20°C)

[a] S_1 refers to the fluorescent state, and hence to the lower of the two states, ^1L_b and ^1L_a [87,88].

[b] Obtained from fluorescence quantum yield measurements (Figure 10). It is assumed that acid-base equilibrium is established during the excited-state lifetime. No correction to the pK_a value is made for the lifetimes of the protonated and unprotonated species [79].

[c] The value reported earlier [18] was the inflection point of the titration curve.

[d] Determined by the half neutralization method.

[e] Not enough material was available after the optical measurements to perform the ground-state titration.

Figure 12. Fluorescence quantum yield of 7-azaindole as a function of pH at 20°C. Measurements are relative to those of 7-azaindole at pH 8.8 and 20°C. These results are slightly different from those of Ingham and El-Bayoumi [58] who only measured the 7-azaindole fluorescence intensity at 390 nm and do not take the spectral shift with pH into account. pH measurements are accurate to ± 0.10 units.

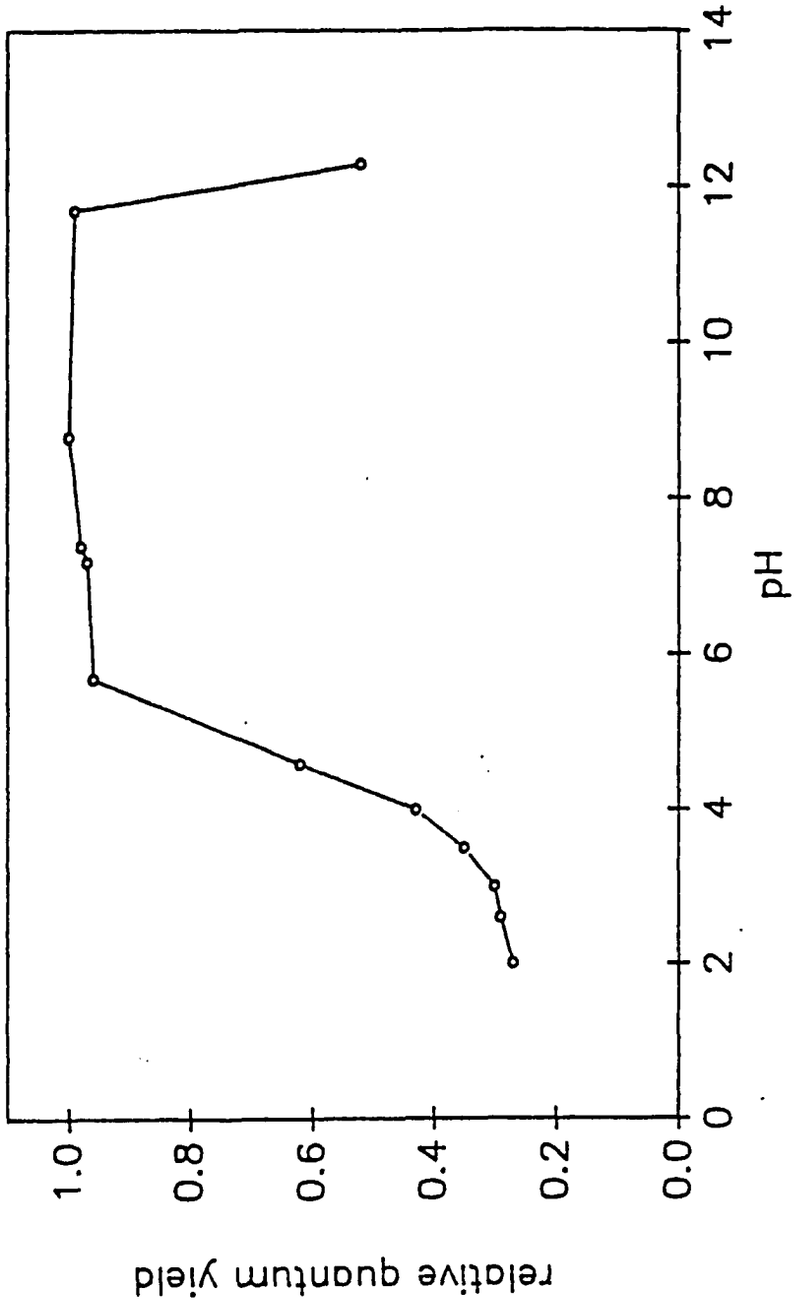
relative quantum yield
1.0
0.8
0.6
0.4
0.2
0.0
0
2
4
6
8
10
12
14
pH

Figure 13. Average fluorescence lifetime as a function of pH of 1M7AI and 7M7AI at 20°C. For 1M7AI, the points a, **b**, and **c** denote double-exponential lifetimes. **a**: 3.2 ns (81%), 5.6 ns (19%); **b**: 2.3 ns (58%), 7.67 ns (42%); **c**: 1.9 ns (54%), 15.2 ns (46%). For 7M7AI, the points **a** and **b** indicate double-exponential lifetimes. **a**: 629 ps (64%), 361 ps (36%); **b**: 603 ps (50%), 403 ps (50%). Titration curves obtained from fluorescence quantum yields of 1M7AI and 7M7AI demonstrate the same behavior.

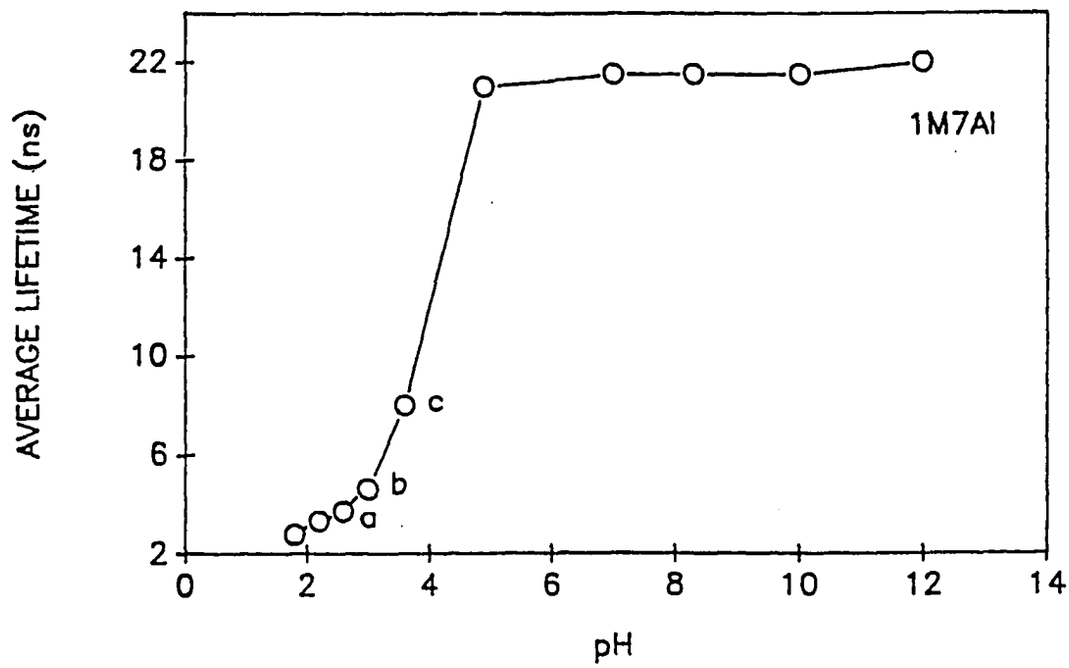
AVERAGE LIFETIME (ns)
22
18
14
10
6
2
0
2
4
6
8
10
12
14
pH
1M7AI
a
b
c

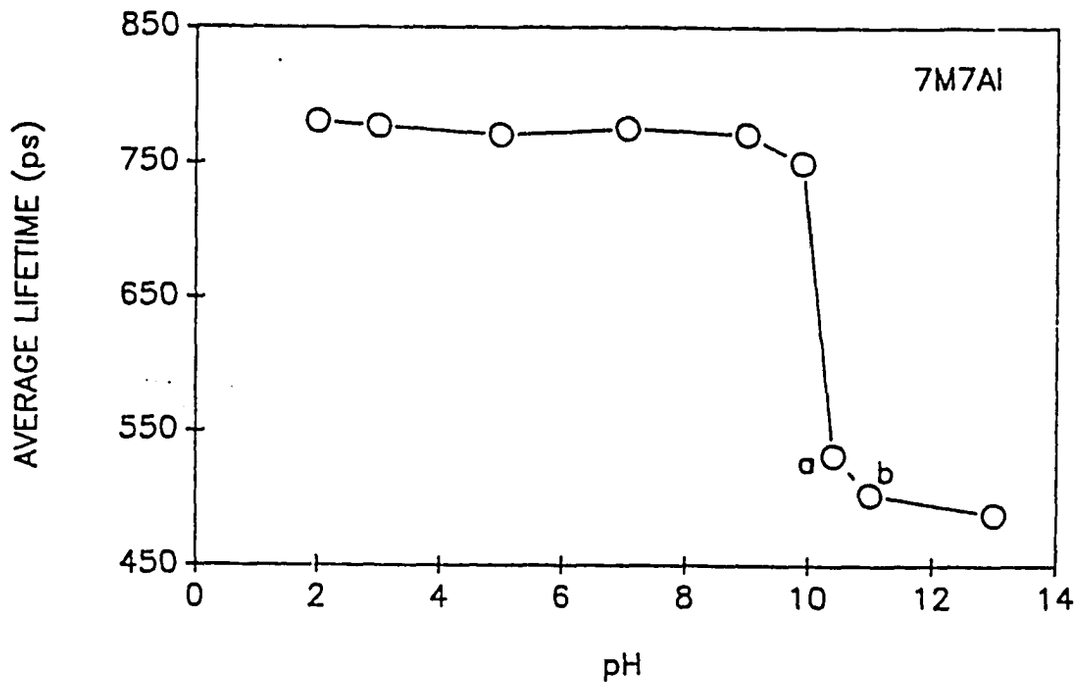
AVERAGE LIFETIME (ps)
850
750
650
550
450
0
2
4
6
8
10
12
14
pH
7M7AI
a
b

as a function of pH (Figure 13) are thus required to clarify the kinetics involved. In particular, we consider the tautomer analog 7M7AI (T) being protonated by water to yield TH^+ at neutral pH.

$$T^* + H_2O \underset{k_{-H\cdot}}{\overset{k_{H\cdot}}{\rightleftharpoons}} TH^{+*} + OH^-$$

$$h\nu_{ex} \qquad k_F^T \qquad\qquad h\nu_{ex} \qquad k_F^{TH\cdot}$$

$$T + H_2O \rightleftharpoons TH^+ + OH^-$$

k_F^T and $k_F^{TH^+}$ are the rates of population decay of the excited-state unprotonated and protonated species, not taking into account k_{H^+} or k_{-H^+}. The solution [68,74,78] to the excited-state rate equations yields two rate constants, λ_1 and λ_2, where λ_1 represents the rate of decay of T^*; λ_2, of TH^{+*}:

$$\lambda_{1,2} = \frac{1}{2}\left[X + Y \mp \left\{(Y - X)^2 + 4k_H'.k_{-H}.[OH^-]\right\}^{1/2}\right] \qquad (5)$$

$k_{H\cdot}' = k_{H\cdot}[H_2O]$, $X = k_F^T + k_{H\cdot}'$, and $Y = k_F^{TH\cdot} + k_{H\cdot}[OH^-]$. The subscript 1 correspondsto the minus sign. Constructing the sum and difference of λ_1 and λ_2, which can be obtained from any point on the titration curve where two exponentially decaying components are present, permits the determination of k'_1, k_{-1}, and K_b (or K_a). For 7M7AI at pH 10.4 and 20°C (Figure 13), $\lambda_1 = (361\ ps)^{-1}$ and $\lambda_2 = (629\ ps)^{-1}$. $k_F^T = (480\ ps)^{-1}$ and

k_F^{TH+} = (780 ps)$^{-1}$; these latter values are the rates of population decay of 7M7AI and protonated 7M7AI in regions far away from the inflection point (Table I). Results are tabulated in Table III. There is only a small change in pK_a between the ground and the excited state for N_7 and N_1; and the change that is observed indicates that in the excited state N_7 doesn't change clearly and N_1 is slightly more basic. This results is contradictory to the suggestion [80] that the driving force for intramolecular tautomerization in molecules such as methyl salicylate is an excited-state pK_a change. Notice that these data are obtained by assuming that acid-base equilibrium is established during the excited-state lifetime.

Figure 14 presents the steady-state fluorescence spectra of 1M7AI and 7M7AI as a function of pH. At pH values below 9, 7M7AI has a maximum at 442 nm; at pH values above 10, the maximum shifts to 510 nm. It is reasonable to assume that the tautomer form of 7-azaindole in water has an N_1 whose pK_a is similar to that of 7M7AI. Therefore, after excited-state, double-proton transfer is effected in 7-azaindole, it is likely that N_1 will very rapidly become protonated and that this cation gives rise to a species with emission maximum at about 440 nm.

Table III contains pK_a data for pyrrole, pyridine, and indole, which serve as reference compounds. Fusion of a benzene ring to pyrrole to yield indole has a small effect on the pK_a of N_1. On the other hand, fusion of pyridine to pyrrole to yield 7-azaindole reduces the ground-state pK_a of N_1 by more than 4 units. For indole the excited-state pK_a change is large, whereas in 7-azaindole, both for N_1 and N_7, it is small as we have mentioned above.

Figure 14. Steady-state emission spectra of 7AI, 1M7AI, and 7M7AI in water, λ_{ex} = 285 nm and 20°C. All spectra are corrected for concentration differences. pH measurements are accurate to ± 0.10 units. The emission maxima as a function of pH are as follows.

For 7AI: pH ≥ 5.70, λ_{max} = 387 nm; pH 4.60, λ_{max} = 394 nm; pH 4.00, λ_{max} = 424 nm; pH 3.50, λ_{max} = 437 nm; pH ≤ 3.00, λ_{max} = 444 nm. These data are more accurate and of higher quality than those presented earlier [2].

For 1M7AI: pH ≥ 4.20, λ_{max} = 395 nm; pH 3.70, λ_{max} = 398 nm; pH 3.20, λ_{max} = 402 nm; pH 2.75, λ_{max} = 435 nm. Not shown are spectra for pH ≤ 2.15. Below pH 2.15, λ_{max} = 454 nm and the peak intensities are significantly less than that at pH 2.75.

For 7M7AI: pH ≤ 9.0, λ_{max} = 444 nm; pH 10.0, λ_{max} = 482 nm; pH ≥ 11.0, λ_{max} = 510 nm.

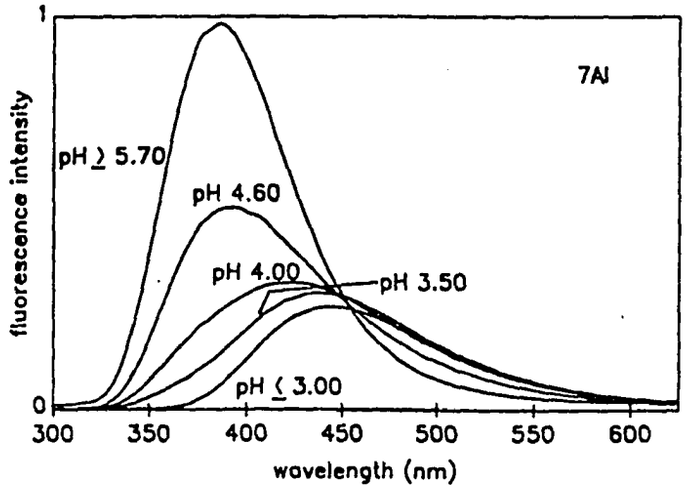
7AI
pH ≥ 5.70
pH 4.60
pH 4.00
pH 3.50
pH ≤ 3.00
fluorescence intensity
wavelength (nm)
1
0
300
350
400
450
500
550
600

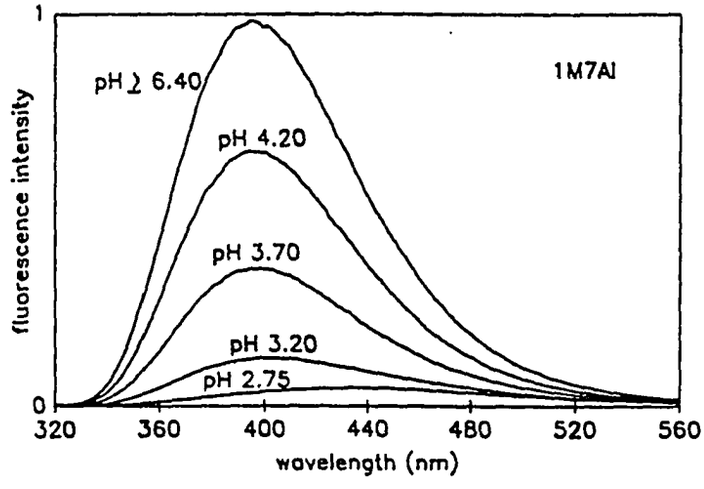
1M7AI
pH ≥ 6.40
pH 4.20
pH 3.70
pH 3.20
pH 2.75
fluorescence intensity
wavelength (nm)
1
0
320
360
400
440
480
520
560

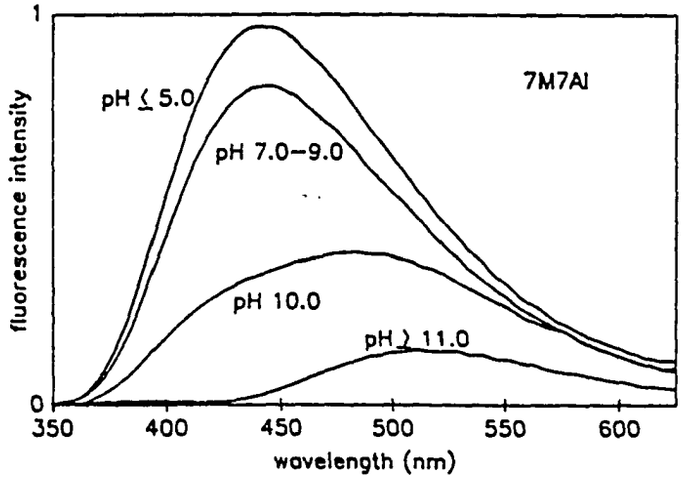
7M7AI
pH ≤ 5.0
pH 7.0–9.0
pH 10.0
pH ≥ 11.0
fluorescence intensity
wavelength (nm)
1
0
350
400
450
500
550
600

D. Discussion

1. The Fluorescent Species in Water

The 70-ps transient that we report elsewhere [19] in the transient absorbance of 7-azaindole is consistent with the rapid component that we measure across the emission spectrum for 7-azaindole and 7-azatryptophan in water at neutral pH (Figure 8). This rapid decay, which is observed for emission wavelengths towards the blue edge of the spectrum, is matched by a rise time of corresponding duration on the red edge of the spectrum. We note, however, that the amplitude of short component never exceeds 20% of the total fluorescence decay for 7-azaindole. This rapid fluorescence decay and rise times clearly indicate that 20% of the excited-state 7-azaindole molecules are undergoing tautomerization. The Arrhenius plots (Figure 11) indicate that this tautomerization is mediated by large-amplitude solvent motion, just as is observed in the alcohols [18,62-64]. Recently two related studies of 7-azaindole have been performed. Chou et al. [85] investigated 7-azaindole in mixtures of water and aprotic solvents. Small additions of water to polar aprotic solvents produced tautomer-like emission. They proposed that excited-state tautomerization is possible only when there are significant concentrations of 1:1 complexes of 7-azaindole and water. They further proposed that in pure water the formation of higher-order aggregates inhibits tautomerization during the excited-state lifetime.

Chapman and Maroncelli have studied 7-azaindole fluorescence in water and in

mixtures of water and diethyl ether [84]. They too observe long-wavelength, tautomer-like emission at low water concentrations. In pure water they also observe a rapid rise time at long wavelengths. They, however, take a different point of view, namely that excited-state tautomerization occurs for the entire 7-azaindole population in pure water and that the 7-azaindole fluorescence lifetime is dominated by this reaction. Using a two-state kinetic model in conjunction with steady-state spectral data they conclude that the rapid rise time is associated with the nonradiative decay rate of the tautomer. They propose that the longer, ~ 900 ps, decay time of the entire emission band is a measure of the tautomerization rate. Their scheme requires that the nonradiative decay rate of the tautomer is greater than the rate of tautomerization. They estimate that the rate of tautomerization is 1.2×10^9 s^{-1}.

Our observations and conclusions more nearly approach those of Chou et al., although there is a small population of 7-azaindole molecules that do tautomerize in addition to the majority of the population in which this reaction is frustrated. That the fluorescence lifetime of 7-azaindole is <u>not</u> dominated by excited-state tautomerization is demonstrated by the observation of three distinct fluorescence lifetimes: ~ 70 ps, the normal decay time; ~ 980 ps (i.e., 1100 ps, Table III), the tautomer decay time; and 910 ps, the decay time of the blocked solute. Further evidence is provided by the spectral inhomogeneity of the emission band (Figures 9 and 10).

At this point, there are two major questions that must be posed:

1. To what does the remaining 80% of the fluorescence decay in water correspond?
2. If excited-state double proton transfer is being effected in water, even for only 20%

of the population, why does the fluorescence spectrum apparently consist of only one band whereas in alcohols, which also mediate tautomerization, two emission bands are observed?

i. The Presence of a "Blocked" Solute Species

To address the first question, we propose that there are three types of species of 7-azaindole in water that give rise to its fluorescence spectrum. These are illustrated in Figure 15. Twenty percent of the population is solvated in such a fashion that excited-state tautomerization can be effected in 70 ps. This population then comprises "normal" and "tautomer" species that are formally equivalent to those observed in linear alcohols. The normal species has a lifetime of 70 ps; and the tautomer, which is protonated, has a lifetime of 1100 ps. We suggest that the fluorescence properties of 7-azaindole in water are dominated by the remaining 80% of the solute molecules, which are "blocked" and unable to tautomerize during the 910 ps lifetime of this species.

In order to check this assignment, we can estimate the fluorescence quantum yield that would be observed if these three species were present and compare this estimated value to the measured fluorescence quantum yield of 7-azaindole in water, $\phi_F = 0.03$ [61] (Table II). The fluorescence intensity as a function of time, when emission is collected over the entire spectrum, is given by the rate at which photons are emitted from all excited states present:

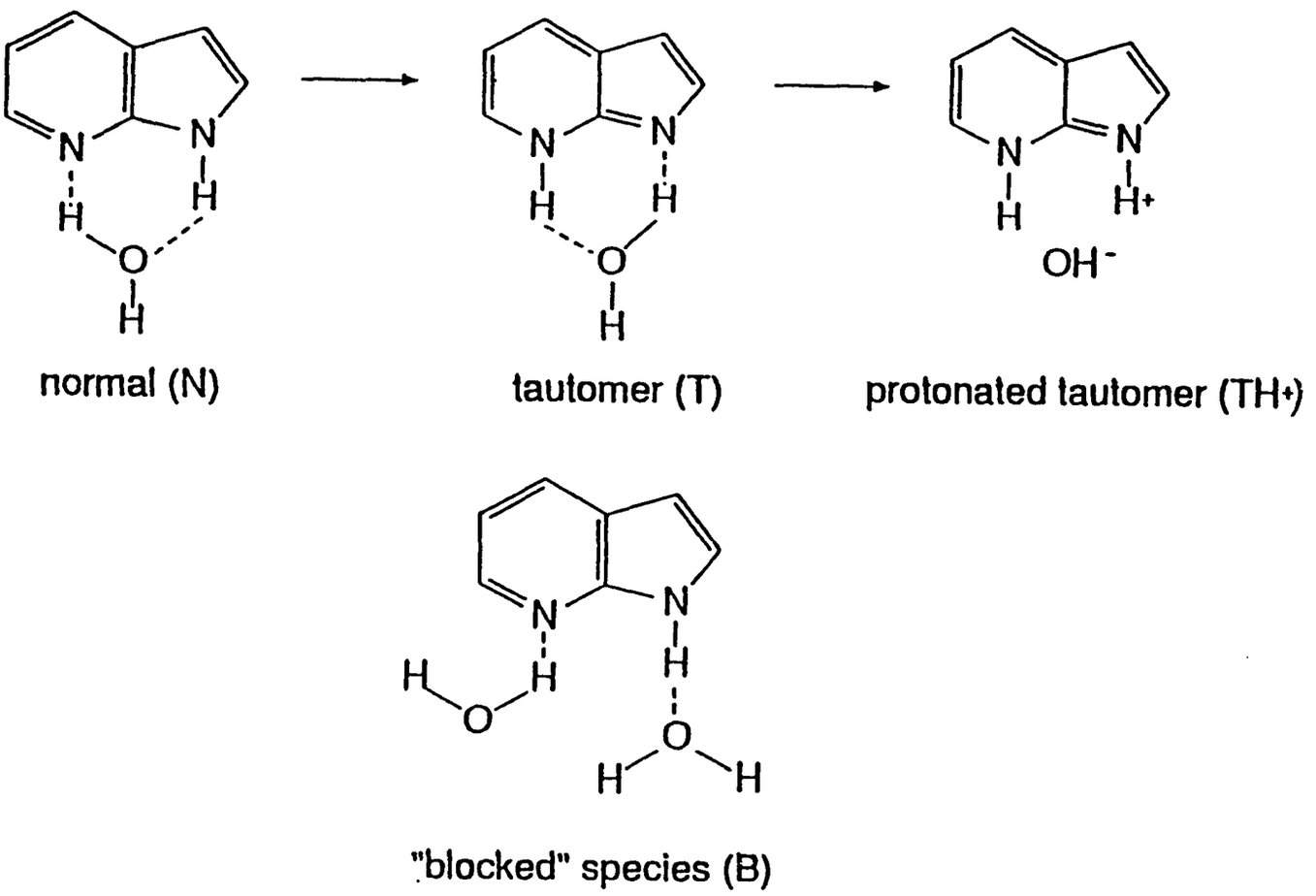

Figure 15. The ideal structure of 7-azaindole in water.

$$I(t) = \sum_i k_R^i F_i(t) \tag{6}$$

where k_R^i is the radiative rate of species i and $F_i(t)$ is the excited-state population at a given time (the fluorescence decay profile) of species i. In our case, $F_i(t)$ is expressed as an exponential decay or as a sum of exponentially rising and decaying components. The fluorescence quantum yield is obtained by integration of this equation over time:

$$\phi_F = \int_0^\infty I(t)dt. \tag{7}$$

We thus obtain:

$$\begin{aligned}\phi_{F,calc} = {} & k_R^{1M7AI}(0.20)(70\ ps) + k_R^{7M7AI(N_1H^+)}(-0.20)(70\ ps) \\ & + k_R^{7M7AI(N_1H^+)}(0.20)(1100\ ps) + k_R^{1M7AI}(0.80)(910\ ps) = 0.025\end{aligned} \tag{8}$$

This estimated result is in good agreement with the measured value of 0.03 when one considers the difficulties in obtaining accurate measurements for quantum yields as well as for the radiative rates and the weight of the short component that represents the 7-azaindole population undergoing tautomerization.

Blocked solvation, referred to above, could be produced if N_1 forms a strong hydrogen bond with water that results in an orientation that is not propitious for proton transfer or if N_7 is also "blocked" by forming another hydrogen bond with a different water molecule (Figure 15). Postulating this state of blocked solvation—and most importantly a strong

hydrogen bonding interaction of N_1 with the solvent—resolves the following paradoxical observations: the maximum of the fluorescence emission of 7-azaindole in water, 386 nm, is closer to that of unprotonated 1M7AI, 395 nm, than to that of protonated or unprotonated 7M7AI, 442 or 510 nm, respectively. On the other hand, the fluorescence lifetime of 7-azaindole in water is more similar to that of protonated or unprotonated 7M7AI, 780 ps or 480 ps, than to that of unprotonated 1M7AI, 21 ns.

The substitution of the hydrogen by a methyl group at N_1 renders 1M7AI incapable of tautomerizing and hence provides a relatively high fluorescence quantum yield, ϕ_F = 0.55-0.64 [61] (Table I). Presumably, the only significant nonradiative decay channels left to 1M7AI are photoionization and intersystem crossing [19].

The fundamental difference between the blocked species and 1M7AI is the proton at N_1, which can interact with the solvent. We propose that the presence of this proton bound to N_1 is responsible for the position and shape of the fluorescence band of the blocked species of 7-azaindole in water—that is, similar to that of 1M7AI. On the other hand, since this proton has a strong hydrogen bonding interacting with solvent, another channel of deactivation may be evolved. We will deal this problem in the following chapter.

It is noteworthy that the fluorescence lifetime and quantum yield of this blocked species are more similar to those of protonated 7AI, 1M7AI, and 7M7AI than to those of the unprotonated tautomer analog, 7M7AI (Table I). This supports the notion that the blocked species is also undergoing an interaction of its N_7 with solvent, as depicted schematically in Figure 14.

ii. The Importance of the Relative Acidities of N_1 and N_7

In order to address the second question raised above, it is important to note that consideration of the steady-state fluorescence spectrum of 7-azaindole in water requires an appreciation of the relative acidities of N_1 and N_7. A considerable amount of confusion may ensue if one expects to observe, for the fraction of molecules undergoing tautomerization, fluorescence emission in the red (λ_{max} ~ 510 nm) as is observed for the tautomer of 7-azaindole in methanol or for 7M7AI in methanol. Instead of bimodal emission at neutral pH, one only detects a long-wavelength tail (Figure 15). This apparent discrepancy is easily resolved when one notes that N_1 in the tautomer (e.g., 7M7AI) is very basic: excited-state pK_a = 10.3 (Figure 13, Table III). Owing to the basicity of N_1, upon excited-state tautomerization of the small subset of appropriately solvated molecules, it is likely that N_1 is immediately protonated. Protonated 7M7AI has an emission maximum at 444 nm; and this is consistent with the shape of the 7-azaindole spectrum at low pH (Figure 15).

2. Population Decay, Tautomerization, and Solvent Reorganization ("Dynamics")

The physical picture that we have so far obtained for the photophysics of the 7-azaindole chromophore in water is the following:

1. At ambient temperature there is a ground-state equilibrium between a set of 7-azaindole molecules that can tautomerize (N) and that is analogous to the normal

species referred to in linear alcohols and a set of 7-azaindole molecules that are solvated in such a fashion that tautomerization is blocked (B).

2. For 7-azaindole, based on the preexponential factors obtained from wavelength-resolved lifetime measurements, we estimate the equilibrium constant to be at most $K = k_1/k_{-1} = [N]/[B] = 0.25$.

3. N and B do not interchange rapidly on the time scale of their fluorescence lifetimes, 70 ps and 910 ps, respectively.

4. The tautomer (T) formed by the decay of N is rapidly ($\lesssim$ 1 ps) protonated (TH^+) owing to the strong basicity of N_1 relative to that of N_7 ($pK_a^*(N_1) = 10.3$ as opposed to $pK_a^*(N_7H^+) = 3.7$).

5. The protonated tautomer decays with a time constant of 1100 ps.

We can construct a reaction scheme that is consistent with these data and conclusions. Scheme

$$\xrightarrow{k_F^B = (910\ \text{ps})^{-1}} B \underset{k_{-1}}{\overset{k_1}{\rightleftharpoons}} \left[N \xrightarrow{k_{PT} = (70\ \text{ps})^{-1}} T \right] \xrightarrow{k_{H^+} > (1\ \text{ps})^{-1}} TH^+ \xrightarrow{k_F^{TH^+} = (1100\ \text{ps})^{-1}}$$

The proposal of a time constant of $\lesssim$ 1 ps for the ultimate protonation step is based on the following. First, fast protonation is facilitated by the availability of the proton from the water molecule that participated in the cyclic complex. Thus, this reaction may be considered as essentially intramolecular, insofar as it depends on a solute-solvent complex, rather than as intermolecular. Second, since no long-wavelength emission is observed, the

unprotonated tautomer must decay as rapidly as it is formed. Third, a time constant of this duration is consistent with the estimated lifetime of a hydrogen bond, ~ 5 ps [82].

In the above discussion, we have tacitly assumed that the 910 ps and 70 ps decay components represent the population decay of B and N respectively and are not significantly perturbed by the rate constants for solvent reorganization, k_1 and k_{-1}. These assumptions then require us to place certain limits on k_1 and k_{-1}.

If we consider only the equilibrium between B and N and their population decays, we obtain the following expressions by solving the rate equations using Laplace transform techniques [83]. Here we assume that at t = 0, the populations of the excited-state blocked and normal species are nonzero and that $[N]_o/[B]_o = 0.25$.

$$[B](t) = \frac{[B]_o}{(\lambda_2 - \lambda_1)}\left[(\lambda_2 - X)e^{-\lambda_1 t} + (X - \lambda_1)e^{-\lambda_2 t}\right] + \frac{k_{-1}[N]_o}{(\lambda_2 - \lambda_1)}(e^{-\lambda_1 t} - e^{-\lambda_2 t}) \tag{9}$$

$$[N](t) = \frac{k_1[B]_o}{(\lambda_2 - \lambda_1)}(e^{-\lambda_1 t} - e^{-\lambda_2 t}) + \frac{[N]_o}{(\lambda_2 - \lambda_1)}\left[(\lambda_2 - Y)e^{-\lambda_1 t} + (Y - \lambda_1)e^{-\lambda_2 t}\right] \tag{10}$$

$$\lambda_{1,2} = \frac{1}{2}\left[X + Y \mp \left\{(Y - X)^2 + 4k_{-1}k_1\right\}^{1/2}\right] \tag{11}$$

where subscript 1 refers to the negative sign; and subscript 2, to the positive. In general, $\lambda_{1,2}$ depend on the nonradiative and radiative pathways of deactivation of B and N as well as on k_1 and k_{-1}. Thus,

$$X = k_1 + k_F^B; \quad Y = k_{-1} + k_F^N \tag{12}$$

where k_F^B and k_F^N are the inverse of the fluorescence lifetimes of B and N, neglecting the contribution from k_1 and k_{-1}.

From Eqns. 10 and 11 it can be seen that if $k_F^B \gg k_1$ and if $k_F^N \gg k_{-1}$, then $\lambda_1 = k_F^B$ and $\lambda_2 = k_F^N$. It is interesting to consider the physical implications of how small k_1 and k_{-1} must be relative to k_F^B and k_F^N in order for $\lambda_1 \sim k_F^B$ and $\lambda_2 \sim k_F^N$. If we arbitrarily choose $k_1 = 0.1 \times 10^9\ s^{-1}$, the equilibrium between B and N requires $k_{-1} = 0.4 \times 10^9\ s^{-1}$. Then from Eqns. 10 and 11 we obtain $1/\lambda_1 = 837$ ps $\sim \tau_F^B$ and $1/\lambda_2 = 68$ ps $\sim \tau_F^N$. In other words, if we require that the solvation step converting B to N occurs on a time scale of 10 ns or longer, we recover decay components that are qualitatively similar to the measured 910 ps and 70 ps that we have attributed to the population decay times of B and N, respectively.

Two additional self-consistency checks arise from these assumptions. First, the total fluorescence intensity, which is proportional to the sum of the transient populations of B and N, assuming that their radiative rates are identical, yields from Eqn. 5 $I(t) = k_R[B](t) + k_R[N](t) \propto 0.80 \exp(-\lambda_1 t) + 0.20 \exp(-\lambda_2 t)$. Thus, we retrieve 20% of a species decaying rapidly, which is in agreement with the experimental observation of the proportion of the 7-azaindole population that is capable of tautomerization. Second, using the above values, we find that $(X - \lambda_1) \sim 0$ and that $[B]_o(\lambda_2 - X)/k_{-1}[N]_o \gg 1$. Thus, B decays essentially as a single exponential, as is observed.

One may ask whether the reorganization of water molecules about the solute can occur on such a slow time scale. It is important to distinguish the time scales involving reorientational dynamics of solvent molecules, which can be extremely rapid [60,84], and "diffusive redistribution" of solvent. In particular, one must distinguish between the kind of solvent reorientation that is induced by dipole moment changes in the excited state of a probe

molecule and reorganization of the solvent that involves the breaking and making of hydrogen bonds. It has been noted that in polyalcohols such as ethylene glycol and glycerol there is a severe deviation, characterized by unusually slow tautomerization, from the good correlation of tautomerization rate with $E_T(30)$ that is observed with monoalcohols [64]. It has been suggested that this deviation is a signature of solvents capable of donating more than one hydrogen bond per molecule and that such solvents reduce the probability of forming solute molecules with the "correct" solvation for tautomerization [64,84]. The detailed mechanism of the rate reduction peculiar to these solvents is still unknown.

E. Conclusions

1. Only a small fraction ($\lesssim$ 20%) of 7-azaindole molecules in pure water are capable of excited-state tautomerization on a 1-ns time scale.
2. The majority of the 7-azaindole molecules are solvated in such a fashion that tautomerization is blocked. More than 10 ns are required to achieve a state of solvation that facilitates tautomerization, that is, to convert the "blocked" species into a "normal" species.
3. No significant emission intensity is observed for 7-azaindole in water at 510 nm because so little tautomer is produced and because the tautomer that is produced is rapidly protonated and has an emission maximum at ~ 440 nm.
4. For 7-azaindole in water, excited-state tautomerization and intersystem crossing seem

to be relatively minor pathways of nonradiative decay. Photoionization from a higher-lying excited singlet has been suggested to be quite facile [19].

5. Most importantly these results clarify the photophysics of 7-azaindole for use as the intrinsic chromophore of the probe molecule, 7-azatryptophan. In particular, the minor amount of tautomerization will contribute to the decay kinetics only if emission is collected at wavelengths red of 505 nm or with a relatively narrow spectral bandpass (with adequate temporal resolution). This is not a serious restriction since experiments are not likely to be performed with such spectral resolution owing to the low fluorescence intensity. When emission is collected over a large spectral region and on a full-scale time base coarser than 3 ns, the tautomerization reaction is imperceptible. On the other hand, the appearance of long-wavelength emission of a protein containing 7-azatryptophan in water would definitely signal a change of environment that facilitates tautomerization.

CHAPTER IV SOLVATION OF 7-AZAINDOLE IN ALCOHOL AND WATER: EVIDENCE FOR CONCERTED, EXCITED-STATE, DOUBLE-PROTON TRANSFER IN ALCOHOLS

A. Introduction

In the previous chapter, we discussed the fluorescent species and reaction dynamics of 7-azaindole in water. In this chapter, we will provide further evidence to support the model of the blocked species and elucidate the nonradiative pathways of it. Also we want more detailed information about the nature of double proton transfer reaction. In alcohols, the tautomerization or double-proton transfer reaction has been traditionally depicted (Figure 16) as being mediated by one solvent molecule, which forms a cyclic complex with the solute. There has been, however, no experimental evidence to verify the concerted nature of this reaction or the involvement of the cyclic complex; and it seems possible that more than one solvent molecule could be involved in the shuttling of the proton from N_1 to N_7 in the excited state. The model of excited-state tautomerization of 7-azaindole in alcohols being mediated by a cyclic solute-solvent complex suggests that only two protons are involved in the transition state for this nonradiative decay process. In water, on the other hand, we have suggested that the majority of 7-azaindole molecules do not execute concerted excited-state double-proton transfer [19, 88-90]. The significantly different behavior observed in water is illustrated by the fluorescence emission with a single maximum at 386 nm and the single-

exponential fluorescence decay when emission is collected with a wide band-pass, 910 ps [19, 89]. We and Chou et al. [85] have attributed the different behavior in alcohols and water to fundamentally different types of solvation. In this work, we present experimental evidence that supports the model of the double-proton transfer reaction in alcohols arising from a two-proton, concerted process that is consistent with a cyclic solute-solvent complex.

Our experimental procedure consists of measuring the fluorescence lifetimes of 7-azaindole in solvent mixtures that vary in the ratio of the amount of the protiated to deuterated component. There are several examples of using ROH/ROD solvent mixtures to elucidate reaction mechanisms in double-proton transfer reactions [91-107]. As we discuss below, the interpretation of our results depends on whether the time scale for proton/deuteron exchange between solute and solvent is shorter than the excited-state lifetime of the solute. If it is, the measured fluorescence lifetimes are rigorously single-exponential; and the data may be interpreted in terms of the Gross-Butler equation [91, 94, 95]. If on the other hand proton exchange is slow, interpreting the excited-state kinetics is more complicated, even if the data are fortuitously well-described by a single, exponentially decaying component. In the Discussion, we consider the results in the limit of both fast and slow exchange with solvent. We conclude that the limit of slow exchange is probably more appropriate. Regardless, however, of whether exchange is rapid or not, the data for alcohols are qualitatively different from those of water and are suggestive of a two-proton, concerted process.

Figure 16. Idealized structures for excited-state tautomerization in (a) dimers of 7-azaindole and in (b) complexes of 7-azaindole with linear alcohols. We have argued [12] that water solvate 7-azaindole in such a fashion (c) that excited-state tautomerization is frustrated. We suggest, however, that abstraction of the N_1 proton by the coordinated water molecule is an important nonradiative pathway (see Figure 21 and the text).

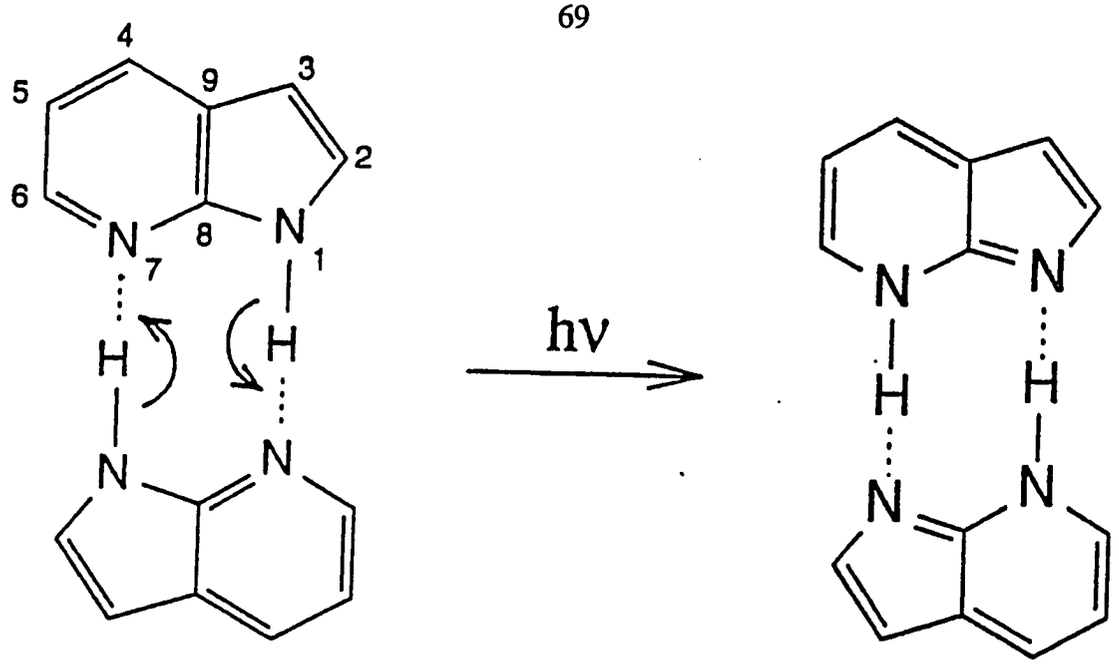

a

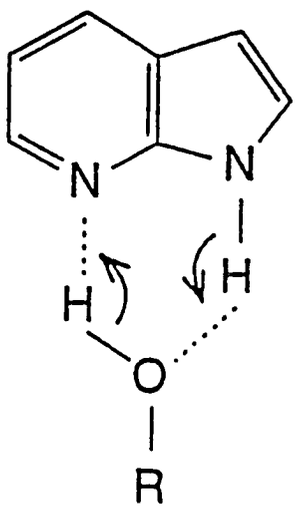

b

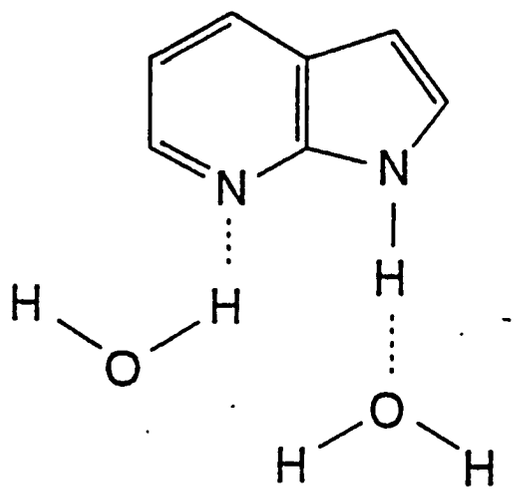

c

B. Experimental

Fluorescence lifetimes of 7-azaindole are obtained by time-correlated single-photon counting. 7-Azaindole was obtained from Sigma. Solvents were purchased from Aldrich; (MeOD and EtOD > 99.5% D; D_2O, 99.9% D). The reported results are the average of 3-4 runs for the MeOH/MeOD and the EtOH/EtOD experiments and 6-8 runs for the H_2O/D_2O experiments. The error in the measured lifetime was never more than 2% of the lifetime. The quality of fit was measured by the χ^2 criterion. 7-Azaindole was either purified as described above or used without purification. The lifetime results were identical. Regardless of the state of purification of the sample, a small percentage of a long lifetime component was always present in the alcohol data (but not in the water data). An extra lifetime component was required in all the fits to take into account its presence (Figure 17). Thus, in the Discussion, when we refer to single and double exponential fits we implicitly ignore the long-lived component. In previous work [18] we had been led to believe that the long-lived component arose from an impurity in the sample.

C. Results

The normal band of 7-azaindole in MeOH/MeOD and EtOH/EtOD mixtures can be fit relatively well to a single exponential fluorescence decay, although a double-exponential always provides a slightly better fit and yields physically reasonable parameters. Results

Figure 17. (a) Fluorescence decay of 7-azaindole in H_2O/D_2O (n = 0.5). A single exponential fit yields F(t) = exp(-t/1665 ps), χ^2 = 1.20. A double-exponential fit yields F(t) = 0.5exp(-t/1665 ps) + 0.5exp(-t/1650 ps), χ^2 = 1.20. The Figure displays the single-exponential fit. (b) Fluorescence decay of 7-azaindole in EtOH/EtOD (n = 0.8). The Figure displays the result for a fit to a sum of three exponentials: F(t) = 0.199exp(-t/271 ps) + 0.798exp(-t/455 ps) + 0.003exp(-t/3600 ps), χ^2 = 1.10. The double-exponential fit yields F(t) = 0.95exp(-t/401 ps) + 0.05exp(-t/852 ps), χ^2 = 1.23. See the Experimental section for a discussion of the significance of the third and second lifetime components in (b).

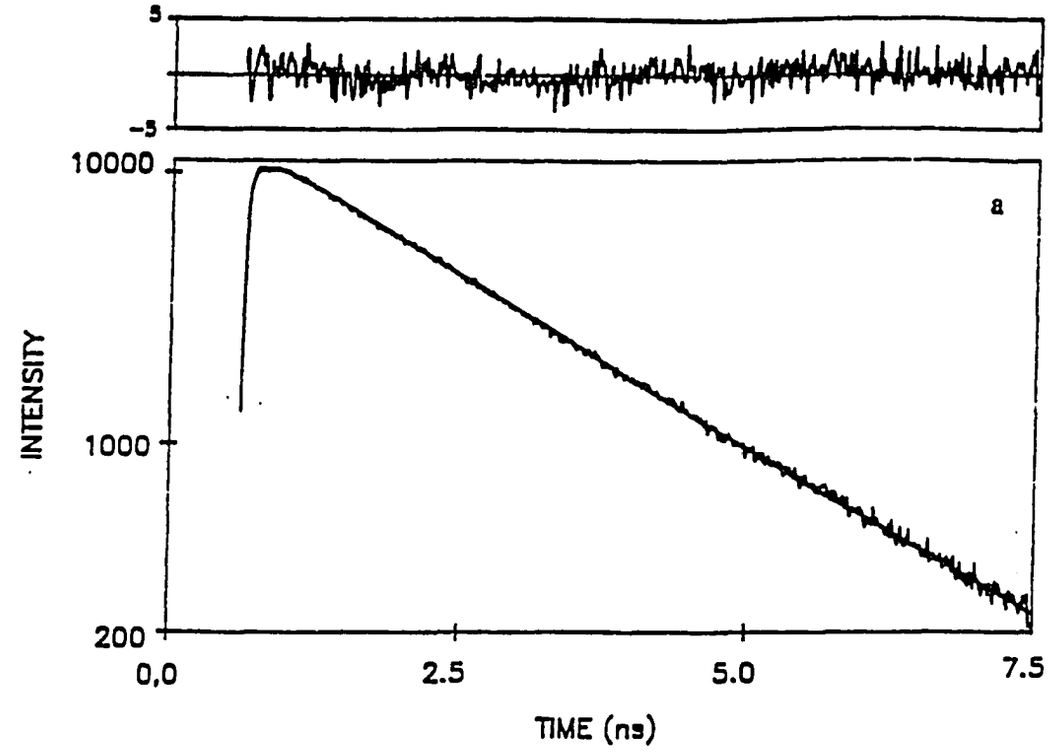
5
-5
10000
1000
200
INTENSITY
a
0,0
2.5
5.0
7.5
TIME (ns)

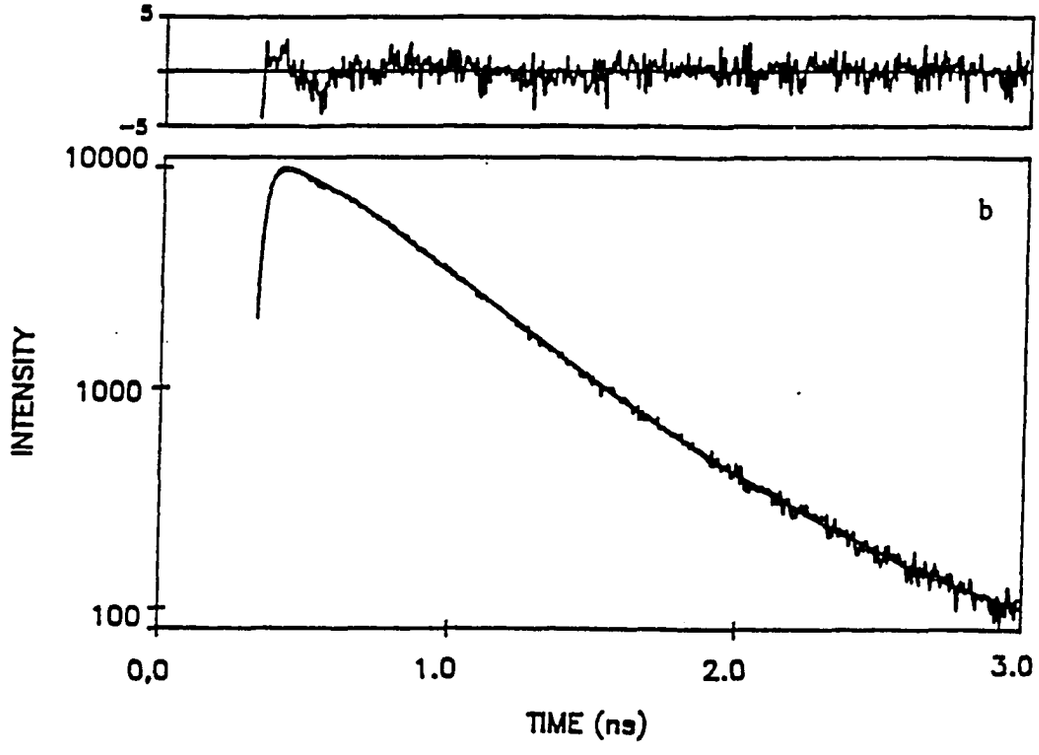
5
-5
10000
1000
100
INTENSITY
b
0,0
1.0
2.0
3.0
TIME (ns)

from both fitting procedures are cited (Tables 4-7). The double-proton transfer rate in the alcohols was estimated to be the inverse of the fluorescence lifetime. For water, the nonradiative decay was also taken to be the inverse of the fluorescence lifetime. Subtraction of the radiative rate [89] has a negligible effect on k_n and k_o. For water, a double-exponential fit was never significantly better than a single exponential fit and always yielded two lifetimes of the same duration. Figure 18 presents the solvent isotope effect k_n/k_o where k_o is the proton transfer rate in the pure undeuterated solvent, and k_n is the proton transfer rate in the solvent mixture whose mole fraction is n in the deuterated solvent. Similar data are presented for 7-azaindole in H_2O/D_2O in Figure 18. The methanol, ethanol, and water data all exhibit downward-bulging curves suggesting the involvement of a multi-proton transition process.

D. Discussion

1. Application and Appropriateness of the Gross-Butler Equation

i. 7-Azaindole in Methanol and Ethanol

The isotope effect on proton transfer reactions is rarely a linear function of solvent deuterium content. Gross and Butler explained this phenomenon by noting that either the H/D composition in the proton site can be different with respect to the solvent or more than

Table 4

Single-Exponential Fluorescence Lifetimes of 7-Azaindole in H/D Solvent Mixtures[a]

n[b]	MeOH/MeOD	EtOH/EtOD	H_2O/D_2O
0.0	139 ± 2	184 ± 2	885 ± 5
0.1	152 ± 2	201 ± 2	988 ± 3
0.2	166 ± 3	219 ± 3	1122 ± 23
0.3	185 ± 2	240 ± 2	1262 ± 6
0.4	196 ± 4	260 ± 2	1453 ± 27
0.5	217 ± 3	292 ± 4	1675 ± 15
0.6	239 ± 2	314 ± 3	1873 ± 17
0.7	267 ± 2	346 ± 4	2178 ± 48
0.8	289 ± 3	395 ± 4	2466 ± 30
0.9	327 ± 3	462 ± 3	2829 ± 23
1.0	365 ± 4	519 ± 4	3247 ± 13

[a] Lifetimes are given in picoseconds (ps). Data are reported for 20 °C.

[b] Mole fraction of deuterated solvent (atom fraction of deuterium in solvent).

Table 5

Double-Exponential Fit of 7-Azaindole Fluorescence Lifetimes in MeOH/MeOD Mixtures[a]

n[b]	τ_1 (ps)	τ_2 (ps)
0.1	139 ± 2	232 ± 3
0.2	144 ± 2	232 ± 10
0.3	155 ± 2	245 ± 2
0.4	166 ± 3	243 ± 6
0.5	167 ± 15	262 ± 5
0.6	172 ± 7	270 ± 4
0.7	184 ± 4	288 ± 5
0.8	199 ± 2	309 ± 4
0.9	207 ± 1	1330 ± 3

[a] Data are obtained at 20 °C. Fluorescence lifetimes are fit to the functional form $F(t) = A_1\exp(-k_1t) + A_2\exp(-k_2t)$. The interpretation of the rate constants (the inverse fluorescence lifetimes) is given in the text. Fluorescence lifetimes for the pure solvents (n = 0 and n = 1.0) are well described by a single exponential and are reported in Table 8.

[b] Mole fraction of deuterated solvent.

Table 6

Double-Exponential Fit of 7-Azaindole Fluorescence Lifetimes in EtOH/EtOD Mixtures[a]

n[b]	τ_1 (ps)	τ_2 (ps)
0.1	187 ± 3	315 ± 3
0.2	193 ± 4	339 ± 8
0.3	203 ± 4	350 ± 1
0.4	217 ± 4	356 ± 2
0.5	225 ± 17	385 ± 25
0.6	234 ± 4	398 ± 10
0.7	261 ± 3	420 ± 3
0.8	275 ± 8	453 ± 3
0.9	287 ± 1	484 ± 11

[a] Data are obtained at 20 °C. Fluorescence lifetimes are fit to the functional form $F(t) = A_1\exp(-k_1t) + A_2\exp(-k_2t)$. The interpretation of the rate constants (the inverse fluorescence lifetimes) is given in the text. Fluorescence lifetimes for the pure solvents (n = 0 and n = 1.0) are well described by a single exponential and are reported in Table I.

[b] Mole fraction of deuterated solvent.

Table 7

Rate Constants ($s^{-1} \times 10^{-9}$) for Proton Transfer Steps[a]

rate constant	MeOH/MeOD	EtOH/EtOD	H_2O/D_2O
k^{HH}	7.19 ± 0.10	5.43 ± 0.08	1.13 ± 0.02
k^{DD}	2.74 ± 0.04	1.9 ± 0.02	0.31 ± 0.01
$(k^{HH}k^{DD})^{1/2}$	4.43 ± 0.05	3.24 ± 0.03	0.59 ± 0.01
$k^{HD,b}$	4.42 ± 0.06	3.25 ± 0.02	
$k^{DH,b}$	4.59 ± 0.04	3.27 ± 0.02	
$k^{HD,c}$	4.29 ± 0.11	3.24 ± 0.09	0.48 ± 0.02

[a] Fluorescence lifetime measurements from which the rate constants were obtained were performed at 20 °C.

[b] Obtained from eqns 18 and 19. See text. Because this method requires fitting the data to a double-exponential fluorescence decay, the corresponding rate constants could not be determined for water, where a single exponential is sufficient to describe the decay curves. The rate constants were determined by assuming that $\phi^R = 1$ in both the ground and the excited states. If, on the other hand, $\phi^R = 1.6$, then, for example, an ethanol mixture where n = 0.5 yields $k^{HD} = 3.22 \pm 0.03 \times 10^9\ s^{-1}$ and $k^{DH} = 4.78 \pm 0.04 \times 10^9\ s^{-1}$. Eliason and Kreevoy [103] have discussed mechanisms by which values for ϕ^R other than 1 may result.

[c] Obtained from eqn 34. This method of analysis assumes that $k^{HD} = k^{DH}$. The reported results were determined by assuming that $\phi^R = 1$ in both the ground and the excited states. If $\phi^R = 1.6$, then for n = 0.5, eqn 34 becomes $k_{n=0.5} = (0.5)(0.385)k^{HH} + (0.5)(0.615)k^{HD} + (0.385)(0.5)k^{DH} + (0.5)(0.615)k^{DD}$. For methanol, ethanol, and water this value of the fractionation factor yields $k^{HD} = 4.88 \pm 0.16 \times 10^9\ s^{-1}$, $3.71 \pm 0.13 \times 10^9\ s^{-1}$, and $5.78 \pm 0.11 \times 10^9\ s^{-1}$, respectively.

Figure 18. (a) Ratio of tautomerization rate of 7-azaindole in MeOH, k_o, to that in a mixture of protiated and deuterated methanol that is mole fraction, n, in MeOD, k_n. The open circles represent k_n/k_o vs n. The solid line through the data represents the fit assuming a two-proton process with $\phi^T = 0.62$. Directly above is plotted the straight line that would result from a one proton process, i.e., the average of k_o and k_1 weighted by the respective mole fractions of protiated and deuterated solvents [16]. The open squares represent $(k_n/k_o)^{1/2}$ vs n. The linearity of this plot verifies the two-proton process in methanol, assuming the validity of the Gross-Butler equation. (b) Similar to part (a) only here the rates are measured in EtOH and EtOD. These data are also consistent with a two-proton process with $\phi^T = 0.60$.

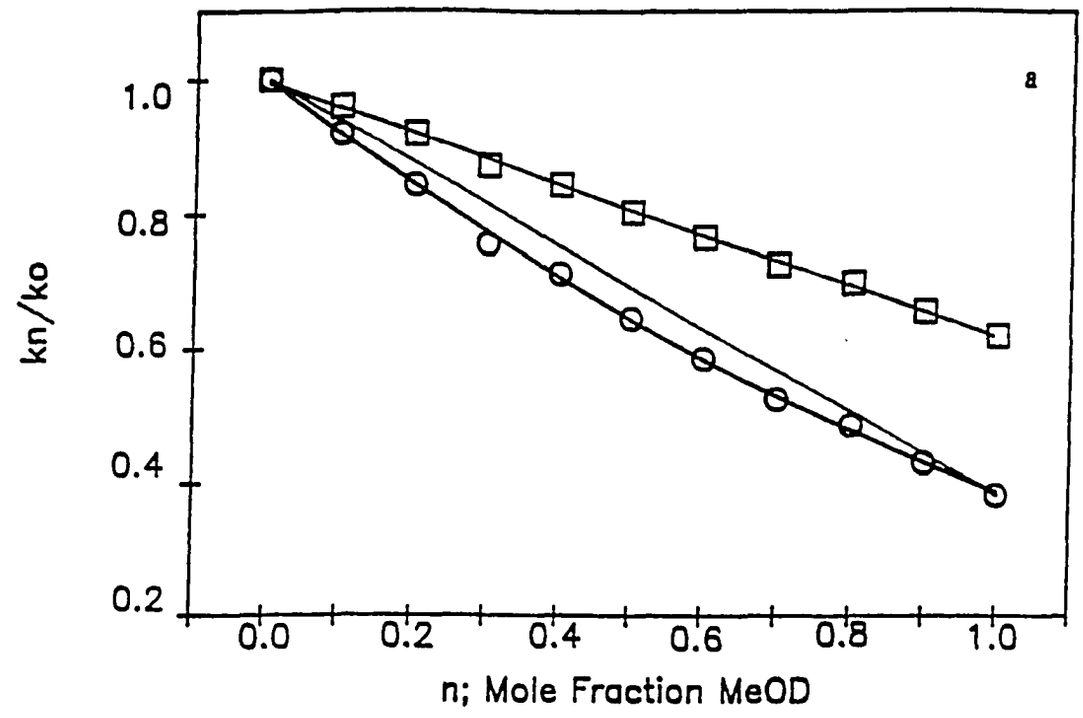
a
1.0
0.8
0.6
0.4
0.2
kn/ko
0.0
0.2
0.4
0.6
0.8
1.0
n; Mole Fraction MeOD

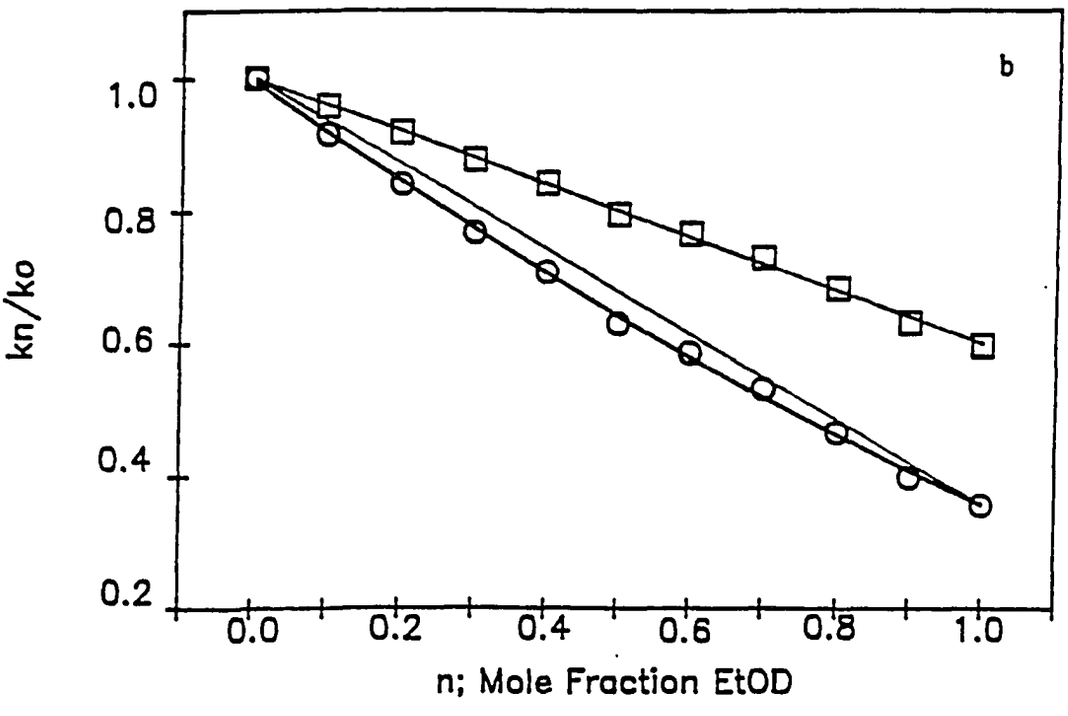
b
1.0
0.8
0.6
0.4
0.2
kn/ko
0.0
0.2
0.4
0.6
0.8
1.0
n; Mole Fraction EtOD

Figure 19. Proton inventory data for 7-azaindole in H_2O and D_2O at 20°C. The open circles represent k_n/k_o vs n. The pH at n=0 is 6.8. The solid line through these data represents the fit assuming a three proton process: $k_n/k_o = (1 - n + 0.48\ n)(1 - n + 0.69\ n)^2$. The straight line plotted directly above is the result expected for a one-proton process. The open triangles represent $(k_n/k_o)^{1/2}$ vs n. The solid line through the open triangles is only meant to guide the eye. This plot deviates significantly from the straight line just above it. Hence, the proton inventory data in water are different from those in the alcohols. Assuming the validity of the Gross-Butler equation, the water data are inconsistent with a two-proton process.

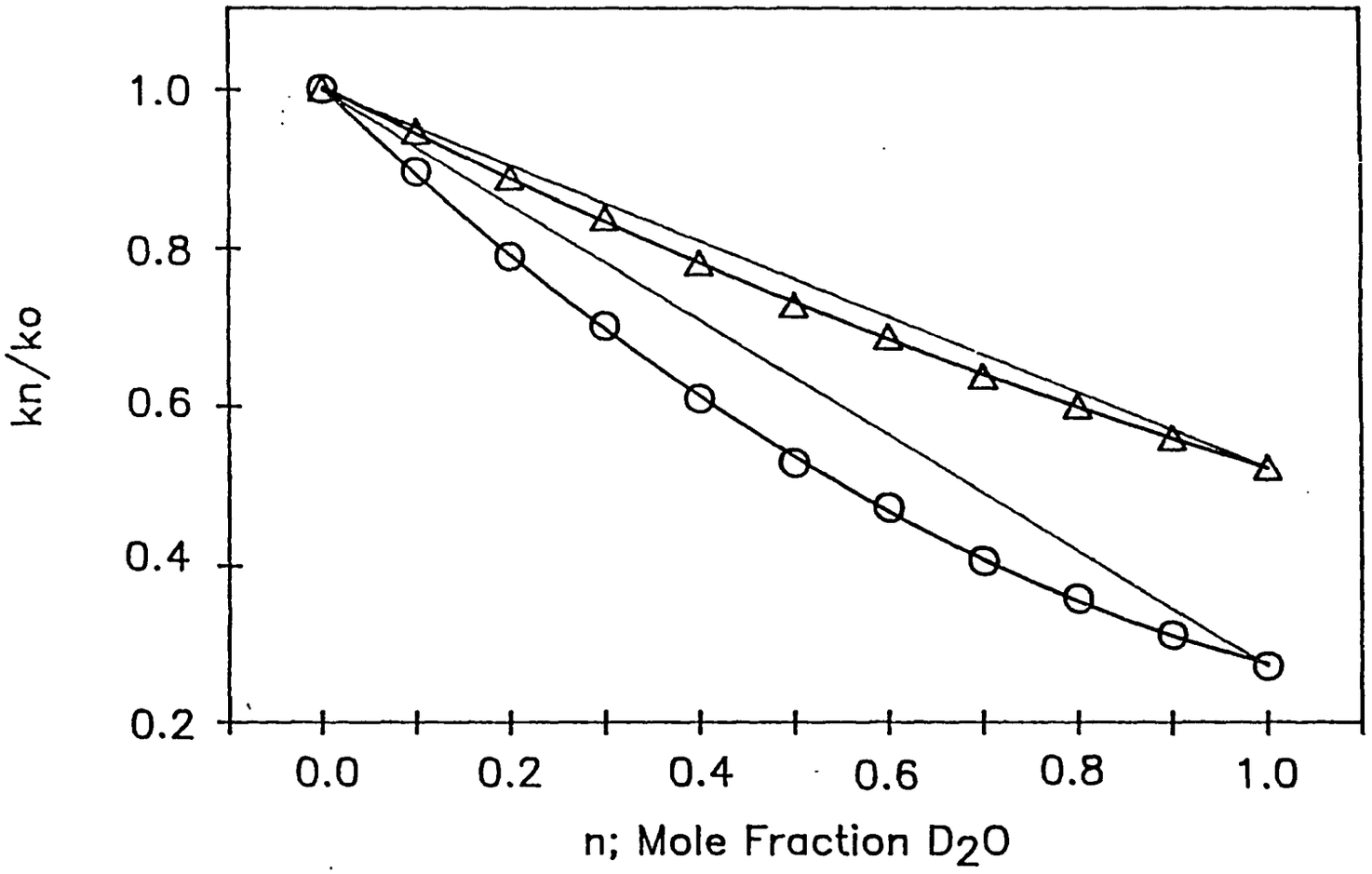
1.0
0.8
0.6
0.4
0.2
kn/ko
0.0
0.2
0.4
0.6
0.8
1.0
n; Mole Fraction D_2O

one proton is in flight during the rate-limiting step. References 91, 94, and 95 provide discussions and derivations of what has come to be called the Gross-Butler equation. This equation relates the rate of the process in the protiated solvent, k_o, to the rate in a solution of mole fraction n of the deuterated solvent and to all the protons in the reactant and transition states involved:

$$k_n = k_o \frac{\prod_i^{\nu} (1-n+n\phi_i^T)}{\prod_i^{\nu} (1-n+n\phi_i^R)} \simeq k_o \prod_i^{\nu} (1-n+n\phi_i^T) \qquad (1)$$

ν is the total number of protons involved. The $\phi^{T,R}$ are the fractionation factors in the transition and the reactant states, respectively. ϕ is the ratio of the preference in a site in a molecule for deuterium over protium relative to the preference for deuterium over protium in a solvent molecule [91,94,95]. In other words, ϕ is the equilibrium constant for the generalized reaction: XH + ROD $\rightleftharpoons$ XD + ROH. It is customary in most analyses to take ϕ^R = 1 for an NH or an OH site, as indicated above. For 7-azaindole, we suggest that ϕ^R = 1 is a reasonable approximation for N_1L (L = H,D) since ϕ^R = 0.92 for R_2N-L and ϕ^R = 0.97 for R_3N^+-L for water [91]. (These ϕ^R are for the ground state. In order to apply them directly to our problem, we must assume that the ϕ^R are identical in the excited state. We have considered this possibility elsewhere [18,89] and also discuss it below.)

We must also take into account that fractionation factors are often estimated for weak acids from the empirical equation $\Delta pK_a = 0.41 + 0.020pK_H$, where $\Delta pK_a = pK_D - pK_H$; and

from the relationship $\phi^R = l^3/(K_D/K_H)$, where l is the fractionation factor for the OH hydrogens of H_3O^+ and is equal to 0.69 [91,103]. If the excited-state species is long lived enough to establish a proton-transfer equilibrium, then the excited-state pK_H of N_1 is somewhere between 10 and 13 [89] (see Discussion) and ϕ^R lies between 1.3 and 1.6. Given, however, that the expression for ΔpK_a is approximately accurate [91] for only 70% of the compounds tabulated by Laughton and Robertson [131] and then only for pK values in the range of 3-10, we tentatively discuss our results using $\phi^R = 1$ for both the ground and the excited state. A more serious problem in the interpretation of the data using eqn 1 is the rate of ligand exchange with the solvent (see below). The downward bulging curves for 7-azaindole in methanol and ethanol (Figure 18) are both such that a plot of $(k_n/k_o)^{1/2}$ vs n yields a straight line. This result suggests that only two protons are involved in the excited-state tautomerization of 7-azaindole in alcohols. This result is also consistent with the "cyclic complex" of 7-azaindole and alcohol (Figure 16) that has been traditionally assumed to be required for the tautomerization to proceed.

ii. 7-Azaindole in Water

The downward bulging of the curve obtained for 7-azaindole in H_2O/D_2O mixtures suggests that more than one proton is involved in the transition state of the nonradiative deactivation process. Fitting k_n/k_o vs n to a quadratic model (i.e., a two-proton process) gives imaginary ϕ^T for the data in water ($\phi^T = 0.43 \pm i0.30$). Imaginary ϕ^T can be obtained when

there are two or more competing parallel pathways and if at least one of the transition states involves at least two protons [91]. We have, however, argued elsewhere [19,89,85] that not more than 20% of the 7-azaindole population in water is capable of executing double proton transfer and that this process can be observed only under conditions of sufficient wavelength and time resolution. In fact, double proton transfer of 7-azaindole in water is a minor nonradiative pathway compared to monophotonic ionization [19,104,105]. The failure of the quadratic model to fit the proton inventory data coupled with the previous evidence against the importance of excited-state tautomerization in water argue against a concerted two-proton process in this solvent. (If two protons are being transferred by 7-azaindole in water, they are not transferred concertedly between N_1 and N_7).

The data are consistent with an infinite number of protons involved in the transition state, whose ϕ^T are all very close to 1. For such a model ln k_n vs n is linear (Figure 20). The data are, however, also in agreement with any number of multi-proton mechanisms ($\nu>2$). For the sake of simplicity and because of experimental precedent with another system, we discuss the proton inventory data of 7-azaindole in water as a three-proton process. This three-proton process involves the abstraction of hydrogen from N_1 by a coordinated water molecule.

For the three-proton process shown in Figure 21, the data in Figure 19 yield an excellent fit to the equation $k_n/k_o = (1-n+0.48n)(1-n+0.69n)^2$. Furthermore, a plot of $(k_n/k_o)^{1/2}$ vs n does not yield a straight line, which is inconsistent with a concerted two-proton process as observed in the alcohols.

Figure 20. Plot of ln k_n vs n for the proton inventory data of 7-azaindole in water (Figure 3). The linear plot is consistent with an "infinite-proton" process [16]. Because the proton inventory data can be fit to a form that is identical with that observed in ribonuclease and because the details of these two systems are so similar (compare Figure 5 with those in refs. 16 and 17) we have chosen to interpret the data in terms of the more intuitive three-proton process discussed in the text.

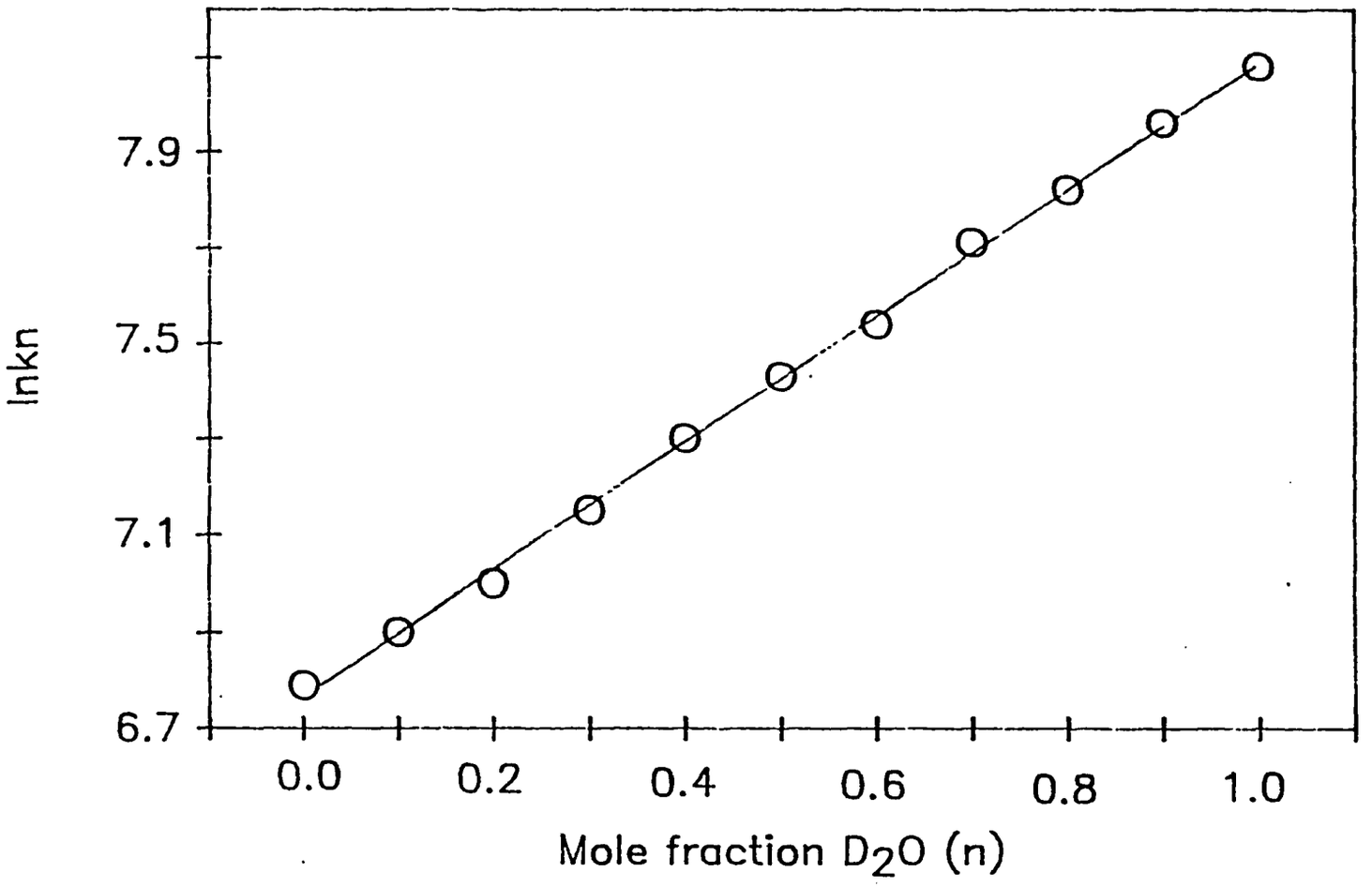
lnkn
7.9
7.5
7.1
6.7
0.0
0.2
0.4
0.6
0.8
1.0
Mole fraction D_2O (n)

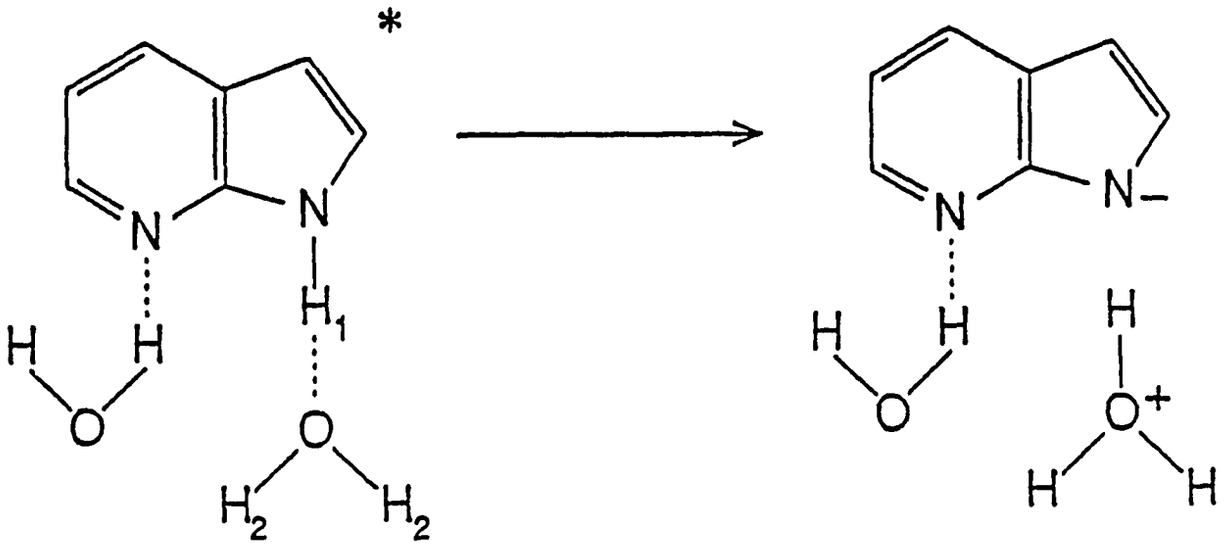

Figure 21. Nonradiative decay of the blocked species of 7-azaindole in water by means of deprotonation of N_1 by a water molecule. The blocked species of 7-azaindole is a complex that solvated by water in such a fashion that concerted, two-proton transfer as depicted in Figure 16 is frustrated.

Wang et al. observed essentially identical behavior in ribonuclease [92]. In this enzyme there is an isomerization between two of its conformations that are characterized by pK_a>8 and pK_a=6.1. These workers measured a solvent isotope effect of 4.7±0.4. Their proton inventory measurements were best described by the relation $k_n/k_o = (1-n+0.46n)(1-n+0.69n)^2$. They assigned the rate-limiting step in this isomerization to proton transfer to a water molecule from the protonated imidazole group of a histidine [91,92]. Within experimental error, the proton inventory rate parameters for 7-azaindole in water are identical to those for the isomerization of ribonuclease. In both cases, the shuttling of a proton from nitrogen to a water molecule is proposed to be the rate-determining step.

A fundamental assumption made in deriving the Gross-Butler equation is that the rate of H/D exchange between the solute and the solvent is significantly greater than the rate of proton transfer being investigated. In other words, the decay of the entire reactant population must be characterized by a rate constant that does not change with time; that is, first-order decay kinetics must be obtained. If solvent exchange is not rapid, then the observed decay is a superposition of the decays of the individual isotopically substituted species. For the case of 7-azaindole, at least four individual rate constants may be involved (see below). In practice, it is often very difficult to distinguish experimentally between genuine first-order kinetics, which are characterized by a single exponential decay time, and the superposition of several single-exponential decays characterized by different time constants. For this reason, we present several different methods of analyzing the 7-azaindole data (Figures 17-19, Tables 4-7).

In order for application of the Gross-Butler equation to the excited-state process of 7-azaindole to be valid, we require that 7-azaindole exchange its N_1 ligand with solvent protium or deuterium much faster than the actual tautomerization reaction discussed in the Introduction and depicted in Figure 16. Since the fluorescence lifetime of 7-azaindole in the solvents used here ranges from 140 to 900 ps, an appropriate time constant for ligand exchange with the solvent would be a few picoseconds. Such a rapid exchange seems unlikely. NMR measurements of ground-state indoles indicate that N_1 exchanges its proton on a time scale of seconds with the solvent [106]. The strong likelihood of slow exchange in the excited state requires us to consider the kinetics in more detail.

2. The Criteria for a Concerted Reaction

Figure 22 presents the four cases that may arise if two protons are involved in the deactivation of excited-state 7-azaindole. In Figure 22, the reactants and products are denoted A and D, respectively. B and C denote intermediates that would exist if the excited-state tautomerization of 7-azaindole proceeded by either the stepwise pathway ABD or ACD involving first the breaking of the N_1-H bond and then the formation of the N_7-H bond, and vice versa. Given such a reaction scheme, in order to demonstrate that the tautomerization is a concerted process, it is necessary, but not sufficient, to show that $k^{HD} = k^{DH}$ and that $k^{HD} = (k^{HH}k^{DD})^{1/2}$. This latter criterion is referred to as "the rule of the geometric mean" and was originally stated by Bigeleisen [107]. Use of the Gross-Butler equation (eqn 13) assumes the

Figure 22. Excited-state tautomerization reactions for each of the four cases of isotopic substitution considered in the text: $N_1HN_7\cdots H$, $N_1HN_7\cdots D$, $N_1DN_7\cdots H$, $N_1DN_7\cdots D$. For each case, the paths ABD and ACD represent stepwise processes where B and C are distinct intermediates. The criteria for a concerted reaction are discussed in the text.

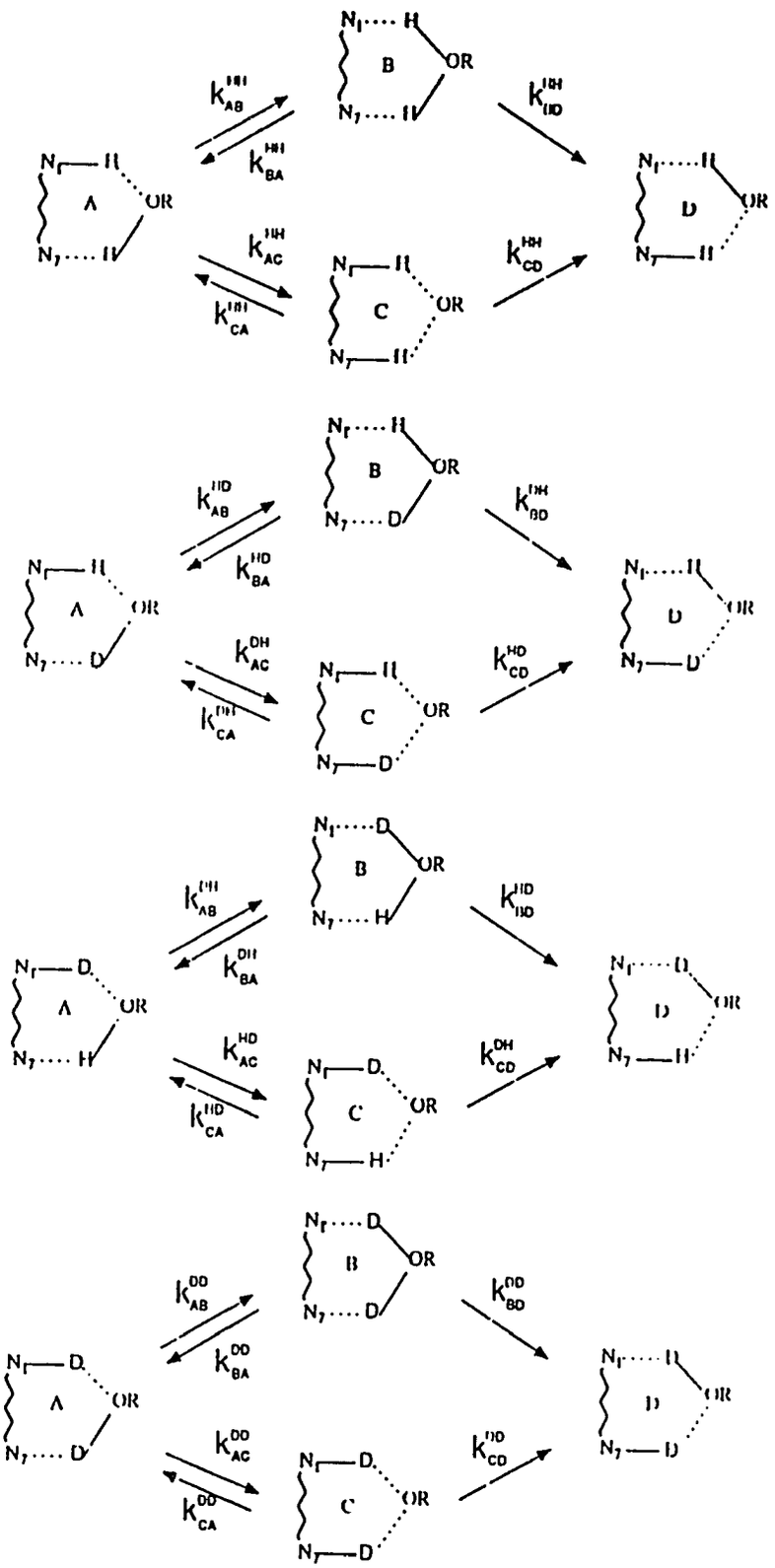

applicability of the rule of the geometric mean (see below). As we shall see, this relationship is very restrictive and demands that many requirements be satisfied. For the examples illustrated in Figure 22, one of the most important of these requirements is that for the concerted double-proton transfer, the secondary isotope effect at the N_7 (or N_1) site is equal to the primary isotope effect at the N_1 (or N_7) site. We shall also see that in order for this relationship to be satisfied, the reaction must be "symmetric"; that is, the rate constants for the decay of the intermediate B (or C) to A and D must be equal.

The significance of the rule of the geometric mean is that if there is a concerted reaction, both protons must be "in flight" in the transition state. Under these circumstances and in the absence of other effects such as tunneling [99], one thus expects the multiple sites in a single transition state to behave independently with respect to isotopic substitution [91, 94-98, 107]. It is useful in the course of this discussion to bear in mind Dewar's distinction between a concerted reaction and a synchronous reaction [108]. A concerted reaction takes place in a single kinetic step, with no reaction intermediate, where some of the changes in bonding take place to different extent in different parts of the reaction. A synchronous reaction is one where all the bond-making and bond-breaking processes take place at the same time and have all proceeded to the same extent in the transition state. Synchronicity is a much more restrictive condition than conceitedness [96, 97, 108]. We shall now show what conditions are required so that the above relations are satisfied so that the tautomerization may be regarded as a concerted reaction. Our discussion is similar to that of Limbach and coworkers [100, 102, 103].

If it is assumed that there is a fast equilibrium between the reactant and the first intermediate [100, 102, 103], then the rate of tautomerization (Figure 22) is given by [104]

$$k_{AD} = \frac{k_{AB}k_{BD}}{k_{BA} + k_{BD}} + \frac{k_{AC}k_{CD}}{k_{CA} + k_{CD}} \qquad (14)$$

where $k_{AD} = k_{ABD} + k_{ACD} = k_{ABD}\,(1 + \frac{k_{ACD}}{k_{ABD}})$. We define the ratio of the overall tautomerization rates to be $\frac{k_{ACD}}{k_{ABD}} = \beta$, for any degree of isotopic substitution. In order to obtain the desired kinetic relationships, it is necessary that:

$$\frac{k_{ACD}^{HH}}{k_{ABD}^{HH}} = \frac{k_{ACD}^{HD}}{k_{ABD}^{HD}} = \frac{k_{ACD}^{DH}}{k_{ABD}^{DH}} = \frac{k_{ACD}^{DD}}{k_{ABD}^{DD}} = \beta\,. \qquad (15)$$

For a given individual, single step represented by the generalized rate constant, k_{ij}, the first superscript H or D refers to the first ligand being transferred; the second superscript refers to the ligand that is not being transferred in the given single step. For the overall rate constants, k_{ABD} and k_{ACD}, the first superscript refers to solute isotopic substitution; and the second, to solvent isotopic substitution. This latter definition will be important when considering eqns 26-29.

The implications of the requirement that all the β are equal (eqn 15) are either that:

1. The intermediates B and C in the upper and the lower branches of a scheme for a particular case of isotopic substitution decay with the same rates to the reactants or the products. The remaining conditions will require that these rates are equal in each of the four schemes displayed in Figure 22. We define a parameter α, which is the ratio of the rates of formation of D and A from the intermediate B (or C). For a "symmetric reaction," where the potential surface of the reactants and the products is identical in the reaction coordinate, α =1. In addition, all the secondary isotope effects are equal to one another; and all the primary isotope effects are equal to one another.

2. Or all the secondary isotope effects are equal to the primary isotope effects, which are in turn all equal to one another.

That these conditions must be fulfilled can be seen from the following. Consider, for example, the left-most equality of eqn 3. The primary isotope effect on the step i→j is defined as [102] $P_{ij}^{H} = \frac{k_{ij}^{HH}}{k_{ij}^{DH}}$, $P_{ij}^{D} = \frac{k_{ij}^{HD}}{k_{ij}^{DD}}$. For the same step, i→j, the secondary isotope effect is defined as [102] $S_{ij}^{H} = \frac{k_{ij}^{HH}}{k_{ij}^{HD}}$, $S_{ij}^{D} = \frac{k_{ij}^{DH}}{k_{ij}^{DD}}$.

Thus from the above requirements, $S^H = S^D = S$ and $P^H = P^D = P$. It follows that

$$\frac{k_{ACD}^{HD}}{k_{ABD}^{HD}} = \frac{k_{AC}^{HH}\, k_{CD}^{HH}}{\frac{1}{P} k_{CA}^{HH} + \frac{1}{S} k_{CD}^{HH}} \frac{\frac{1}{S} k_{BA}^{HH} + \frac{1}{P} k_{BD}^{HH}}{k_{AB}^{HH}\, k_{BD}^{HH}}. \qquad (16)$$

If the intermediates C and B decay into the products and reactants with the same rate, then $k_{CA}^{HH} = k_{CD}^{HH}$ and $k_{BA}^{HH} = k_{BD}^{HH}$, and $\frac{k_{ACD}^{HH}}{k_{ABD}^{HH}} = \frac{k_{ACD}^{HD}}{k_{ABD}^{HD}}$. Alternatively, even if $k_{CA}^{HH} \neq k_{CD}^{HH}$ and $k_{BA}^{HH} \neq k_{BD}^{HH}$, if S = P, then we also obtain $\frac{k_{ACD}^{HH}}{k_{ABD}^{HH}} = \frac{k_{ACD}^{HD}}{k_{ABD}^{HD}}$.

In order to obtain the desired expression for the rule of the geometric mean, it will be shown that it is necessary that both conditions 1 and 2 above hold.

Given these definitions,

$$k_{AD}^{HH} = (1 + \beta)\frac{k_{AB}^{HH} k_{BD}^{HH}}{k_{BA}^{HH} + k_{BD}^{HH}} \qquad (17a)$$

$$k_{AD}^{HD} = (1 + \beta)\frac{k_{AB}^{HD} k_{BD}^{DH}}{k_{BA}^{HD} + k_{BD}^{DH}} \qquad (17b)$$

$$k_{AD}^{DH} = (1 + \beta)\frac{k_{AB}^{DH}k_{BD}^{HD}}{k_{BA}^{DH} + k_{BD}^{HD}} \tag{17c}$$

$$k_{AD}^{DD} = (1 + \beta)\frac{k_{AB}^{DD}k_{BD}^{DD}}{k_{BA}^{DD} + k_{BD}^{DD}}. \tag{17d}$$

It follows that

$$\frac{k_{AD}^{HD}}{k_{AD}^{HH}} = \frac{k_{AB}^{HD}k_{BD}^{DH}}{k_{AB}^{HH}k_{BD}^{HH}}\left(\frac{k_{BA}^{HH} + k_{BD}^{HH}}{k_{BA}^{HD} + k_{BD}^{DH}}\right). \tag{18}$$

For the rest of this discussion i,j = A, B, D (that is, only the upper branches in Figure 22 are considered) and $i \neq j$.

We may now write eqn 18 (since $\alpha = \frac{k_{BA}^{HH}}{k_{BD}^{HH}}$) as

$$\frac{k_{AD}^{HD}}{k_{AD}^{HH}} = (S_{AB}^{H})^{-1}(P_{BD}^{H})^{-1}\ \frac{1 + \frac{k_{BD}^{HH}}{k_{BA}^{HH}}}{\frac{k_{BA}^{HD}}{k_{BA}^{HH}} + \frac{k_{BD}^{DH}}{k_{BA}^{HH}}} = (S_{AB}^{H})^{-1}(P_{BD}^{H})^{-1}\ \frac{1 + \alpha^{-1}}{(S_{BA}^{H})^{-1} + (\alpha P_{BD}^{H})^{-1}} \tag{19a}$$

and similarly

$$\frac{k_{AD}^{DH}}{k_{AD}^{HH}} = (P_{AB}^{H})^{-1}(S_{BD}^{H})^{-1} \quad \frac{1 + \alpha^{-1}}{(P_{BA}^{H})^{-1} + (\alpha S_{BD}^{H})^{-1}} \tag{19b}$$

$$\frac{k_{AD}^{HH}}{k_{AD}^{DD}} = (S_{AB}^{H})(P_{AB}^{D})(S_{BD}^{H})(P_{BD}^{D}) \frac{(P_{BA}^{D})^{-1}+(\alpha P_{BA}^{D})^{-1}}{(S_{BA}^{H}) + (\alpha^{-1}S_{BA}^{H})} \tag{19c}$$

$$\frac{k_{AD}^{DH}}{k_{AD}^{DD}} = (S_{AB}^{H})(P_{BD}^{D}) \frac{1 + \alpha^{-1}}{(S_{BA}^{D}) + (\alpha^{-1}P_{BD}^{D})} \tag{19d}$$

These equations present two extreme possibilities.

First, if all the secondary isotope effects are equal to one, then eqns 19a and 19b become

$$\frac{k_{AD}^{HD}}{k_{AD}^{HH}} = \frac{1 + \alpha^{-1}}{(P_{BD}^{H}) + \alpha^{-1}} \tag{20a}$$

$$\frac{k_{AD}^{DH}}{k_{AD}^{HH}} = \frac{1 + \alpha^{-1}}{1 + \alpha^{-1}(P_{AB}^{H})}. \tag{20b}$$

Under these conditions, when $\alpha = 1$ ($k_{AD}^{HD} = k_{AD}^{DH}$) and if $P_{AB}^{H} = P_{BA}^{H}$,

$$\frac{k_{AD}^{HD}}{k_{AD}^{HH}} = \frac{k_{AD}^{DH}}{k_{AD}^{HH}} = \frac{2}{1 + (P^{H})}. \qquad (21a)$$

Similarly,

$$\frac{k_{AD}^{DH}}{k_{AD}^{DD}} = \frac{k_{AD}^{HD}}{k_{AD}^{DD}} = \frac{2}{1 + (P^{D})^{-1}} \qquad (21b)$$

From eqn 19c, $\frac{k_{AD}^{HH}}{k_{AD}^{DD}} = P_{BD}^{D} = P^{D}$, which substituted into eqn 21b yields

$$k_{AD}^{HD} = k_{AD}^{DH} = \frac{2k_{AD}^{DD}}{1 + \frac{k_{AD}^{DD}}{k_{AD}^{HH}}}. \qquad (22)$$

This is equivalent to the result obtained by Limbach and coworkers [100,101]. As they point out, the above equation clearly contravenes the rule of the geometric mean and is suggestive of a step-wise rather than a concerted process.

Second, if $\alpha = 1$, $S^{H} = S^{D} = S$, and $P^{H} = P^{D} = P$, then from eqn 19a,

$$\frac{k_{AD}^{HD}}{k_{AD}^{HH}} = \frac{2P^{-1}\,S^{-1}}{P^{-1} + S^{-1}} \qquad (23)$$

and from eqn 19c, $\frac{k_{AD}^{HH}}{k_{AD}^{DD}} = P \cdot S$, which upon substitution into eqn 23 yields

$$\frac{k_{AD}^{HD}}{k_{AD}^{DD}} = \frac{2}{S^{-1} + P^{-1}}. \tag{24}$$

For the concerted tautomerization, the secondary isotope effect is equal to the primary isotope effect (S = P), and we obtain from eqns 23 and 24

$$\frac{k^{HD}}{k^{HH}} = \frac{k^{DD}}{k^{HD}}. \tag{25}$$

Determination of the Individual Rate Constants, k^{HH}, k^{HD}, k^{DH}, k^{DD}

Formally, the excited-state tautomerization of 7-azaindole (N_1H) with alcohols or water (ROH) can be considered to be a biomolecular reaction. In pure protiated solvent,

$$\frac{d[N_1H]}{dt} = -k^{HH'}[N_1H]\ [ROH] = -k^{HH}[N_1H], \tag{26}$$

where $k^{HH} = k^{HH'}[ROH]$ and the measured lifetime is $\tau_F^{HH} = 1/k^{HH}$. In pure deuterated solvent,

$$\frac{d[N_1D]}{dt} = -k^{DD'}[N_1D]\ [ROD] = -k^{DD}[N_1D], \qquad (27)$$

where $k^{DD} = k^{DD'}[ROD]$ and the measured lifetime is $\tau_F^{DD} = 1/k^{DD}$.

For mixed solvents, ROH/ROD, we must consider the decay of at least four different species $N_1HN_7\cdots H$, $N_1HN_7\cdots D$, $N_1DN_7\cdots H$, $N_1DN_7\cdots D$ characterized by the overall biomolecular rate constants $k^{HH'}$, $k^{HD'}$, $k^{HD'}$, $k^{DD'}$. These rate constants refer to the sum of k_{ABD} and k_{ACD}, as mentioned earlier. Similarly, the significance of the superscripts is different from that when individual steps are being considered (see above). If n is the mole fraction of the deuterated solvent, [ROD] = n[ROL], [ROH] = (1 - n)[ROL], and [ROL] = [ROH] + [ROD], where L is H or D. The decay of both species where N_1 is bound to H is thus

$$\frac{d[N_1H]}{dt} = -k^{HH'}[N_1H]\ [ROH] - k^{HD'}[N_1H]\ [ROD]$$

$$= -\{(1 - n)k^{HH'}[ROL] + nk^{HD'}[ROL]\}[N_1H] = -\{(1 - n)k^{HH} + nk^{HD}\}[N_1H], \qquad (28)$$

where as above we have introduced the pseudo first-order rate constants. For the two species where N_1 is bound to D,

$$\frac{d[N_1D]}{dt} = -\{(1 - n)k^{DH} + nk^{DD}\}[N_1D]. \qquad (29)$$

Eqns 28 and 29 do not depend on which ligand is at N_7 and therefore do not assume

the presence of a cyclic complex (Figure 16), whose formation has been proposed to be necessary for the excited-state tautomerization (see below). We assume that the proton exchange rate for N_1L is much smaller than $1/\tau_F$, the inverse of the fluorescence lifetime, and we then can apply the following treatment. If in the ground state, the fractionation factor, $\phi^R = 1$, then $[N_1H]/[N_1D] = [ROH]/[ROD]$. The rate of decay for protiated 7-azaindole (N_1H) may then be written as

$$\frac{d[N_1H]}{dt} = -k_1[N_1H], \text{ where } k_1 = k^{HH} + (k^{HD} - k^{HH})n. \qquad (30)$$

Similarly,

$$\frac{d[N_1D]}{dt} = -k_2[N_1D], \text{ where } k_2 = k^{DH} + (k^{DD} - k^{DH})n. \qquad (31)$$

The assumption that proton exchange is slow requires that the fluorescence decay curves, F(t), be fit to a sum of two exponentials:

$$F(t) = A_1\exp(-k_1t) + A_2\exp(-k_2t). \qquad (32)$$

The ratio of the preexponential factors, A_1/A_2, is known from the solvent composition and the assumed value of ϕ^R. These parameters may thus be fixed during the fit, which yields k_1 and k_2. Since k^{HH} and k^{DD} are known from the experiments in the pure solvents, k^{HD} and k^{DH} may be obtained independently as demonstrated in Figures 23 and 24. We have assumed that for all cases of isotopic substitution the radiative rate is the same [89].

Another method of analyzing the data involves fitting (or force fitting) the data to a

Figure 23. (a) k_1 vs (1 - n) for MeOH/MeOD mixtures. (b) k_2 vs n for MeOH/MeOD mixtures. n is the mole fraction of the deuterated solvent. The slopes and intercepts of these plots permit the determination of k^{HD} and k^{DH}. See text.

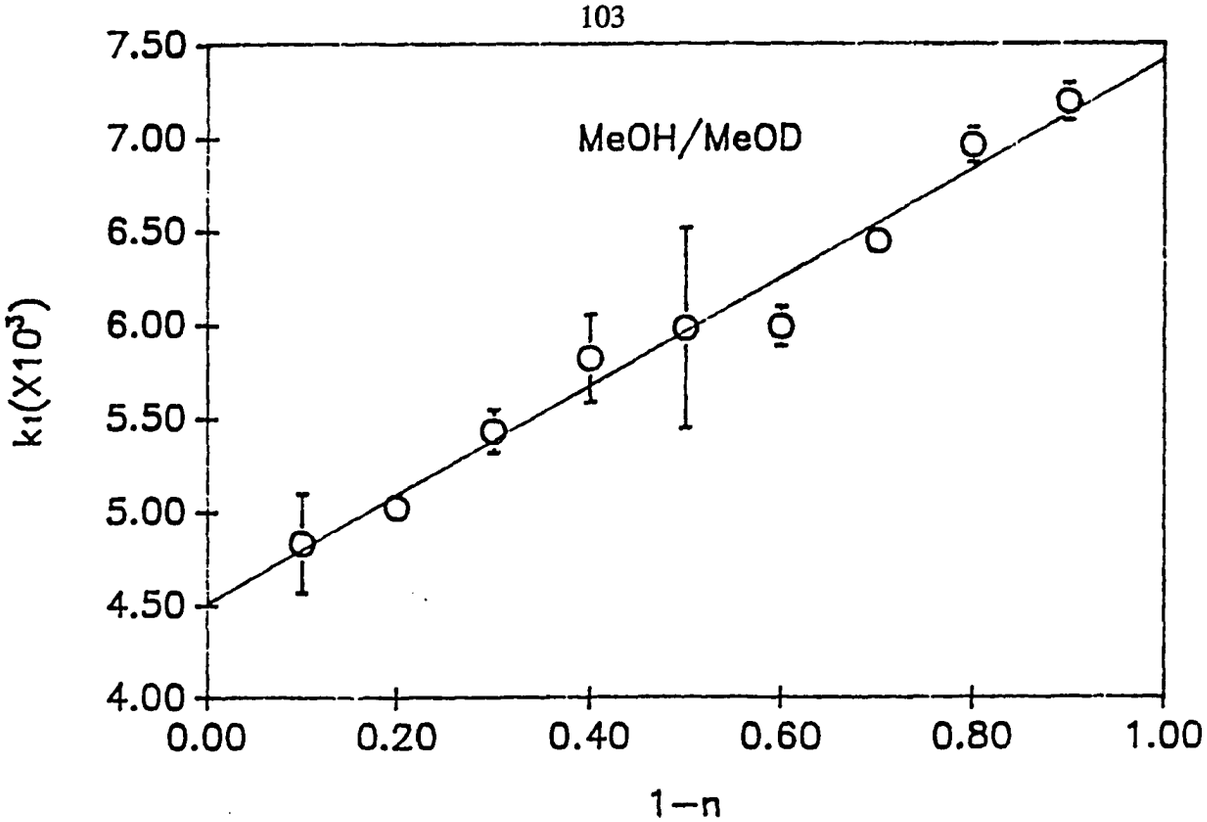
MeOH/MeOD
k1(X10³)
7.50
7.00
6.50
6.00
5.50
5.00
4.50
4.00
0.00
0.20
0.40
0.60
0.80
1.00
1−n

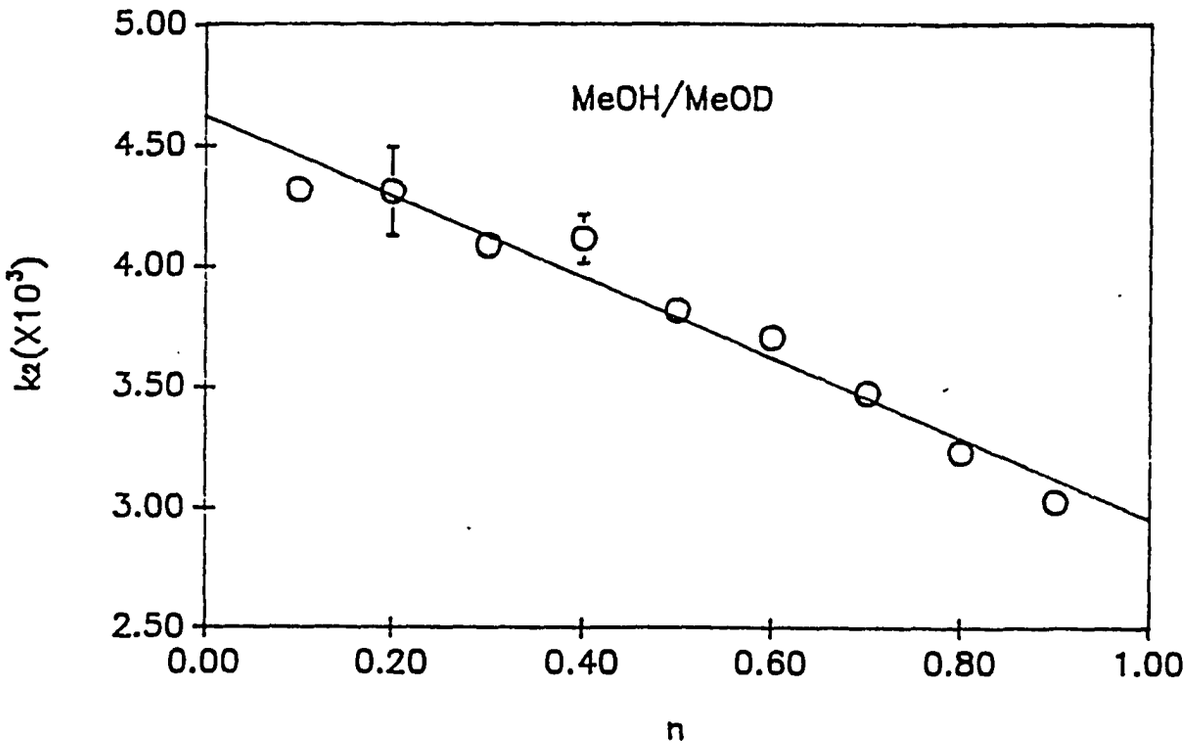
MeOH/MeOD
k2(X10³)
5.00
4.50
4.00
3.50
3.00
2.50
0.00
0.20
0.40
0.60
0.80
1.00
n

Figure 24. (a) k_1 vs (1 - n) for EtOH/EtOD mixtures. (b) k_2 vs n for EtOH/EtOD mixtures. n is the mole fraction of the deuterated solvent. The slopes and intercepts of these plots permit the determination of k^{HD} and k^{DH}. See text.

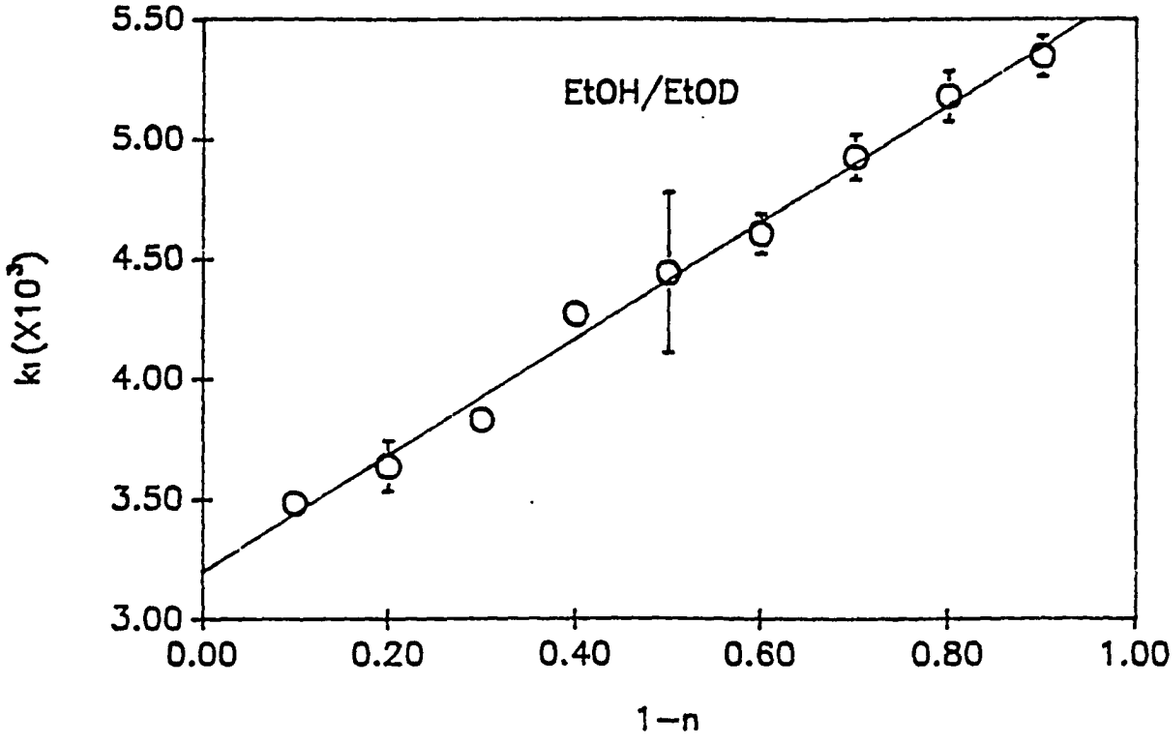
EtOH/EtOD
5.50
5.00
4.50
4.00
3.50
3.00
0.00
0.20
0.40
0.60
0.80
1.00
k1(X10³)
1−n

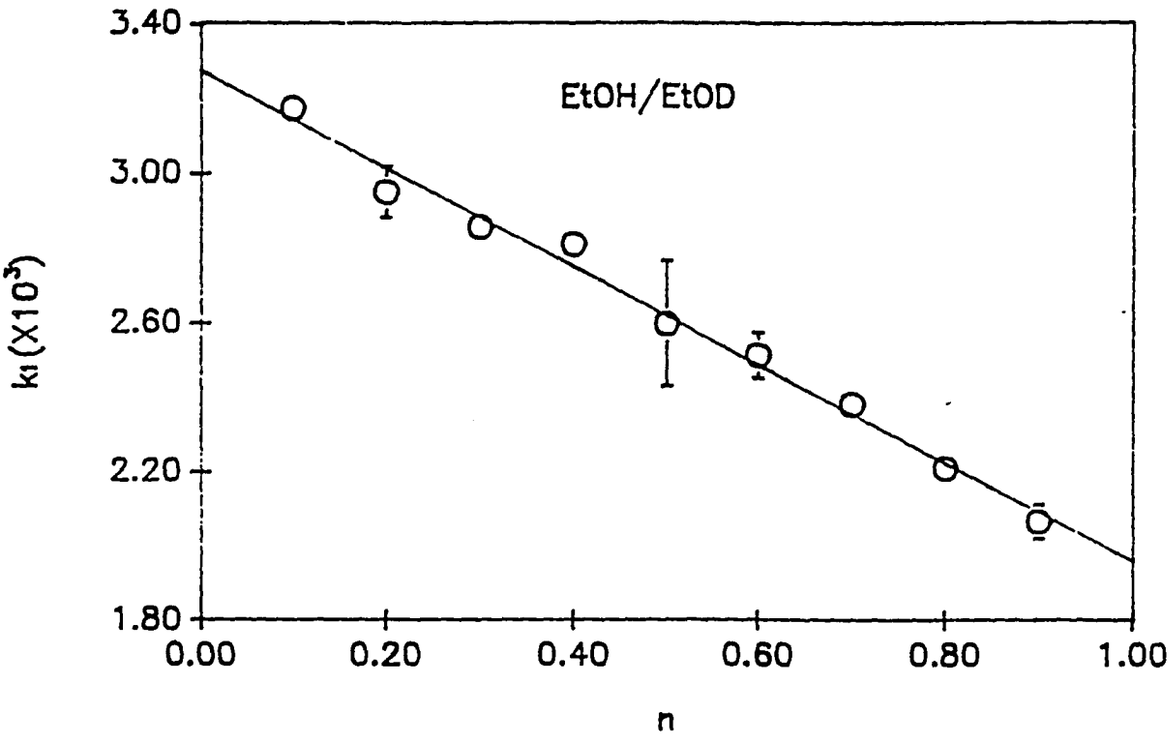
EtOH/EtOD
3.40
3.00
2.60
2.20
1.80
0.00
0.20
0.40
0.60
0.80
1.00
k1(X10³)
n

single exponential decay. Even if proton exchange is slow compared to the fluorescence lifetime, we can define an apparent first-order rate constant for the decay of the entire 7-azaindole population at time zero, $k_n(t = 0)$, where $k_n(t = 0)[N_1L] = k_1(1\text{-}n)[N_1L] + k_2n[N_1L]$. More specifically, if proton exchange is slow, the measured time constant for fluorescence decay is time dependent, $\tau_F = 1/k_n(t)$, and the decay of the excited state population is, if $k^{HD} = k^{DH}$,

$$\exp[-k_n(t)t] = (1 - n)^2\exp(-k^{HH}t) + 2(1 - n)n\exp(-k^{HD}t) + n^2\exp(-k^{DD}t). \qquad (33)$$

The prefactors in the above expression are a result of the assumption that $\phi^R = 1$. Differentiating this equation with respect to t and setting t = 0 yields

$$k_n(t = 0) = (1 - n)^2k^{HH} + 2(1 - n)nk^{HD} + n^2k^{DD}. \qquad (34)$$

Using eqn 34, k^{HD} may be extracted from a knowledge of the fluorescence lifetime, $1/k_n$, the lifetimes in the fully protonated and deuterated solvents, $1/k^{HH}$ and $1/k^{DD}$, and the mole fraction of deuterated solvent, n.

If we assume

$$\frac{k^{HD}}{k^{HH}} = \frac{k^{DD}}{k^{HD}} = \phi^T \text{ and that } \frac{k^{DD}}{k^{HH}} = \phi^{T^2}, \qquad (35)$$

which actually are the requirements of the rule of the geometric mean[95,97].

Substitution of eqn 23 into eqn 22 yields

$$k_n(t = 0) = k^{HH}(1 - n + \phi^T n)^2, \quad (36)$$

which is formally equivalent to the Gross-Butler equation (eqn 13) and is identical to it in the limit of fast exchange. Table 7 summarizes the results of these analyses and indicates that the rule of the geometric mean is satisfied for methanol and ethanol, but not for water, assuming $\phi^R = 1$ (see above and notes to Table 7).

3. The Nonradiative Process in 7-Azaindole and the Mechanism of Double proton-Transfer process

Glasser and Lami [110] and Wallace and coworkers [111] have discussed the importance of fission of the NH bond as a nonradiative process in gas phase indole. Barkley and coworkers [112] have performed detailed investigations of the deuterium isotope effect on the photophysics of tryptophan, indole, and some of their derivatives. They have proposed at least six different mechanisms to explain the isotope effect ranging from photoionization, hydride transfer from the NH, proton transfer from the solvent to the ring, solvent mediated NH exchange, tautomerization resulting in NH abstraction, and exciplex formation.

We propose that the isotope effect observed in indole derivatives can be rationalized

by the same mechanism that we illustrate for 7-azaindole in Figure 6. We suggest that in indole this process is much less efficient because there is no N_7 nitrogen coordinated with a solvent proton. Such an interaction could establish a partial positive charge on N_7 that would help to stabilize the negative charge generated on N_1. Proton inventory experiments on indole could in principle help to sort out the numerous nonradiative mechanisms catalogued above for indole. Even with the excellent precision afforded by our experimental system, we have not, however, undertaken such experiments because the solvent isotope effect for indole is only 1.3 [89]. Schowen has noted [94] that for an isotope effect of 1.5, to distinguish between a one- and a two-proton process precision in the data of 1% is required. To distinguish between a two- and a three-proton process, precision of 0.4% is required.

We must comment on the origin of the isotope effect. In large part because of the rapid (1.4 ps) tautomerization observed in dimers of 7-azaindole [60], the tautomerization of dilute solutions of 7-azaindole in alcohols has been discussed in terms of a two-step process [62-64, 89]. The first step involves obtaining the correct solvation of the solute by the alcohol; the second step, double-proton transfer. The interpretation of our isotopic substitution experiments depends on whether the two-step model is appropriate and, if it is, whether the solvation step is slow, fast, or comparable to tautomerization. If the rate-limiting step in the double-proton transfer reaction is the formation of the cyclic complex, then the isotope effects we discuss above require reinterpretation. Figure 27 presents a plot of the time constant for excited-state proton transfer in 7-azaindole at 20°C against pK_{auto} for a wide range of solvents. K_{auto} is the equilibrium constant for autoprotolysis and characterizes both

the proton accepting and proton donating abilities of a solvent (S) for the reaction: $2SH \leftrightharpoons SH_2^+ + S^-$ [30]. The correlation is exceptionally good, especially when one considers that previous correlations attempted between the proton transfer times and viscosity or polarity ($E_T(30)$) are strongly dependent upon the molecular structure of the solvent (e.g., primary as opposed to secondary alcohols or polyalcohols or water) and in general are quite scattered [63,84]. The liner free energy relation presented in Figure 3, however, comprises very disparate kinds of solvents. Even water fits well into this relationship. This correlation is consistent with the requirement of a cyclic solute-solvent complex for excited-state tautomerization and with the proton-transfer event being the rate-limiting step. The larger the autoprotolys is constant (the smaller the pK_{auto}), the easier it is for the solvent to accept a proton from N_1 and to donate a proton to N_7. In addition, dimers of 7-azaindole may not be an appropriate paradigm for the tautomerization of the 7-azaindole-alcohol complex. For example, Fuke and Kaya [113] observe that in supersonic jets the rate of excited-state double-proton transfer of 7-azaindole dimers is 10^{12} s^{-1} while in dimers of 1-azacarbazole and in complexes of 7-azaindole with 1-azacarbazole the rate is 10^9 s^{-1}. The reduction in rate by a factor of 10^3 is initially surprising given the very similar hydrogen bonding in the three types of complexes. It is therefore most likely premature to assume that tautomerization in a 7-azaindole complex occurs as rapidly as in a 7-azaindole dimer. Fuke and Kaya suggest that detailed considerations of the coupling of proton motion with intermolecular vibrational motion are required in order to predict the rate of such tautomerization reactions [113].

Figure 25. Correlation of the time constant for excited-state tautomerization of 7-azaindole in various solvents with pK_{auto} [31]. (1) 2,2,2-trifluoroethanol [13]; (2) water; (3) ethylene glycol; (4) methanol; (5) propylene glycol; (6) ethanol; (7) 1-propanol [13]; (8) 1-pentanol [13]; (9) 1-butanol; (10) 2-propanol [13]; (11) 2-methyl-1-propanol [13]; (12) 2-butanol [13]; (13) 2-methyl-2-propanol [13]. For 2,2,2-trifluoroethanol, the pK_{auto} is estimated from the pK_a.

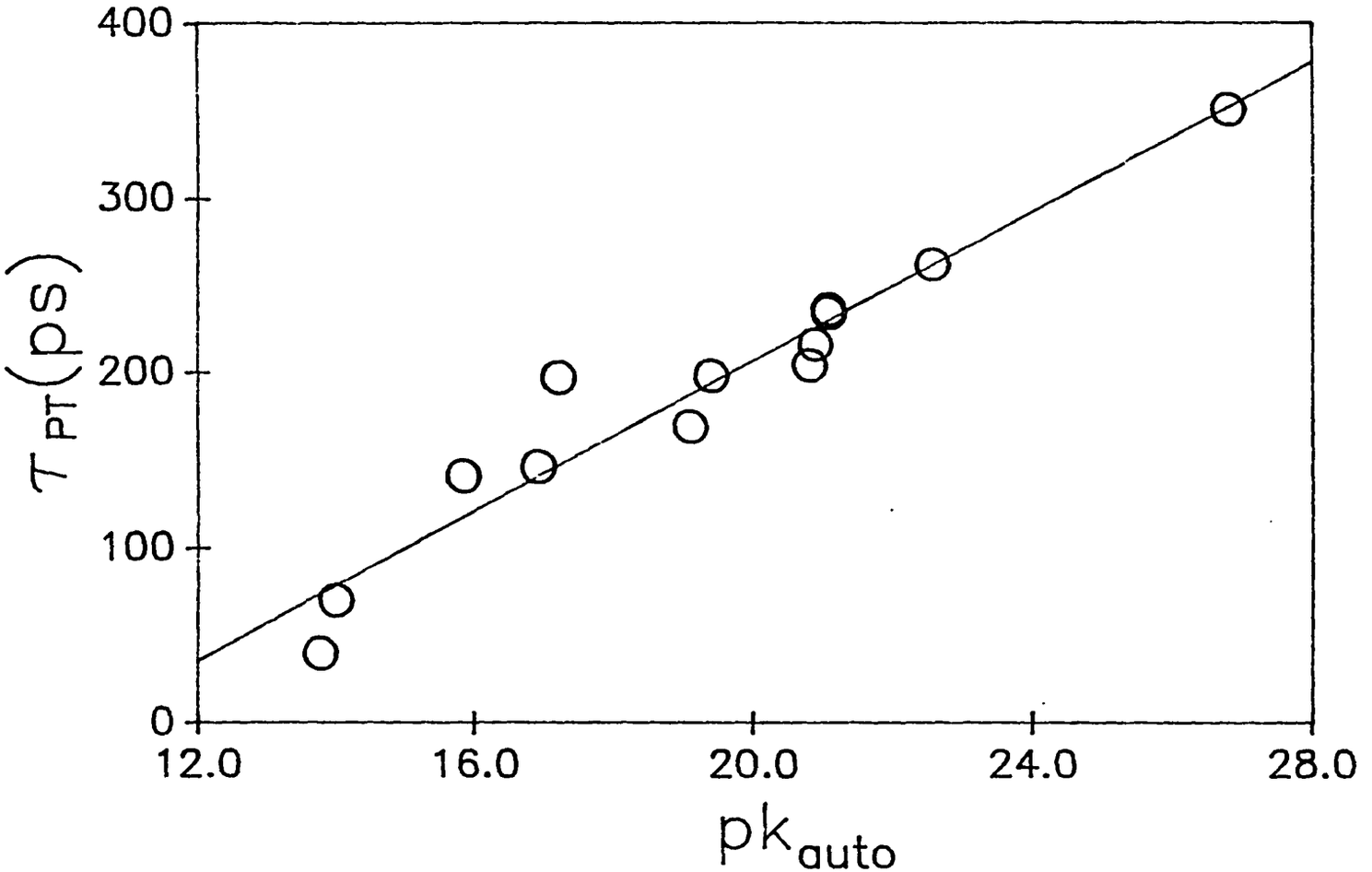
400
300
200
100
0
τ_{PT} (ps)
12.0
16.0
20.0
24.0
28.0
pk_{auto}

E. Conclusions

1. We have performed the first application of the proton inventory technique to an excited-state process. The data suggest that the excited-state tautomerization of 7-azaindole in alcohols proceeds by a concerted, two-proton process that is consistent with the structure of the cyclic solute solvent complex presented in Figure 16. (There is the possibility that the double proton transfer involving N_1 and N_7 occurs via two different alcohol molecules that interact with each other sufficiently strongly to effect the concerted reaction.)

2. Interpretation of the data in terms of a concerted process is based on several methods of analysis. All of these methods require as a criterion of conceitedness that the rule of the geometric mean be fulfilled. The first, employing the Gross-Butler equation, is the most easily interpreted but assumes rapid ligand exchange between solute and solvent, which may not be likely. Alternatively, explicit consideration of the double-proton transfer reaction in terms of nominally stepwise processes taking into account the four possible permutations of isotopic substitution (Figure 22) provides a similar result. The rule of the geometric mean is shown to hold within experimental error for methanol and ethanol, but not for water (Table 7). We note, however, that the rule of the geometric mean is satisfied only in very special cases: namely that the reaction be symmetrical ($\alpha = 1$) and that S = P. There are also instances where the reaction is concerted but the rule of the geometric mean breaks down because of contributions

from tunnelling [994, 100]. Finally, the rule of the geometric mean may apply even for a stepwise process, if it proceeds by what Limbach and coworkers refer to as a "compressed state" [102]--an orientation where the reactants are so near that the barrier to proton transfer vanishes [102]. (In such a state there is no difference between a concerted and a stepwise transfer.)

3. Further evidence is provided to support the model (Figure 20) of 7-azaindole being solvated by water in such a way that double-proton transfer--as it occurs in alcohols--is negligible [19, 89, 90].

4. Proton inventory experiments of 7-azaindole in H_2O/D_2O mixtures are interpreted in terms of a three-proton process involving the hydrogen of N_1 and the two protons of a water molecule coordinated to it. These data are consistent with measurements of proton abstraction in ribonuclease [94, 95].

5. The poor correlation of the proton-transfer rate with solvent viscosity [63], the results of proton inventory experiments [116], and the excellent correlation of proton-transfer rate with pK_{auto} for a wide variety of solvents including water suggest that for 7-azaindole in dilute solutions the actual tautomerization and not the formation of a cyclic complex is the rate-limiting step in the proton transfer reaction.

CHAPTER V SOLVATION OF 7-AZAINDOLE IN ALCOHOL AND WATER

A. Introduction

We have shown that only a minor amount (≤ 20%) of the population of 7-azaindole in water undergoes excited-state tautomerization [89]. The majority of the population exists in a "blocked" state of solvation that frustrates excited-state tautomerization (Figure 16). A similar picture has been proposed by Chou et al. [85], but these workers do not resolve the small fraction of solute molecules capable of tautomerization. Measurements of the nonradiative processes of 7-azaindole in solvent mixtures containing varying amounts of the protiated and the deuterated solvent (the proton inventory) further indicate that the majority of the excited-state population of 7-azaindole in water decays by a process other than double-proton transfer (Chapter IV).

In alcohols, the emission spectral of 7-azaindole is bimodal. The normal band can always be fit to a double exponential with the long lifetime component only accounting a small amount at room temperature [18]. The central question then becomes whether solvation of 7-azaindole by alcohols is fundamentally different than by water. In this chapter we argue that the small contribution (at room temperature) of the longer-lived fluorescence lifetime component of 7-azaindole in alcohols that has been dismissed as an impurity [18, 64, 67] actually results from a small population of solute molecules that are solvated such that tautomerization is hindered.

B. Experimental

7-Azaindole (Sigma) was either purified by flash chromatography as described in chapter III or used without further purification. The significantly increased purity of our 7-azaindole preparation is supported by the superimposability of the excitation spectra obtained at three different wavelengths in water at neutral pH (Figure 6).

Time-correlated, single-photon counting measurements were performed in order to determine fluorescence lifetimes. Only emission from the normal band was collected: 320 nm < λ_{em} < 460 nm. Fluorescence decays were fit to a sum of two exponentials: $F(t) = A_1\exp(-t/\tau_1) + A_2\exp(-t/\tau_2)$. The first component is attributed to the excited-state tautomerization reaction; the second component, to the long-lived species that has heretofore been attributed to an impurity but which we now discuss in terms of a differently solvated species.

C. Results

Figure 26 presents the fluorescence decay of the normal band of 7-azaindole in butanol as a function of temperature. At ambient temperature, The fluorescence decay of the normal band of 7-azaindole (unpurified or purified) in alcohols can always be fit well by a single exponential plus a small amount of longer-lived component. When, however, the fluorescence lifetime of unpurified or purified 7-azaindole in water is obtained (at neutral pH

and using a relatively wide bandpass), it is always well characterized by a single exponential with a decay time of 910 ps at 20°C.

Figure 27 presents the amplitudes of the longer-lived component of 7-azaindole in three alcohols as a function of temperature. The amplitude of the longer-lived component increases as the temperature decreases. For example in butanol, the amplitude of the longer-lived component increases from about 5% at 20°C to about 44% at -6°C. This result renders the assignment of this component in alcohols to an impurity untenable. Assuming that the extinction coefficient and the radiative rate of a putative impurity are relatively insensitive to temperature, such a large change in the amplitude is unlikely. The longer-lived component is predominant in polyalcohols even at 20°C: ethylene glycol, $F(t) = 0.31\exp(-t/141ps) + 0.69\exp(-t/461ps)$; and propylene glycol, $F(t) = 0.31\exp(-t/197ps) + 0.69\exp(-t/816ps)$. (The shapes of the normal and tautomer bands in butanol do not change between 22°C and -2°C. Furthermore, the dominant presence of the longer-lived component at ambient temperature in the polyalcohols indicates that its observation in the normal alcohols is not an artifact arising from a shift, for example, in the spectrum of the tautomer band.)

Based on these results we conclude that trace impurities in the commercial preparations of 7-azaindole do not impair our consideration of its photophysics and that the resulting fluorescence decays contain no detectable information concerning the impurities. If this is indeed the case, it is important to understand the origin of the longer-lived component observed in the fluorescence decay of 7-azaindole in alcohols.

Figure 26. Fluorescence decay of the normal band of 7-azaindole in 1-butanol as a function of temperature (320 nm < λ_{em} < 460 nm): (a) F(t) = 0.95exp(-t/234 ps) + 0.05exp(-t/1818 ps); (b) F(t) = 0.92exp(-t/280 ps) + 0.08exp(-t/1406 ps); (c) F(t) = 0.83exp(-t/329 ps) + 0.17exp(-t/916 ps); (d) F(t) = 0.56exp(-t/360 ps) + 0.44exp(-t/760 ps). Because the full-scale time base for the photon-counting measurement is only three nanoseconds, an accurate determination of the duration of the longer-lived component is difficult, especially if it comprises only a few percent of the fluorescence decay.

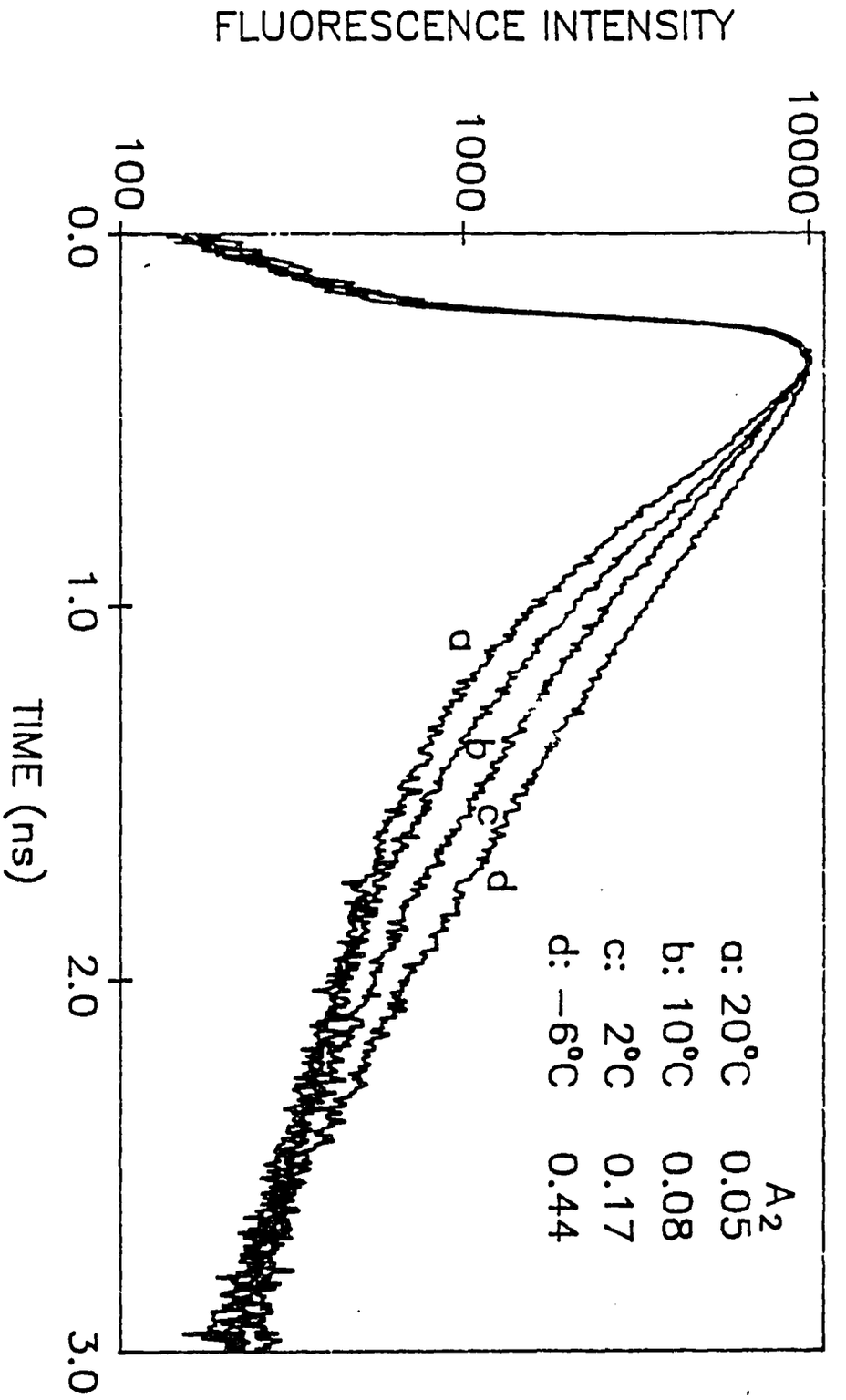
FLUORESCENCE INTENSITY
100
1000
10000
0.0
1.0
2.0
3.0
TIME (ns)
a
b
c
d
A2
a: 20°C 0.05
b: 10°C 0.08
c: 2°C 0.17
d: −6°C 0.44

Figure 27. Amplitude (A_2) of the long-lived component of the fluorescence decay of the normal band of 7-azaindole in 1-butanol, methanol, and deuterated methanol as a function of temperature. We interpret the different behavior between MeOH and MeOD to reflect an isotope effect in the ground state solvation process.

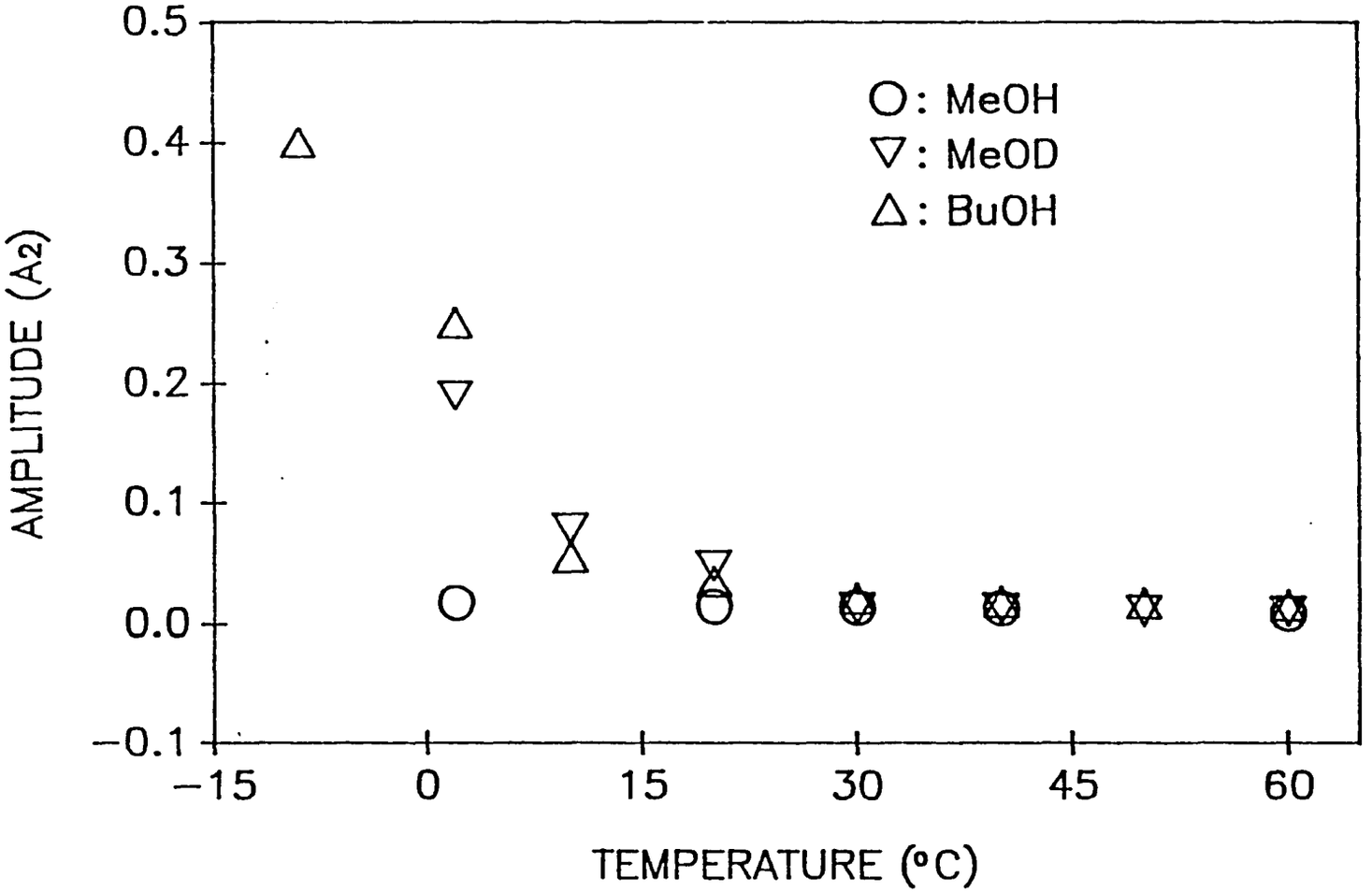
0.5
0.4
0.3
0.2
0.1
0.0
−0.1
AMPLITUDE (A2)
−15
0
15
30
45
60
TEMPERATURE (°C)
○: MeOH
▽: MeOD
△: BuOH

D. Discussion

1. Temperature Dependence of the Amplitude of the Longer-lived Fluorescence Decay Component in Alcohols: Comparisons with Aqueous Solvation

In order to understand the solvation of 7-azaindole by alcohols, it is most useful to consider the problem in the light of what is known concerning aqueous solvation of 7-azaindole. Unlike the bimodal fluorescence spectrum of 7-azaindole in alcohols, the fluorescence spectrum in water has a single maximum at 386 nm. Two extreme explanations of this phenomenon have appeared: either the entire population of 7-azaindole in water tautomerizes [84] or the entire population is prohibited from tautomerization [85]. We have investigated this problem by studying 7-azaindole and its 1- and 7-methylated derivatives over the entire pH range with time-resolved fluorescence spectroscopy [89]. We conclude that solvation of 7-azaindole by water lies between these two extremes. That the fluorescence lifetime of 7-azaindole is not dominated by excited-state tautomerization is demonstrated by the observation of three distinct fluorescence lifetimes: ~ 70 ps, the decay time of the normal species; 1100 ps, the decay time of the tautomer; and 910 ps, the decay time of the "blocked" solute in which tautomerization is prohibited. These results have been summarized in chapter III.

By analogy with the types of solvation possible in water, we propose that the long-

lived fluorescence decay component observed for 7-azaindole in alcohols can be understood by attributing it to a "blocked" form of solvation. In other words, alcohols and water represent different extremes of solvation; but in neither case is excited-state tautomerization completely permitted or completely prohibited.

In the ground state, the two different solvation configurations, "cyclic" (C) and "blocked" (B), are in equilibrium; and their relative populations are determined by the temperature dependent equilibrium constant. The estimated time for conversion between C anb B (10 ns in water) precludes interconversion of these species in the excited state owing to the subnanosecond lifetimes of the normal species. At ambient temperature in normal alcohols, the rapid (several hundred picosecond) decay component comprises the majority of the fluorescence decay and is attributable to excited-state tautomerization; the second, longer-lived, component comprises only a few percent of the total fluorescence intensity. As the temperature is lowered, however, the amplitude of this component becomes much more significant. As we noted above, in ethylene glycol and propylene glycol, the longer-lived component comprises more than 60% of the fluorescence decay at 20°C. The dependence of the amplitude of the longer-lived component is most easily interpreted in terms of the ground-state, standard free energy difference between C and B. Upon light absorption, the relative proportions of C and B are projected into the excited state; but because of the slow interconversion between the two solvation states, only C effects proton transfer.

Similar states of solvation have been observed in argon matrices at 10 K for the much studied model of excited-state proton transfer, 3-hydroxyflavone [127]. The groups of

Barbara [128, 129], Kasha [130], and Harris [131] have discussed the importance of intermolecular hydrogen bonding, cyclic hydrogen-bonded complexes with one solvent molecule, and doubly solvated hydrogen bonded complexes. Strandjord and Barbara [128] have argued that the absence of a significant correlation between viscosity and the excited-state proton transfer rate argues against desolvation of the doubly hydrogen bonded species to form the appropriate intermediate as being an important step in the proton-transfer reaction. McMorrow and Kasha have suggested that such a doubly hydrogen-bonded species would be much longer lived than the excited state of 3-hydroxyflavone and hence could not participate in the proton-transfer reaction [130]. On the other hand, it has recently been suggested that in 3-hydroxyflavone the solvation dynamics of the doubly hydrogen-bonded species may be rapid enough to participate in excited-state proton transfer [131].

E. Conclusions

The longer-lived component of the fluorescence decay of the normal band of 7-azaindole in alcohols is attributed to a blocked state of solvation, which prohibits excited-state tautomerization. This component is present even in carefully purified preparations of 7-azaindole and can not be assigned to an impurity. The presence of this component indicates that the solvation of 7-azaindole by alcohols and by water is much more similar than has previously been realized. Alcohols and water both afford cyclic and blocked solvation states, but in different proportions.

CHAPTER VI THE SINGLE EXPONENTIAL DECAY OF 7-AZATRYPTOPHAN IN WATER

A. Introduction

We have discussed the solvation and dynamics of 7-azaindole and 7-azatryptophan in water. As an optical probe to study protein structure and motion, 7-azatryptophan has several advantage over tryptophan. The most important is 7-azatryptophan is single exponential decay over most of the pH scale. Tryptophan has been study for tens of years. Several models have been proposed to explain the property of nonexponential decay in water. Among them, different conformer combining with different charge transfer rate to side chain gives reasonable and acceptable explanations. We would expect that 7-azatryptophan exist similar conformer in water as tryptophan, here is the question: why tryptophan is nonexponential decay while 7-azatryptophan is single?

In a previous chapter, we have shown that, like 7-azaindole, in water the fluorescence decay of 7-azatryptophan was dominated by the blocked species with a time constant of 780 ps. We also proposed the proton transfer of N1-H as a possible nonradiative decay process. From these studies, two possible reasons accounting for the single exponential decay of 7-azatryptophan might come to our mind: in 7-azatryptophan, the charge-transfer process to side chain is deactivated (the emission spectra of 7-azatryptophan red shift 50nm comparing to tryptophan) or there is a more efficient process that competes with it (like proton transfer).

It is conceivable that in some cases 7-azatryptophan may have a nonexponential fluorescence decay when it is incorporated into the protein matrix. If a situation should arise in which 7-azatryptophan does exhibit a nonexponential fluorescence decay in a protein, we shall know with certainty that this decay is due to the protein matrix and we shall not be obliged to take into account the contributions from the adjacent peptide bonds as we are with tryptophan.

B. Experimental

Time-correlated single-photon counting measurements were performed with the apparatus described above. The dryness of the polar aprotic solvents was determined by the absence of a tautomer band in the fluorescence spectrum of 7-azaindole and 7-azatryptophan. The similarity of the absorption spectra of 7-azaindole and 7-azatryptophan in these solvents indicates that aggregation of 7-azatryptophan does not occur. The nonexponential fluorescence decay of tryptophan is considered here in terms of a finite number of conformational isomers [1-7], but distributions of isomers have been discussed as well [114].

C. Theory of Electron Transfer

Electron transfer, one of the simplest of chemical events, profoundly effects chemical reactivity by inverting normal electron densities in an electron donor-acceptor path, thus

activating previously inaccessible reaction models. The interest of this process is not surprising considering its ubiquity in chemistry, physics, and biology. The theoretical developments include semiclassical extensions of the classical formalism as well as quantum-mechanical treatments deriving from application of Fermi's golden rule. Despite the multitude of formalism, there is general agreement now that the crux of the electron transfer problem is the change in equilibrium nuclear configuration that occurs when a molecule or ion gains or loses an electron.

1. Marcus Theory

Assuming there is very little spatial overlap of the electronic orbital of the two reacting molecules in the activated complex, Marcus presented his landmark paper on electron-transfer reaction in solution [135]. The reaction scheme of Marcus' theory is indeed simple:

$$A + B \underset{k_{-1}}{\overset{k_1}{\rightleftharpoons}} X^* \qquad (37)$$

$$X^* \underset{k_{-2}}{\overset{k_2}{\rightleftharpoons}} X \qquad (38)$$

$$X \xrightarrow{k_3} \text{products} \qquad (39)$$

When the reactants are near each other, a suitable solvent fluctuation can result in the state X^*. The state X^*, whose atomic configuration of the reacting pair and of the solvent is that of the activated complex, can either reform the reactants by disorganization of some of the oriented solvent molecules, or it can form the state X by an electronic transition. This new state has an atomic configuration as that of X^* but has an electronic configuration as that of the products. The pair of state X^* and X constitute the activated complex. If the electronic interaction between them were large, the formation of one from the other would be very rapid and one need then not speak of them separately. For electron-transfer, only a slight electronic interaction may be sufficient to couple the two molecules and permit it to occur. In the steady-state description, one finds that the overall rate constant is:

$$k_{bi} = k_1/[1+(1+k_{-2}/k_3)k_{-1}/k_2] \tag{40}$$

When the forward step in reaction eqn 38 is more probable:

$$k_{bi} \cong k_1 \tag{41}$$

Using nonequilibrium dielectric polarization theory [136], Marcus calculated the free energy of activation for an ion pair (A, B) near constant r, to reach the transition state with rigid inner coordination shell, gave the following familiar expression:

$$k_1 = Z \exp(-\Delta G^*/kT) \tag{42}$$

$$\Delta G^* = \frac{1}{4}(\Delta e)^2\left(\frac{1}{2a_1} + \frac{1}{2a_2} - \frac{1}{R}\right)\left(\frac{1}{\varepsilon_\infty} - \frac{1}{\varepsilon_o}\right) \qquad (43)$$

Where $\Delta e = e_A^R - e_A^P = -e_B^R + e_B^P$ is the charge transferred. a is the ionic radii. ε_∞, ε_o are high- and low-frequency solvent dielectric constant.

Later on, Marcus gave a more clear insight into the actual mechanism of the electron transfer [137] by the introduction of the potential energy surface described in Fig. 28. The treatment was extended so as to include changes in bonding property in the inner coordination shell in terms of statistical mechanism. Based on the assumption of (i) dielectric continuum model for solvent, (ii) harmonic forces in the inner coordination shell, (iii) spherical reactants, (iv) negligible correlation of fluctuation of coordinates inside and outside this shell in the activated complex, Marcus derived a parabolic expression for the free energy of activation $\Delta G^{\neq}$:

$$\Delta G^{\neq} = \frac{Z_1 Z_2 e^2 f}{D r_{12}} + \frac{\lambda}{4}\left(1 + \frac{\Delta G^{o'}}{\lambda}\right)^2 \qquad (44)$$

$$\Delta G^{o'} = \Delta G^o + (Z_1 - Z_2 - 1)\frac{e^2 f}{D_{12}} \qquad (45)$$

Where $\Delta G^{o'}$ is corrected standard free energy change of electron transfer step. $\lambda = \lambda_i + \lambda_{out}$, are bond and solvent reorganization energies (inner and outer). The resulting highly successful Marcus theory for the reaction rate constant k is a transition-sate theory description, in which the rate depends on the polar solvent free energetics but not on the solvent dynamics.

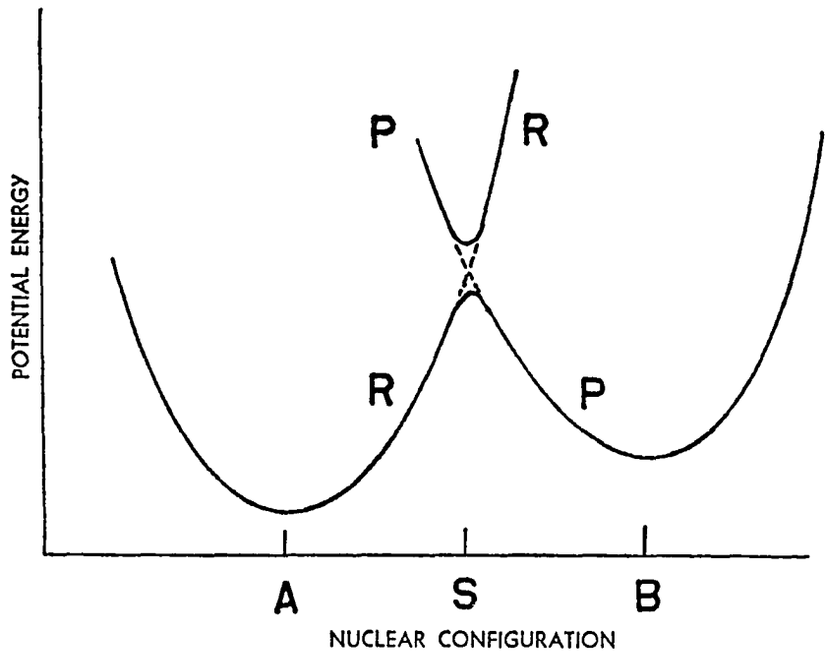

Figure 28. Profile of potential energy surface of reactants (R) and that of products (P), plotted versus nuclear configuration of all the atoms in the system. ---, surface for zero electronic interaction of the reacting species. —,adiabatic surface.

Probably the most fascinating prediction of the Marcus theory is the "inverted region" where the electron transfer rate constant decreases with the increasing driving force in the exothermic region. The first unambiguous experimental evidence for such a region was given by G. L. Closs and J. R. Miller [138].

2. Adiabatic and Nonadiabatic Process

Electron transfer reaction are generally categorized as being "adiabatic" or "nonadiabatic" process [139]. A simple qualitatively description can be made from Fig. 29 as follows: when the system passes the intersection region with high velocity, there is little time for electron transfer; when the velocity is low there is usually time. In the first case, the system will usually "jump" from the lower R surface to the upper R surface on the intersection region. In the second case, the system will usually remain on the lower solid "adiabatic" surface. When the system jumps from one solid "adiabatic" surface to the other on passing through the intersection region, the process of jumping is called a "Nonadiabatic act".

A good description of adiabatic and nonadiabatic reactions is given by Hans Frauenfelder and Peter G. Wolynes [140].

Consider two state s, q, if the matrix element V_{sq} connecting them is zero, the resulting diabatic energy curves (Fig. 29) cross each other. If V_{sq} is very large compared to the kinetic energy of nuclear motion, k_BT, the upper electronic state will be thermally

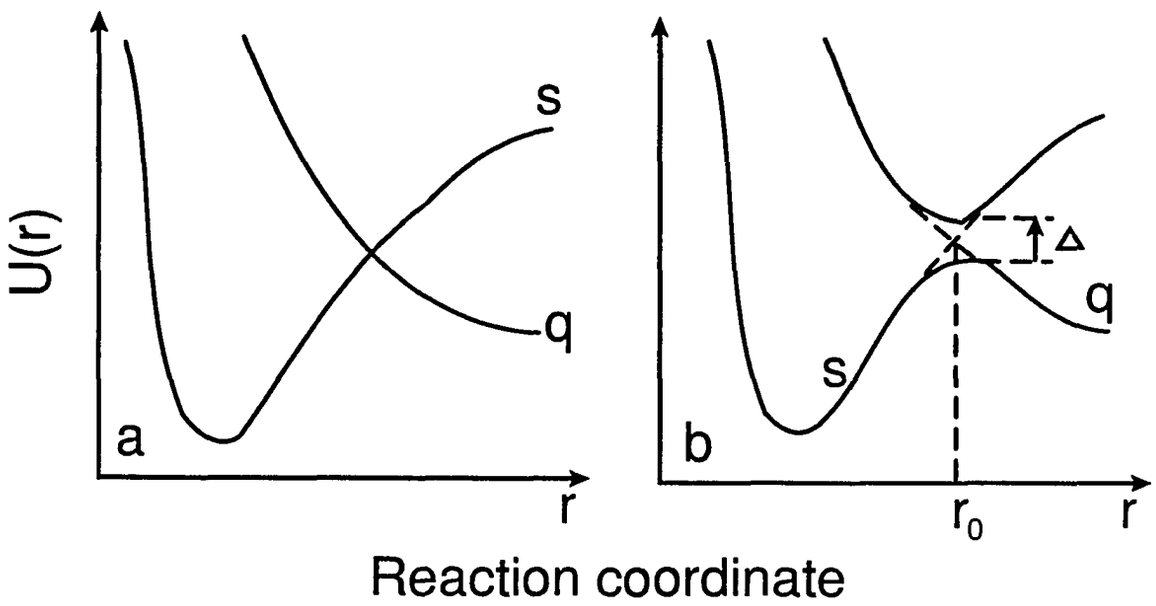

Figure 29. Schematic representation of the potential energy curves. (a) diabatic energy levels; (b) adiabatic energy levels.

inaccessible, the transition will stay on the lower adiabatic surface [Fig. 29].

When $\Delta < k_BT$, thermodynamics considerations alone do not determine whether the electronic states can change. Adiabaticity will depend on the relative time scale of electron and nuclear motion. Using the uncertainty relation, if the energy uncertainty of the system in the mixing region (Landau-Zener region) is small compared to the splitting $\Delta=2|V_{sq}|$, the transition will be adiabatic. The energy uncertainty is given by $\hbar/\tau_{LZ}$, τ_{LZ} is the time spent in the mixing region. The adiabaticity parameter γ_{LZ}, is defined as the ratio of the splitting Δ to the energy uncertainty:

$$\gamma_{LZ} = \frac{\Delta}{\hbar/\tau_{LZ}} = \frac{\Delta^2}{\hbar v|F_2-F_1|} \tag{46}$$

Where v is nuclear moving velocity, F_1, F_2 are the slopes of diabatic curves at the avoided crossing r_o.

If $\gamma_{LZ} >> 1$, the transition is adiabatic. If $\gamma_{LZ} < 1$, the probability P for electronic structure change on a single crossing is:

$$P = 1 - \exp(-\pi\gamma_{LZ}/2) \tag{47}$$

If $\gamma_{LZ} << 1$, the following expression is obtained:

$$P = \frac{\pi}{2}\frac{\Delta^2}{\hbar v|F_2-F_1|} \tag{48}$$

The probability is proportional to Δ^2, which is the hallmark of a highly nonadiabatic reaction.

Correspondingly, the adiabaticity will affect the reaction rate. For an adiabatic reaction, the simplest theory of rate coefficients is the transition state theory (TST). Its keystone is the assumption that a typical reactive trajectory crosses the barrier from reactant to product only once before being trapped for a very long time, later recrossings are unrelated:

$$k_{TST} = \frac{\omega}{2\pi} e^{-\Delta G^{\ddagger}/k_B T} \tag{49}$$

$\Delta G^{\ddagger}$ include the entropy contribution.

Transition state theory overestimates the rate coefficient. By considering the recrossing and dynamical effect, or friction, which is the effect of energy and momentum exchange on the reaction coordination, Kramers [141] realized that the rate coefficient should contain a transmission coefficient, κ which represents the fact that even when the system is poised at the transition state and is moving toward product, it will not necessarily get there. The fundamental results of Kramers are: at low friction the transmission factor is proportional and at high friction inversely proportional, to the friction coefficient. For nonadiabatic reaction, friction will also affect the rate by causing the system to spend more time in the transition region. The Landau-Zener theory represents an upper bound much like the one provided by TST for adiabatic reaction.

3. Electron Transfer Reaction

Generally, the activation-controlled rate constant can be written by: [37]

$$k_{act} = K_A K_n \nu_{eff} = K_A \nu_{eff} \exp\left(\frac{-\Delta G_n^{\ddagger}}{RT}\right) \qquad (50)$$

K_A is the stability constant of the precursor complex, ν_{eff} is electron-hopping frequency. There are a variety of formalisms--classical, semiclassical, and quantum mechanical--available for treating the activation and electron hopping events represented by the above equation. Marcus gave an excellent description in the classical formalism. When one consider nonadiabatic or nuclear tunneling effects, the simple Transition-State Theory implementation of eqn 50 must be modified. Using time-dependent perturbation theory (the golden rule approach), one has [37, 139]:

$$K_n \nu_{eff} = \frac{4\pi^2}{h Z_p} \sum_{v,w} \exp\left[-\frac{E_{pv}}{RT}\right] \sum_{w} |H_{pv,sw}|^2 \delta(E_{pv} - E_{sw} - \Delta E_o) \qquad (51)$$

Where E_{pv}, E_{sw} are vibronic energies of precursor and successor complex. $H_{pv,sw}$ is a vibronic matrix element:

$$H_{pv,sw} = \int X^{o}_{pv} H_{ps} X_{sw} dq \qquad (52)$$

Which can be factored (the Condon Approximation) into the product of a nuclear overlap integral and the electronic coupling electronic coupling element, H_{ps} (q).

The Dirac delta function can be evaluated by [142, 143]:

$$\delta(E_{pv} - E_{sw} - \Delta E_o) = \frac{2\pi}{h} \int_{-\infty}^{\infty} dt \exp(-it(E_{pv} - E_{sw} - \Delta E_o)) \qquad (53)$$

For the case of a single harmonic mode, a simple semiclassical theory (SCT) gives results identical with the quantum mechanical theory (QMT).

We know that the rates of electron transfer in solution are primarily determined by the configuration change accompanying the electron transfer, that is by the nuclear factors for the reaction. Sometime the electronic factors can become dominant when the reorganization barrier is reduced by the exothermicity of the reaction or when the reaction are kept far apart, for example, in biological systems or in frozen media. The electronic interaction can be represented by the electronic coupling element, H_{ps}, and can be calculated by choosing a suitable expression for the electronic basis and the Hamitonion. M. D. Newton [144] has given a detailed description of the nature of this interaction. Many procedures are available for evaluating the electronic coupling element such as ab initio molecular orbital calculations. The electronic interaction of the two redox centers decreases with increasing separation. John R. Miller [138] and Stefan Franzen et al. [145] have performed detail studies on distance dependence of electron-transfer reactions. The dependence on distance will be reflected mostly in the coupling matrix element, although the reorganization energy also shows a distance dependence.

The most common expression for the distance dependence of the electron-transfer rate can be derived from following eqn 54, which assumes an exponential decay of the wave function and the coupling matrix element:

$$H_{ps} = H^{o}_{ps} \exp[-\beta(R-R_o)/2] \qquad (54)$$

Here H^{o}_{ps} is the coupling matrix element for a donor-acceptor pair at van der Waals separation R_o, and β is a constant scaling the distance dependence. If the reorganization

energy was distance independent, an equivalent expression could be written for electron-transfer rate:

$$k = k_0 \exp[-\beta(R-R_0)] \tag{55}$$

The above two equation are right for a through-space mechanism.

4. The Role of the Solvent

Theoretical understanding of solution phase electron-transfer reactions with regard to the role played by solvent dynamics has progressed rapidly in the last ten years [146, 147]. A solvent can influence a chemical reaction in a number of ways. It can act in a static sense to change the energy of the reactants and products and exert a major influence on the free energy of activation $\Delta G^{\ddagger}$. It can also enter into the proceedings in a more dynamic way by exchanging energy and momentum with reacting species and by responding to their changing distributions of charge. The latter case is so-called dynamical solvent effects and will appear in the frequency factor of rate constant expression. As we know, the rate of decay of the reorganized medium is primarily determined by the solvent dynamics, specifically by the rate of reorientation of the solvent molecules. The latter, in turn, can be related to the frequency dependence of the dielectric constant of the medium and governed by a relaxation time. The dielectric function of many solvents is adequately represented by the phenomenological Debye form:

$$\varepsilon(\omega) = \varepsilon_\infty + \frac{\varepsilon_0 - \varepsilon_\infty}{1 + i\omega\tau_D} \tag{56}$$

Simple continuum models predict that solvents with this type of dielectric function have an exponential solvation response:

$$S(t) = \exp(-t/\tau_L) \tag{57}$$

τ_L is the so-called "longitudinal" relaxation time;

$$\tau_L = (\varepsilon_\infty/\varepsilon_0)\tau_D \tag{58}$$

Since reorganization of the solvent involves a change in polarization at constant change, it is reasonable to identify the relaxation time for this reorganization with τ_L, so solvation is indeed much faster than diffusion.

Dynamical solvent effects are expected to be observed only in reactions for which the dominant contribution to the activation energy comes from the solvent. In such cases, the energy of the reacting system is mainly a function of the solvent configuration. With this initial condition in mind, the dynamical solvent effect depends on the adiabatic or nonadiabatic character of the reaction.

When the coupling between reactant and product states in the ET process is weak, a appropriate nonadiabatic description, the probability for electron transfer is very low and ET is rate limiting; solvent dynamics do not dictate the overall rate.

The opposite extreme is the adiabatic limit. The ET reaction is treated in terms of nuclear (solvent) motion on a single potential energy surface, just as in "normal" chemical reaction. The ET rates in the adiabatic regime are predicted to be directly proportional to

solvation rates. Most theories of ET have thus far used Debye-type continuum models for the solvent, and they therefore predict $k \propto \tau_L$. More recently, the observed solvation time may be faster than the τ_L under some conditions [147]. A more general prediction of electron transfer might be $k \propto \langle\tau\rangle_{obs}$. $\langle\tau\rangle_{obs}$ is the experimentally observed solvation time.

D. Results

1. Spectroscopic Distinguishability of 7-Azatryptophan

An important feature of 7-azatryptophan that renders it preferable to tryptophan as an optical probe is its distinguishability in absorption and fluorescence spectra and its single-exponential fluorescence lifetime [17, 20, 89]. Recently, there have been reports suggesting that 5-hydroxytryptophan is a useful biological probe as well [115]. While in some cases 5-hydroxytryptophan may prove useful (if relatively long excitation wavelengths, ~320 nm, are employed), Figure 25 demonstrates that because its fluorescence spectrum and lifetime are similar to those of tryptophyl chromophores, it is much more difficult to distinguish from tryptophan than is 7-azatryptophan. This is due in large part to the 3.8-ns lifetime of 5-hydroxytryptophan, which is similar to that of the long component of tryptophan. Figure 30 indicates that in mixtures of 5-hydroxytryptophan and the tryptophyl chromophore, NATA, in a ratio as high as 1/10, the presence of 5-hydroxytryptophan cannot be discriminated from the mixture. This is demonstrated by the identical χ^2 values obtained from fits to single

exponential and double exponential functions. On the other hand, even when this ratio is as low as 1/40 in 7-azatryptophan, the 7-azatryptophan can be detected in the mixture.

2. pH Dependence of the Fluorescence Lifetime of 7-Azatryptophan

There are several states of ionization available for 7-azatryptophan in water. Like tryptophan, the cationic, zwitterionic, and anionic forms of the side chain may be present. We must, however, also take into account N_7, which we know to be titratable based on previous work [18, 89]. For 7-azaindole, the pK_a of N_7 is 4.5. Potentiometric titrations of 7-azatryptophan similar to those for 7-azaindole [18] indicate that its ground-state pK_a values are 2.70, 3.85, and 9.35. The pK_a values correspond to the following groups, respectively: $-CO_2H$; $-N_7-$; and $-NH_2$. Below pH 2, both the amino group and N_7 (as well as the acid group) are protonated, yielding a dication. When $2 < pH < 4$, three species can coexist in equilibrium: the dication mentioned above; the zwitterion protonated at N_7; and the zwitterion deprotonated at N_7 (the conventional zwitterion). From pH 4 to 9, the predominant form is the zwitterion. From pH 10 to 13, the anion predominates.

The dependence of the average fluorescence lifetime of 7-azatryptophan on pH is illustrated in Figure 26. For $pH < 4$, double-exponential fluorescence decay is observed. Above pH 4, the fluorescence lifetime is single exponential. Between pH 4 and 10, the lifetime is constant at ~780 ps. At $pH > 10$, the lifetime remains single exponential; but it decreases.

Figure 30. Spectroscopic distinguishability of 7-azatryptophan and 5-hydroxytryptophan with respect to tryptophyl absorption and emission at 20° C and neutral pH. In all cases, λ_{ex} = 305 nm and $\lambda_{em} \geq$ 335 nm. In water, the fluorescence maximum of 7-azatryptophan is 395 nm; that of 5-hydroxytryptophan, 340 nm. For each panel, (a) refers to 5HT/NATA mixtures; (b), to 7AT/NATA mixtures. Panels A, B, and C present the results of fitting the fluorescence decays of mixtures of 7-azatryptophan (7AT) or 5-hydroxytryptophan (5HT) and NATA. (A) [7AT]/[NATA] = [5HT]/[NATA] = 1/10. 5HT/NATA: single exponential fit, τ = 3240 ps, χ^2 = 1.32; double exponential fit, F(t) = 0.35 exp(-t/3220 ps) + 0.65 exp(-t/3250 ps), χ^2 = 1.32. 7AT/NATA: single exponential fit, χ^2 = 2390 ps, χ^2 = 20.0; double exponential fit, F(t) = 0.42 exp(-t/822 ps) + 0.58 exp(-t/3000 ps), χ^2 = 1.16. (B) [7AT]/[NATA] = [5HT]/[NATA] = 1/20. 5HT/NATA: single exponential fit, τ = 3200 ps, χ^2 = 1.29; double exponential fit, F(t) = 0.33 exp(-t/3220 ps) + 0.67 exp(-t/3190 ps), χ^2 = 1.30. 7AT/NATA: single exponential fit, τ = 2660 ps, χ^2 = 9.3; double exponential fit, F(t) = 0.24 exp(-t/736 ps) + 0.76 exp(-t/2950 ps), χ^2 = 1.19. (C) [7AT]/[NATA] = [5HT]/[NATA] = 1/40. 5HT/NATA: single exponential fit, τ = 3120 ps, χ^2 = 1.25; double exponential fit, F(t) = 0.48 exp(-t/3500 ps) + 0.52 exp(-t/2773 ps), χ^2 = 1.24. 7AT/NATA: single exponential fit, τ = 2760 ps, χ^2 = 4.1; double exponential fit, F(t) = 0.16 exp(-t/732 ps) + 0.84 exp(-t/2950 ps), χ^2 = 1.24.

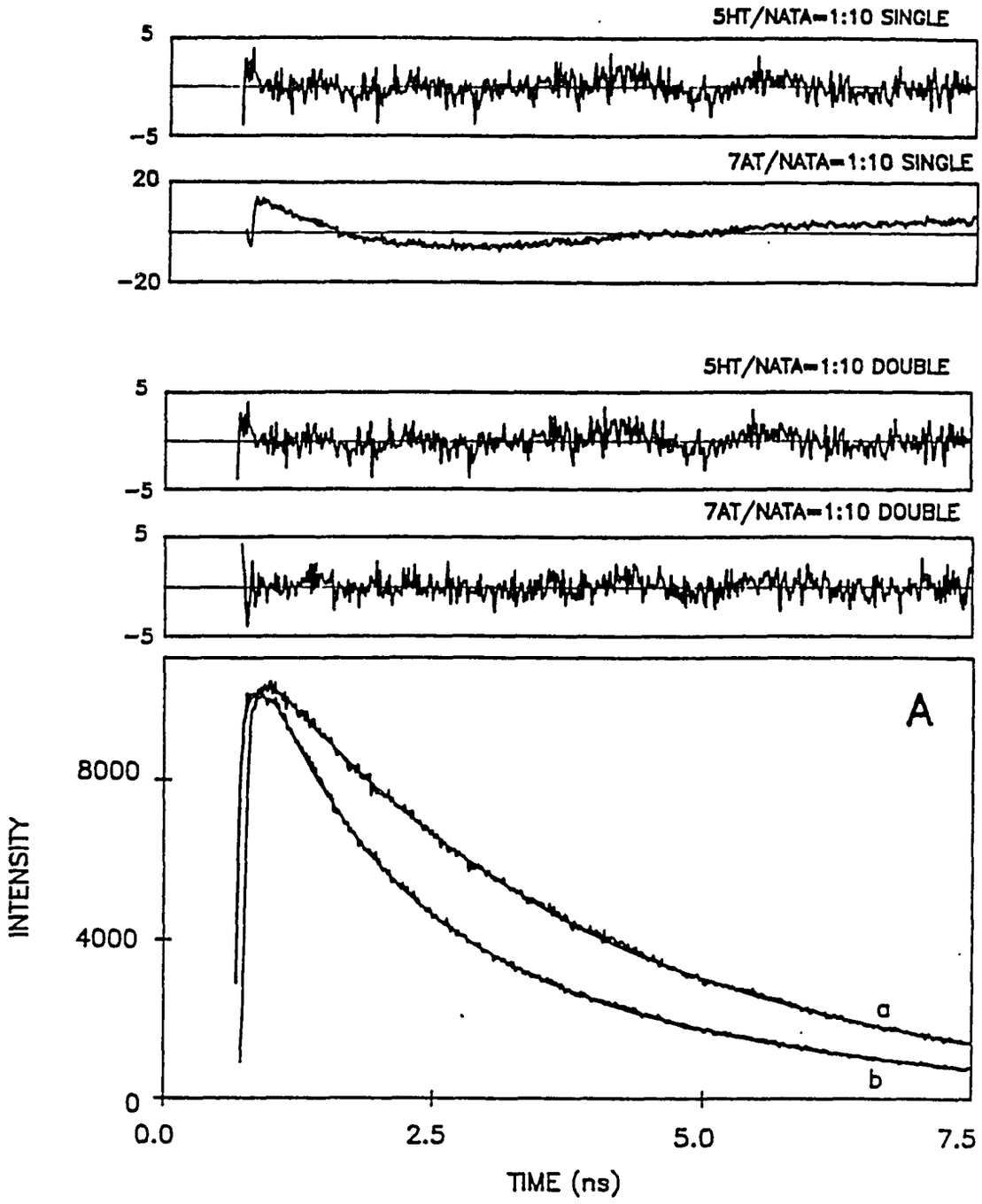
5HT/NATA=1:10 SINGLE
5
-5
7AT/NATA=1:10 SINGLE
20
-20
5HT/NATA=1:10 DOUBLE
5
-5
7AT/NATA=1:10 DOUBLE
5
-5
A
8000
4000
0
INTENSITY
a
b
0.0
2.5
5.0
7.5
TIME (ns)

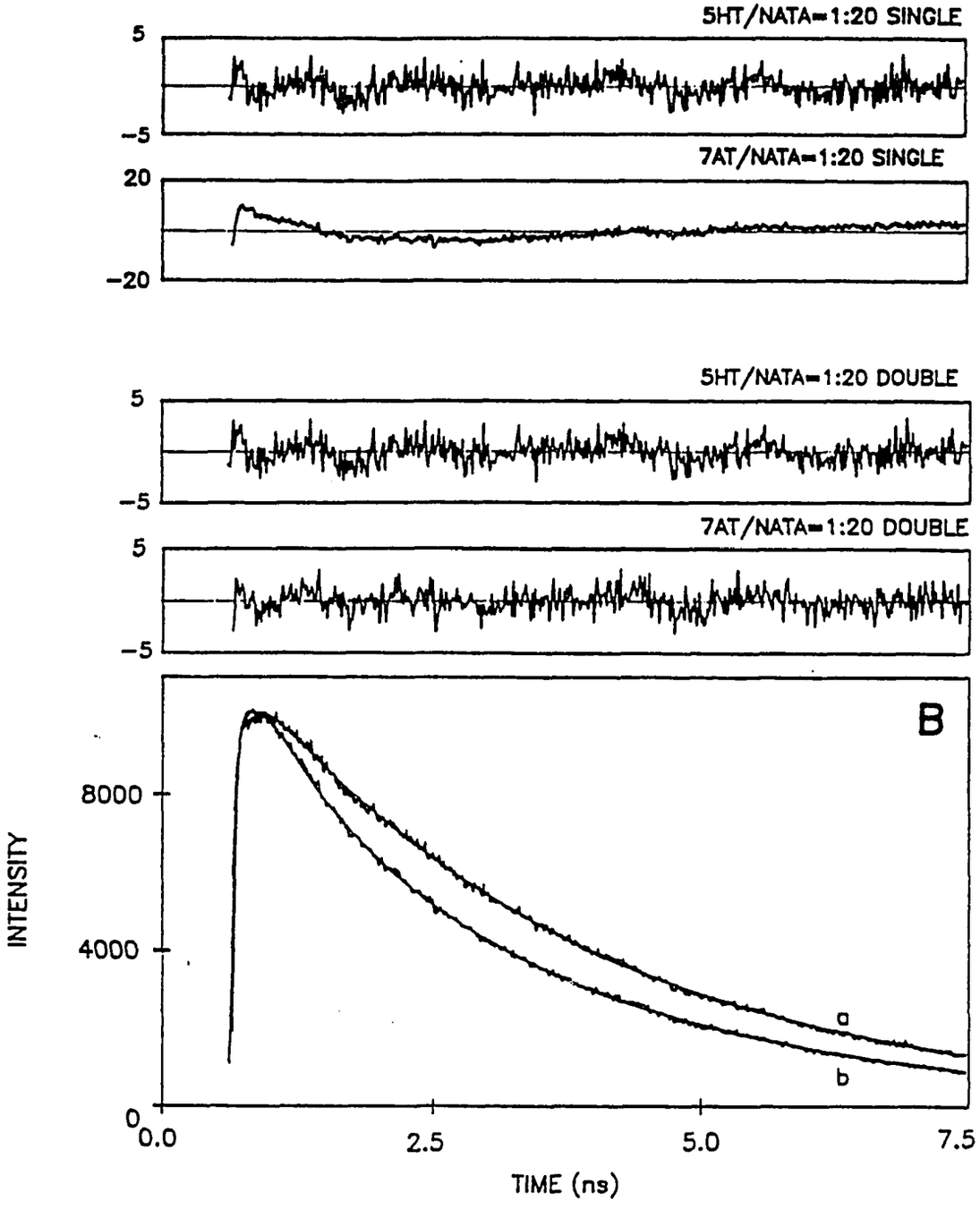

Figure 30. (continued)

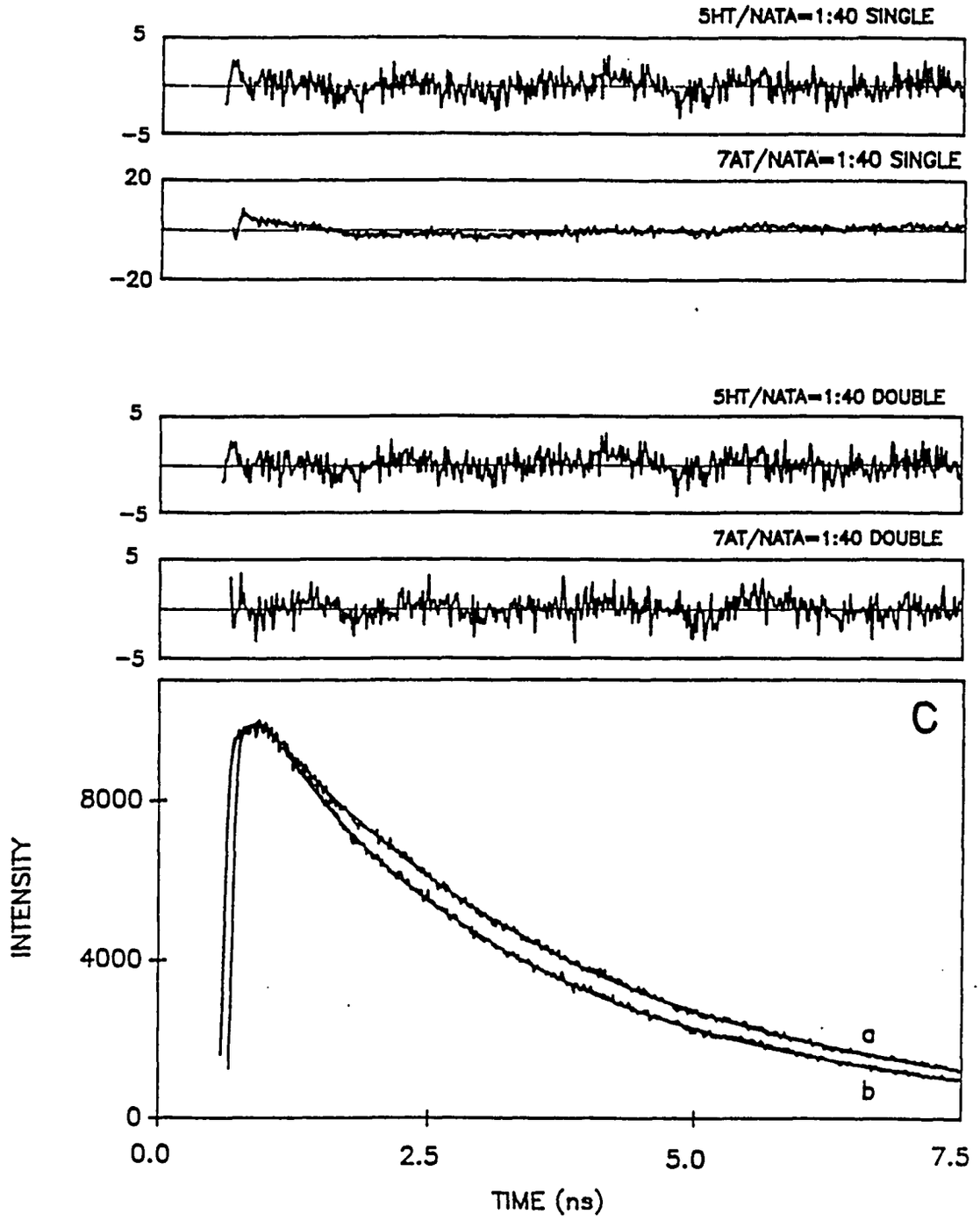

Figure 30. (continued)

A problem of considerable interest for understanding the excited-state tautomerization reaction of 7-azaindole in alcohols [89] and the nonradiative process for 7-azaindole in water [116] and for interpreting proton inventory data [116] is the determination of the excited-state pK_a values. For pH values between 2 and 4, the species NH^+_3-$N_7{}^+H$-CO_2H, NH^+_3-$N_7{}^+H$-CO^-_2, and NH^+_3-N_7-CO^-_2 are in equilibrium. Although we know with certainty the fluorescence lifetime of the last form, the deprotonated zwitterion, we do not know the lifetimes of the first two species, and thus any calculation of the excited state pK_a of the first two species becomes intractable. For pH > 9 there is a ground-state equilibrium between the deprotonated zwitterion and the anion, NH^+_3-N_7-CO^-_2 and NH_2-N_7-CO^-_2. In the ground state it is known for glycine [117] that the rate for the back reaction (the protonation of the amino group by water) is only $48 \times 10^5\ s^{-1}$. Even if in the excited state the rate for the back transfer is several orders of magnitude larger, equilibrium between the conjugate acid and base will not be established owing to the relatively short lived excited states involved ($\leq$ 1ns), and the excited-state pK_a cannot be determined.

3. Fluorescence Lifetime of 7-Azatryptophan in Mixtures of H_2O and D_2O: The Proton Inventory

In chapter IV we examined the nonradiative processes of 7-azaindole in ROH/ROD solvent mixtures, where R = CH_3, CH_3CH_2, or H. These proton inventory experiments [118]

Figure 31. Fluorescence lifetime titration of 7-azatryptophan at 20° C. The lettered points indicate pH values where the fluorescence lifetime is nonexponential. (a) pH 2.9, F(t) = 0.95exp(-t/430 ps) + 0.05exp(-t/848 ps). (b) pH 3.4; F(t) = 0.73exp(-t/421 ps) + 0.27exp(-t/778 ps). (c) pH 3.9; F(t) = 0.30exp(-t/360 ps) + 0.70exp(-t/750 ps). At all the other pH values investigated the fluorescence lifetime was single exponential.

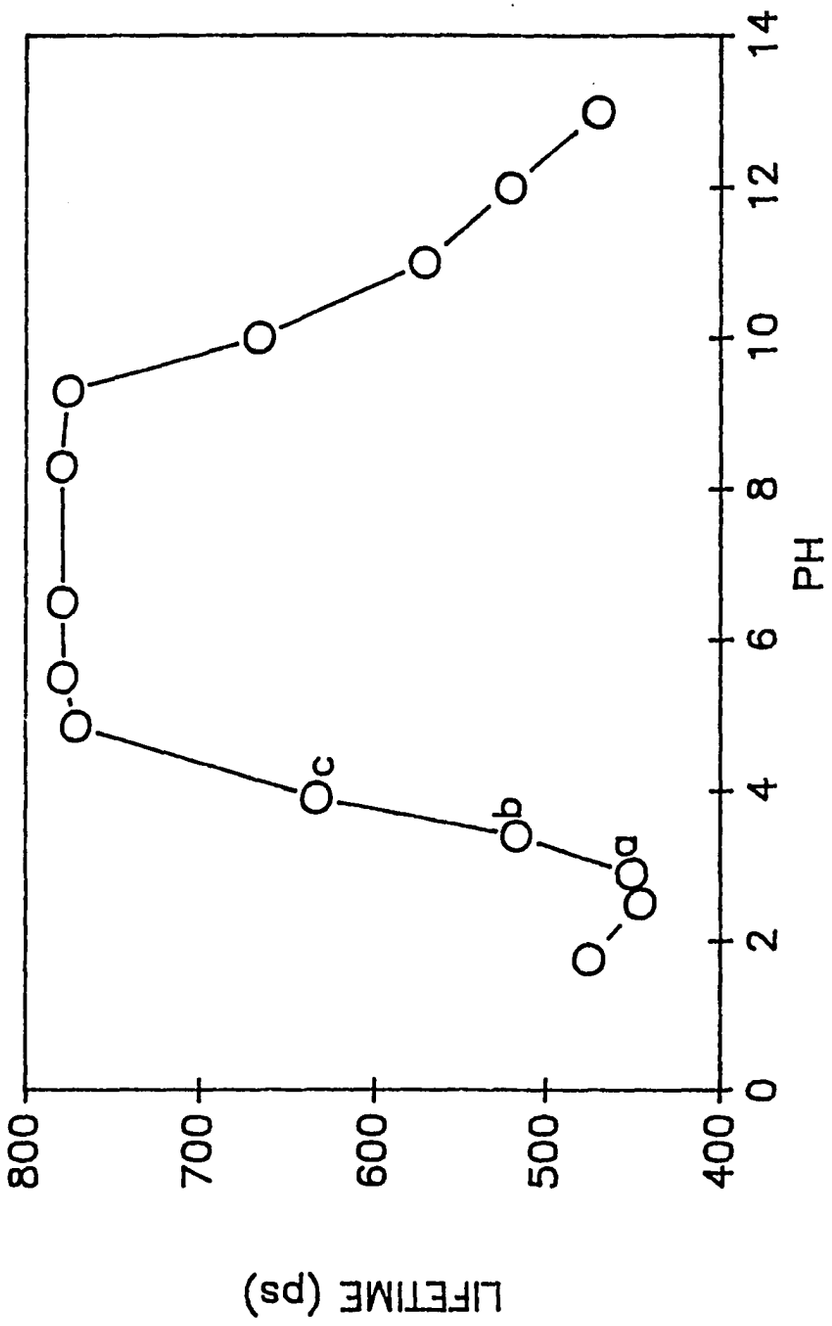
LIFETIME (ps)
800
700
600
500
400
0
2
4
6
8
10
12
14
PH
a
b
c

are designed to determine the number of protons involved in the nonradiative process and whether this process is stepwise or concerted. The proton inventory data for 7-azatryptophan are remarkably similar to those for 7-azaindole (Figure 27 and Tables 8 and 9). These data for 7-azatryptophan argue against any significant involvement of the side chain in the proton transfer step in this pH region and suggest that the nonradiative process involving the N_1 ligand in H_2O/D_2O mixtures is fundamentally different from that in alcohols.

We note that the interpretation of the proton inventory data is subject to several assumptions. Among the most important of these involves the rate of H or D exchange of the solute with the solvent and the value of the fractionation factor.

4. Dependence of the Fluorescence Lifetime of 7-Azatryptophan on Solvent

It is important to understand why 7-azatryptophan is characterized by a 780 ps lifetime in water at 20°C at neutral pH and, most importantly, why its lifetime is single-exponential. To this end, we have performed fluorescence lifetime measurements of 7-azatryptophan in a variety of solvents. The results are summarized in Table III. The significant result, which shall be discussed in detail below, is that in solvents that shift the fluorescence maximum of 7-azatryptophan to higher energies, nonexponential fluorescence decay is observed.

Figure 32. Proton inventory data for 7-azatryptophan in H_2O and D_2O at 20° C. The open circles represent k_n/k_o vs n, where n is the mole fraction (atom fraction) of the deuterated solvent. The pH at n = 0 is 6. The solid line through the open circles represents the fit to the expression $k_n/k_o = (1 - n + 0.52n)(1 - n + 0.69n)^2$. The straight line plotted directly above is the result expected for a one-proton process. The open triangles represent $(k_n/k_o)^{1/2}$ vs. n. The solid line through the open triangles is only meant to guide the eye. This plot deviates significantly from the straight line just above it. Hence, the proton inventory data in water for 7-azatryptophan are, like those for 7-azaindole, inconsistent with the two-proton process observed in alcohols. See reference 7 for a more detailed discussion of the analysis and the significance of these data.

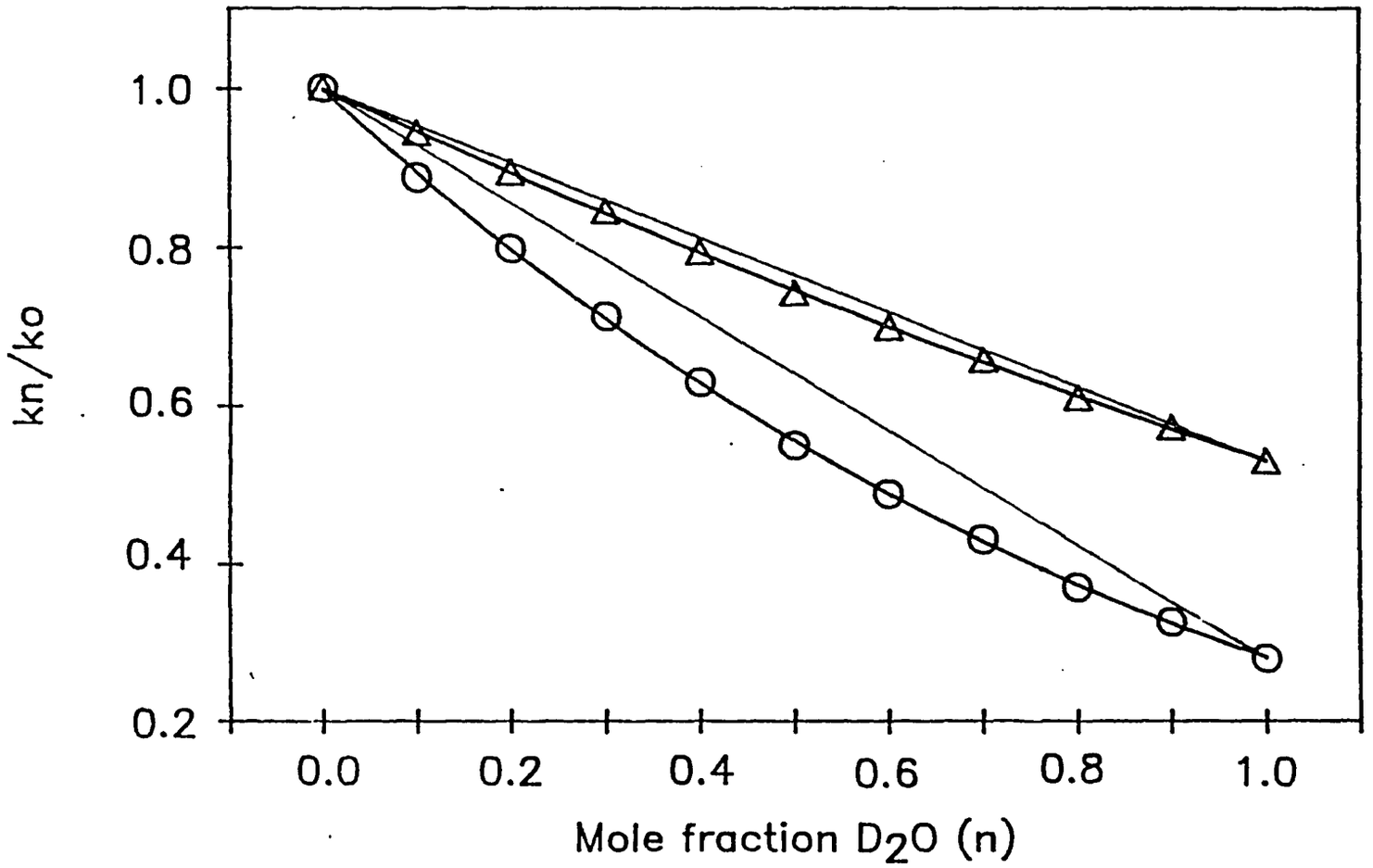
1.0
0.8
0.6
0.4
0.2
kn/ko
0.0
0.2
0.4
0.6
0.8
1.0
Mole fraction D_2O (n)

Table 8

Proton Inventory for 7-Azatryptophan at 20° C[a]

n (mole fraction D_2O)	τ_F (ps)
0.0	780 ± 10
0.1	882 ± 10
0.2	977 ± 8
0.3	1084 ± 10
0.4	1235 ± 15
0.5	1407 ± 17
0.6	1596 ± 8
0.7	1808 ± 15
0.8	2103 ± 10
0.9	2385 ± 15
1.0	2780 ± 20

[a] The isotope effect on the fluorescence lifetime is only slightly dependent on the state of protonation of 7-azatryptophan: $\tau_F(pD=7)/\tau_F(pH=7)$ = 2780 ps/780 ps = 3.56; $\tau_F(pD=11)/\tau_F(pH=11)$ = 1970 ps/570 ps = 3.46.

Table 9

Rate Constants for Proton Transfer Steps

in 7-Azatryptophan [a]

proton transfer step	rate constant ($s^{-1} \times 10^{-9}$)
k^{HH}	1.28 ± 0.02
k^{DD}	0.36 ± 0.01
$(k^{HH}k^{DD})^{1/2}$	0.68 ± 0.01
$k^{HD,b}$	0.60 ± 0.01

[a] Fluorescence lifetime measurements from which the rate constants were obtained were performed at 20°C.

[b] Obtained from eqn 22 in reference 116. This method of analysis assumes that $k^{HD} = k^{DH}$. The reported results were determined by assuming that isotopic fractionation factor $\phi^R = 1$ in both the ground and the excited states. If $\phi^R = 1.6$, then $k^{HD} = 0.72 \pm 0.01 \times 10^9\ s^{-1}$. The methods of analysis of the proton inventory data are discussed in detail in above chapter.

Table 10

Comparison of Fluorescence Lifetimes[a]

compound	solvent	λ^{em}_{max}(nm)	A_1[b]	τ_1 (ps)	τ_2 (ps)
7-azaindole	H_2O	385	1.00	900±15	
7-azatryptophan[c]	H_2O	397	1.00	780±10	
indole	H_2O	341	1.00	4550±20	
tryptophan[c]	H_2O	351	0.22±0.01	670±50	3200±100 [10]
tryptophan ethyl ester,	pH 5[d]	345	0.59±0.06	260±20	870±50 [10]
tryptophan ethyl ester,	pH 9[d]	354	0.27±0.05	930±30	2400±200 [10]
5-hydroxytryptophan	H_2O	335	1.00	3800±100	
7-azaindole	MeOH	364	1.00	140±3 [e]	
7-azatryptophan	MeOH	382	1.00	140±3 [e]	
indole	MeOH	330	1.00	3400±100	
tryptophan	MeOH	340	0.05	200±100	1900±50[f][33]
7-azaindole	DMSO	361	1.00	9300±200	
7-azatryptophan	DMSO	385	0.10±0.02	1080±50	19200±60
indole	DMSO	330	1.00	4800±200	
tryptophan	DMSO	344	0.12±0.02	1200±200	7200±400
tryptophan ethyl ester	DMSO	339	0.48±0.02	480±30	1820±80
7-azaindole	CH_3CN	353	1.00	5700±200	
7-azatryptophan	CH_3CN	374	0.43±0.02	1050±100	11000±400

[a] Experiments are performed at 20° C.

[b] Lifetimes are fit to a double exponential of the form $F(t) = A_1 \exp(-t/\tau_1) + A_2 \exp(-t/\tau_2)$, where $A_1 + A_2 = 1.00$.

[c] Zwitterionic form.

[d] $pK_a \sim 7$. Hydrochloride salt.

[e] Emission is collected from the "normal" band: 320 nm < λ^{em} < 480 nm.

[f] The fluorescence decay for tryptophan in methanol is fit well to a triple exponential. The third component comprises 10% of the emission intensity and has a lifetime of 7 ns. This component is attributed to the anionic form of tryptophan [3].

E. Discussion

1. Comparison of 7-Azatryptophan and Tryptophan

It has been proposed that the nonexponential fluorescence decay of tryptophan arises from different conformational isomers of the side chains with respect to the indole ring that have different excited-state charge transfer rates [2]. It seems likely that 7-azatryptophan would exist in similar conformational isomers. Why, then, is the fluorescence lifetime of 7-azatryptophan in water single exponential (when emission is collected over most of the band [19, 20]) and what is the role of the side chains in the photophysics of 7-azatryptophan? There are two possible answers to these questions: In 7-azatryptophan, the charge-transfer process to the side chain is deactivated or there is a more efficient process that competes with charge transfer in water. We shall consider both possibilities.

We have shown that in water 7-azatryptophan exhibits behavior that is very similar to that of 7-azaindole. The majority of solute molecules are solvated in such a fashion that excited-state tautomerization is blocked. The fluorescence lifetimes of these blocked states are 910 ps for 7-azaindole and 780 ps for 7-azatryptophan at 20°C. It is possible that the nonradiative process responsible for the 780-ps lifetime in 7-azatryptophan has a rate greater than, or at least comparable to, the rates of charge transfer from the 7-azaindole ring to side chain groups.

Evidence for the existence of such a process is provided by a proton inventory [116, 118] of the excited-state pathways of decay of 7-azatryptophan. The results of these experiments indicate [116] that the majority of the excited-state population of 7-azaindole in water does not decay by a two-proton process similar to that observed in alcohols, as has been proposed. Another mechanism for the nonradiative decay of 7-azaindole is suggested: Proton abstraction from the N_1 nitrogen by a coordinated water molecule. The proton inventory data are nearly identical for 7-azatryptophan (Figure 27, Tables 8 and 9), and we propose that here proton abstraction from N_1 is also an efficient nonradiative decay pathway that is responsible for the 780-ps lifetime [112, 116].

While the proton inventory experiments suggest another significant nonradiative process, they do not address the question of whether charge transfer to the side chain is still a viable mode of nonradiative decay. In order to answer this question, experiments were performed in nonaqueous solvents (Table 10). Alcohols that are polar and protic are represented in Table 10 by methanol. Methanol is capable of forming the idealized cyclic intermediate that is proposed to be crucial to the execution of excited-state tautomerization of 7-azaindole. In methanol this process occurs in 140 ps. In most linear alcohols it occurs on an ~200-ps time scale [18, 119]. We have already argued that the population of such a cyclic intermediate is negligible in water. It is also unlikely that a stable cyclic intermediate could be formed with polar aprotic solvents like DMSO or CH_3CN. In the polar aprotic solvents 7-azatryptophan, on the other hand, now displays a nonexponential fluorescence decay as does tryptophan.

Because of the evidence for nonradiative decay by charge transfer in tryptophan in both aqueous [2] and nonaqueous solvents and because nonexponential fluorescence decay is induced in 7-azatryptophan in DMSO and CH_3CN, we propose that charge transfer to the side chain is an effective nonradiative pathway for 7-azatryptophan in these solvents. That the side chain is responsible for the observed nonexponential decay is demonstrated by the single exponential fluorescence decay of 7-azaindole in the same solvents (Table 10). If charge transfer to the side chain is a significant pathway of nonradiative decay in these polar aprotic solvents, it is important to understand why. The answer to this question may be found by noting that nonexponential fluorescence decay in 7-azatryptophan is accompanied by a shift in the fluorescence maximum to higher energies (Table 10). On the other hand 7-azatryptophan in methanol yields the same result as 7-azaindole: a single-exponential lifetime of 140 ps. Apparently, double-proton transfer competes effectively with charge transfer to the side chain in this solvent.

If the blue shift in the emission maximum of 7-azatryptophan observed upon changing solvent from H_2O to DMSO or CH_3CN may be attributed to destabilization of the excited state (which seems likely considering the sensitivity of the indole excited state to solvent perturbation [88, 120]), then one may apply an argument based on charge transfer theory [121] to explain the nonexponential decay of 7-azatryptophan in polar aprotic solvents. The free energy change for the charge transfer process is related to the excited state energy of the donor, $E(S_1)$, by the following relation [31, 32]:

$$-\Delta G^\circ = E(S_1) - E(D/D^+) + E(A/A^-) + e^2/\varepsilon R \qquad (59)$$

Figure 33. Application of eqn 41 to the nonradiative rates obtained from the two lifetime components [10, 11] of zwitterionic tryptophan as a function of temperature. Both lifetime components yield the same activation energy of 5.63 kcal/mol. The prefactor, A, for the short-lived component is 3.96×10^{14} s^{-1} $K^{-½}$; for the long-lived component, 8.40×10^{13} s^{-1} $K^{-½}$.

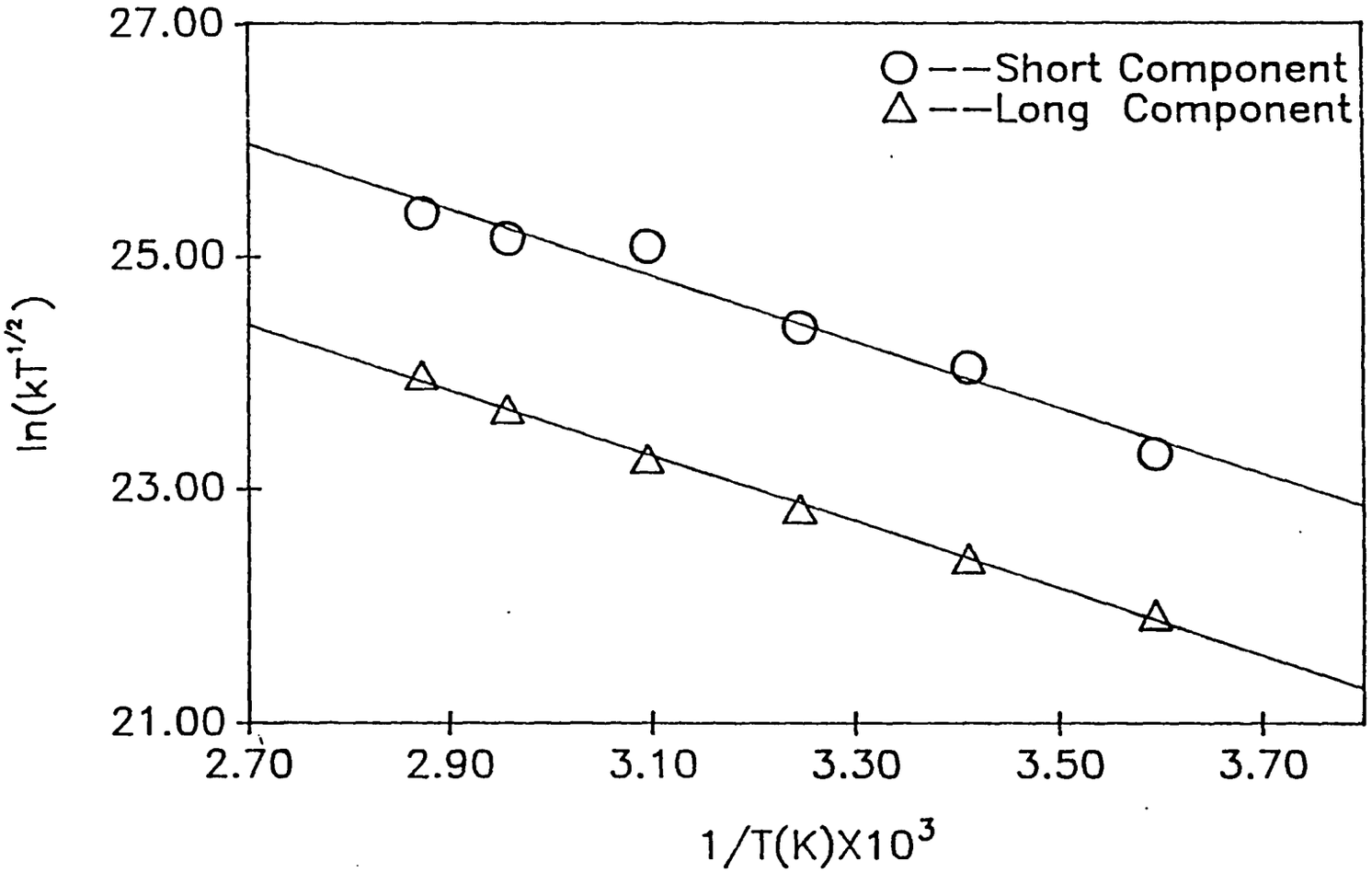
27.00
25.00
23.00
21.00
2.70
2.90
3.10
3.30
3.50
3.70
ln(kT^1/2)
1/T(K)X10^3
O--Short Component
Δ--Long Component

where $E(D/D^+)$ is the oxidation potential of the donor, $E(A/A^-)$ is the reduction potential of the acceptor, and the last term is a correction for the coulombic energy of interaction of the charge separated pair. The coulombic term is often neglected in order to take into account charge delocalization. If, then, in changing the solvent from water to DMSO or CH_3CN the relative oxidation and reduction potentials of the donor and accepter undergo little change, the largest contribution to the free energy for charge transfer must be attributed to the excited-state energy of the donor species. This change in solvent renders the charge transfer reactions more exothermic (see below and Figure 32).

To summarize, if charge transfer to the side chain is possible for 7-azatryptophan in water, it is not observed because of the presence of another nonradiative process with a greater rate. We propose that this process is abstraction of the N_1 proton by a coordinated water molecule. In polar, aprotic solvents, however, proton abstraction from N_1 is no longer feasible and nonexponential fluorescence decay can be observed because the donor, the excited-state 7-azaindole moiety, lies higher in energy than it does in water.

2. The Rate of Charge Transfer to the Side Chain: Comparison of Tryptophan and 7-Azatryptophan

The expression for the rate of nonadiabatic charge (electron) transfer is [121]

$$k = 2\pi/\hbar\ |H_{DA}|^2\ (FC). \qquad (60)$$

Figure 34. Schematic energy diagrams for tryptophan and 7-azatryptophan in water illustrating the role of reaction exothermicity on the rate of charge transfer. In problems dealing with charge (electron) transfer, it is customary to equate the energy, E, with the free energy, G, because the entropy and the product of pressure and volume is expected to remain constant between the reactants and the products. In the main part of the Figure, the solid ^1L_a surface represents tryptophan. The dashed ^1L_a surface represents 7-azatryptophan and is consequently lower in energy by an amount corresponding to its excited-state singlet energy difference with respect to tryptophan. The two ^1L_a states intersect the charge transfer species. The reaction coordinate is referred to as a "charge transfer coordinate" and is assumed to incorporate both the presence of the amino acid side chain as well as the solvent. For further details concerning these surfaces, see reference 8. The inset depicts dependence of the charge transfer rate on reaction exothermicity, $-\Delta G°$, the difference between the minima of the ^1L_a surfaces and that of the charge transfer state. The solid inverted parabola represents the behavior of the rate predicted from eqns 39 and 40. The "normal Marcus region," corresponding to activated processes, lies to the left of the maximum. The lower singlet energy of 7-azatryptophan places it below tryptophan on this curve. In other words, if the 7-azatryptophan potential surface is similar to that of tryptophan, decreasing $-\Delta G°$ will also raise the barrier to charge transfer.

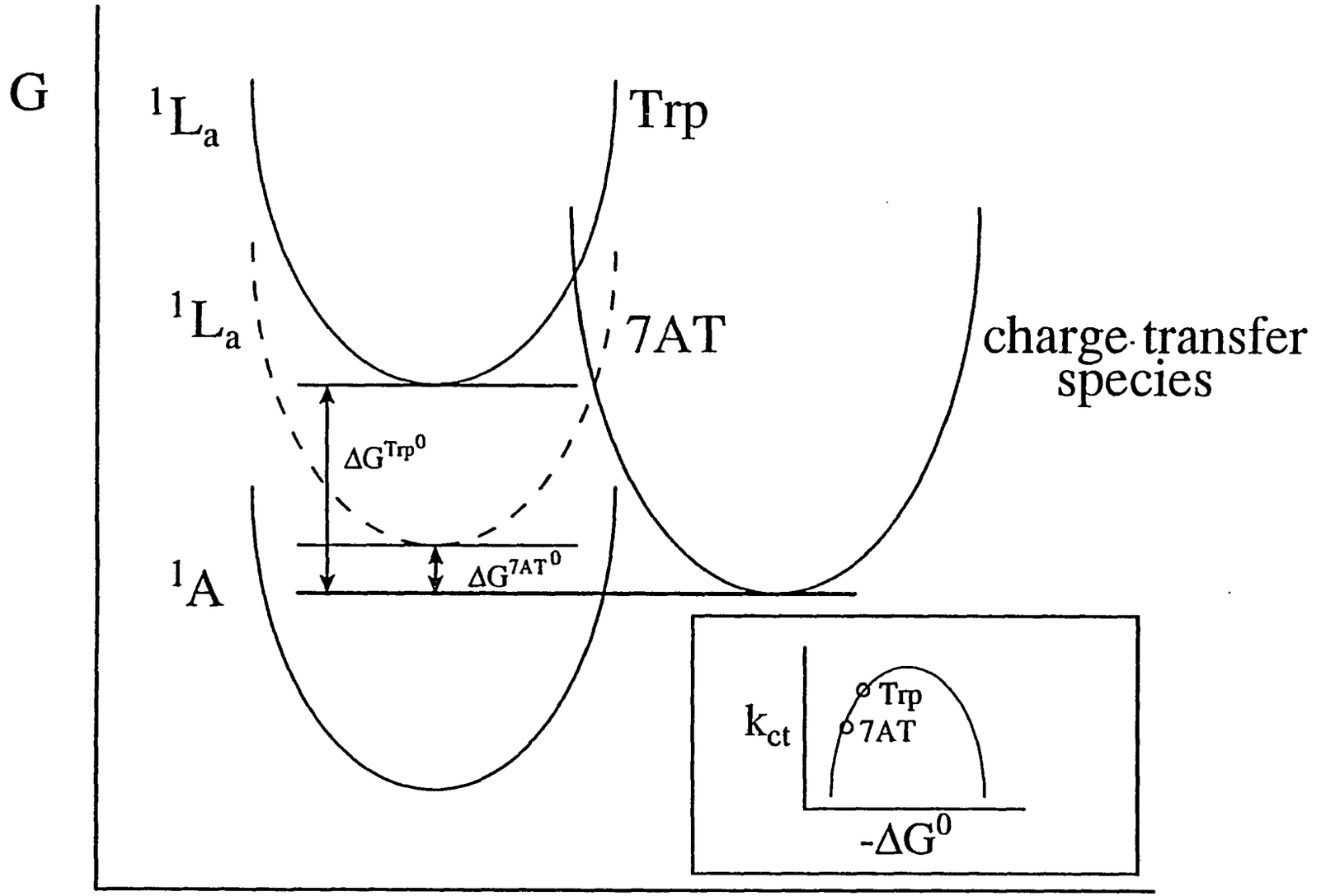
G
^1L_a
Trp
^1L_a
7AT
charge-transfer species
ΔG^{Trp^0}
ΔG^{7AT^0}
^1A
k_{ct}
Trp
7AT
$-\Delta G^0$
charge transfer coordinate

H_{DA} is the matrix element coupling the donor, D, and the acceptor, A, and FC is the nuclear Franck-Condon factor, which may be estimated quantum mechanically, semiclassically, or classically. In the classical limit the Franck-Condon factor is given by

$$FC = [1/(4\pi\lambda RT)]^{1/2} \exp\{-[(\Delta G^\circ + \lambda)^2/(4\lambda RT)]\}, \quad (61)$$

where ΔG° is the standard free energy change for the reaction, and λ is the reorganization energy, which contains both solvent and vibrational contributions. From these equations an expression may be obtained that relates the rate of charge transfer to the absolute temperature:

$$\ell n(kT^{1/2}) = \ell nA - (\Delta G^\ddagger/RT), \quad (62)$$

where $\Delta G^\ddagger = (\Delta G^\circ + \lambda)^2/4\lambda$ is the free energy of activation and $A = |H_{DA}|^2/(2\hbar\lambda R)$. The nonradiative rates obtained from the two lifetime components of zwitterionic tryptophan [39, 3] are plotted according to eqn 62. Here we assume that charge transfer is the major nonradiative pathway. Figure 33 indicates that the slopes are parallel and thus yield the same activation energies. For zwitterionic tryptophan, therefore, $\Delta G^\ddagger$ is the same for each of the conformers present in solution. Consequently it is likely that the charge transfer process for each conformer is characterized by the same ΔG° and λ.

Now let us consider the tryptophan conformer whose charge transfer rate in water is measured to be $(600\ ps)^{-1}$. We assume that the analogous conformer in 7-azatryptophan has

the same values of λ and H_{DA}. If this is the case, then as we suggested earlier, the 46 nm (9.8 kcal/mol) difference in the emission maxima of tryptophan and 7-azatryptophan may be attributed to $\Delta G°$. The drastic reduction in charge transfer rate in 7-azatryptophan with respect to tryptophan may be interpreted in terms of a much reduced reaction exothermicity. In other words, the activated nature of the charge transfer process from tryptophan demonstrated in Figure 33 puts the reaction in the "normal Marcus region." Because of its decreased singlet energy with respect to that of tryptophan, 7-azatryptophan will lie even further into the normal region and hence have a smaller charge transfer rate (Figure 34).

3. The Tryptophan and 7-Azatryptophan Population in Nonaqueous Solvents

The interpretation of the fluorescence lifetime data for 7-azatryptophan proposed above depends not only on the intrinsic electrophilicity of the sidechain to be maintained in the solvents being compared but also on the homogeneity of the sample. If there are specific changes in protonation in going from water to DMSO or CH_3CN, then the conclusions drawn above may be called into question. For example, at neutral pH tryptophan and 7-azatryptophan exist as zwitterions. We must ask whether in DMSO or CH_3CN they are also zwitterionic or what the relative populations of uncharged, cationic, anionic, and zwitterionic species are.

Ware and coworkers [122] have argued, based on trends of dissociation constants as a function of dielectric constant, that in DMSO tryptophan exists exclusively in the

zwitterionic form. Greenstein and Winitz [123] have tabulated data for a water-ethanol mixture that is 65% ethanol (dielectric constant of 40). With respect to pure water, the pK_a of the acid groups investigated is never raised by more than about 1.5 units; and the pK_a of the basic groups investigated is raised or lowered on the average by about half a unit. We note that these studies were not performed on tryptophan, presumably because of its limited solubility. For purposes of comparison, the dielectric constants of DMSO and CH_3CN are 36.7 and 36.0, respectively [124].

Wada et al. [125] measured the equilibrium constant of zwitterionic and uncharged forms of glycine in mixtures of water containing varying proportions of a nonaqueous component: $K_D = [NH_3^+CH_2CO_2^-]/[NH_2CH_2CO_2H]$. They found that while in pure water $K_D = 2.36 \times 10^5$, in solutions where the mole fraction of DMSO and CH_3CN were 0.100 and 0.300, respectively, the values of K_D decreased to 5.76×10^4 and 2.28×10^4. The extrapolated data of Wada et al. for methanol suggest that for pure solution in the nonaqueous component an upper limit for K_D is likely to be 10^2.

For tryptophan in methanol, Ware and coworkers observe a triple-exponential fluorescence decay, the third component of which has an amplitude of 10% and a lifetime of 7 ns. They attribute this third component to an anionic species. Neither they nor we, however, observe a third component in DMSO (Table III). Furthermore, we do not observe a third component in CH_3CN.

Previously we had argued that a criterion for nonexponential fluorescence decay in tryptophan was a protonated amino group, which functions to "activate" the carboxylate and

render it a good electron acceptor [2, 126]. This conclusion was drawn from noting that anionic tryptophan yields a single exponential fluorescence decay. In tryptophan, the carboxylate group is essential for nonexponential decay since both protonated or deprotonated tryptamine yield single exponential fluorescence decays. In order to exhibit nonexponential decay in DMSO and CH_3CN, both protonation of the amino group and deprotonation of the acid group are thus essential. We conclude that the tryptophan and 7-azatryptophan populations in DMSO and CH_3CN are largely zwitterionic.

It is interesting to note that the fluorescence lifetime of tryptophan ethyl ester in DMSO is double exponential with lifetimes and amplitudes similar to that in water. Both protonated and deprotonated tryptophan ethyl ester (pH 5 and 9) exhibit nonexponential fluorescence decay because the ester group is a sufficiently good electrophile in each case [2]. This observation, which does not depend upon the state of ionization of the solute, is consistent with the conclusion drawn earlier that the most important factor in inducing nonexponential fluorescence decay in 7-azatryptophan upon changing solvent from water to DMSO or CH_3CN is the change in free energy.

F. Conclusions

We have proposed 7-azatryptophan as a powerful alternative to tryptophan as an optical probe of protein structure and dynamics. We have investigated the nonradiative processes of 7-azatryptophan and explored why its fluorescence decay in water is so different

from that of tryptophan. Despite the similarities between the 7-azaindole and the indole chromophores such as the presence of two closely spaced excited states [87, 88] and the importance of monophotonic ionization as a pathway of nonradiative decay [120], this difference is most strongly manifested in the single-exponential fluorescence decay of 7-azatryptophan and its spectroscopic distinguishability with respect to tryptophan [17,19,20,89] and the other nonnatural amino acid probe that has been proposed, 5-hydroxytryptophan (Figure 25). We have suggested that the key to understanding this difference lies in the photolability of the proton attached to N_1 [116]. In 7-azaindole, the reactivity of this proton has been demonstrated by the excited-state tautomerization of its dimers [56] and of its complexes with alcohols [18, 117]. Although in water this excited-state double-proton transfer is prohibited owing to the peculiarities of the solute-solvent interactions, this does not imply that the N_1 proton is not reactive. Our proton inventory work on 7-azaindole [116] and on 7-azatryptophan indicate that although this proton is involved in a fundamentally different type of excited-state process in water than in alcohols, it is still a participant in the most important nonradiative process--after the monophotonic ionization event that occurs immediately upon photon absorption [19, 120].

The rate of this nonradiative pathway, which we have postulated to be the abstraction of the N_1 proton by water, is at least comparable to, and most likely greater than, the rate of charge transfer to side chain in 7-azatryptophan. We propose that the relative insignificance of charge transfer in 7-azatryptophan in water (and hence the absence of nonexponential fluorescence decay) in terms of an unfavorable free energy of reaction that results from the

low energy of the excited state (Figure 34). This explanation is confirmed by the appearance of nonexponential fluorescence decay of 7-azatryptophan in DMSO and CH_3CN, where the excited-state energy is raised from that in water by 10 and 19 nm, respectively.

REFERENCES

1. Chang, M. C.; Petrich, J. W.; McDonald, D. B.; Fleming, G. R. *J. Am. Chem. Soc.* **1983**, *105*, 3819.
2. Petrich, J. W.; Chang, M. C.; McDonald, D. B.; Fleming, G. R. *J. Am. Chem. Soc.* **1983**, *105*, 3824.
3. Petrich, J. W. Thesis, The University of Chicago, 1985.
4. Szabo, A. G. and Rayner, D. M. *J. Am. Chem. Soc.* **1980**, *102*, 554.
5. Engh, R. A.; Chen, L. X.-Q.; Fleming, G. R. *Chem. Phys. Lett.* **1986**, *126*, 365.
6. Tilstra, L.; Sattler, M. C.; Cherry, W. R.; Barkley, M. D. *J. Am. Chem. Soc.* **1990**, *112*, 9176.
7. Creed, D. *Photochem. Photobiol.* **1984**, *39*, 537.
8. Eftink, M. R.; Ghiron, C. A. *Biochemistry* **1976,** *15,* 692.
9. Szabo, A. G.; Stepanik, T. M.; Wayner, D. M.; Young, N. M. *Biophys. J.* **1983,** *14,* 233.
10. Petrich, J. W.; Longworth, J. W.; Fleming, G. R. *Biochemitry* **1987**, *26*, 2711.
11. Eftink, M. R.; Wasylewski, Z.; Ghiron, C. A. *Biochemistry* **1987**, *26*, 8338.
12. Grinvald, A.; Schlessinger, J.; Pecht, I.; Steinberg, I. Z. *Biochemistry* **1975**, *14*, 1921.
13. Chen, L. X.-Q.; Longworth, J. W.; Fleming, G. R. *Biophys. J.* **1987**, *51*, 865.
14. James, D. R.; Demmer, D. R.; Steer, R. P.; Verrall, R. E. *Biochemistry* **1985**, *24*, 5517.

15. Delbaere, L. T.; Hutcheon, W. L. B.; James, M. N. G.; Thiessen, W. E. *Nature* **1987**, *257*, 758.

16. Smith, E. L.; Delange, R. J.; Evans, W. H.; Landon, M.; Markland, F. S. *J. Biol. Chem.* **1968**,*243*, 2184.

17. Négrerie, M.; Bellefeuille, S. M.; Whitham, S.; Petrich, J. W.; Thornburg, R. W. *J. Am. Chem. Soc.* **1990**, *112*, 7419.

18. Négrerie, M.; Gai, F.; Bellefeuille, S. M.; Petrich, J. W. *J. Phys. Chem.* **1991**, *95*, 8663.

19. Gai, F.; Chen, Y.; Petrich, J. W. *J. Am. Chem. Soc.* **1992**, *114*, 8343.

20. Rich, R. L.; Négrerie, M.; Li, J.; Elliott, S.; Thornburg, R. W.; Petrich, J. W. *Photochem. Photobiol.* **1993**, *58*, 28.

21. Clark, J. H.; Shapiro, S. L.; Campillo, A. J. and Winn, K. R. *J. Am. Chem. Soc.* **1979**, *101*, 746.

22. Nachliel, E.; Opphir, Z.; Gutman, M. *J. Am. Chem. Soc.* **1987,** *109*, 1342.

23. Huppert, D.; Kolodney, E. *Chem. Phys.* **1981**, *63*. 401.

24. Robinson, G. W.; Thistlethwaite, P. J.; Lee, J. *J. Chem. Phys.* **1986**. *90*. 4224.

25. Mansueto, E. S.; Wight, C. A. *J. Am. Chem. Soc.* **1989**. *111*. 1900.

26. Gutman, M. *Methods Biochem. Anal.* **1984**. *30*. 1.

27. Politi, M. J.; Chaimovich, H. *J.Phys. Chem.* **1986.** *90*. 282.

28. Bardez, E.; Monier, E.; Valleur, B. *J. Phys. Chem.* **1985**. *89*. 5031.

29. Acuna, A. U.; Costela, A.; Munoz, J. M. *J. Phys. Chem.* **1986**. *90*. 2807.

30. Il'chev, Y. V.; Solntsev, K. M.; Demyashkevich, A. B.; Kuzmin, M. G.; Femmetyinen, H.; Vuorimaa, E. *Chem. Phys. Lett.* **1992**. *193*. 128.

31. Nishiya, T.; Yamauchi, S.; Hirota, N.; Baba, M.; Hanazaki, I. *J. Phys. Chem.* **1986**. *90*. 5730.

32. Weber, K. *Z. Phys. Chem.* **1931**. *B15*. 18.

33. Forster, T. *Z. Elektrochem.* **1950**. *54*. 43.

34. Weller, A. *Naturwiss.* **1955**. *42*. 175.

35. Hupppert, D.; Gutman, M.; Kaufman, K. *J. Adv. Chem. Phys.* **1981**. *47*.(part 2) 643.

36. Kosower, E. M.; Huppert, D. *Ann. Rev. Phys. Chem.* **1986**. *37*. 127.

37. Newton, M. D.; Sutin, N. *Annv. Rev. Phys. Chem.* **1984**. *35*. 437.

38. Marcus, R. A.; Sutin, N. *Biochim. Biopphys. Acta.* **1985**. *811*. 265.

39. Rehm, D.; Weller, A. *Isr. J. Chem.* **1970**. *8*. 259.

40. Hopfield, J. J. *Biophys. J.* **1977**. *81*. 311.

41. Cross, A. J.; Fleming, G. R. *Biophys. J.* **1984**, *46*, 45.

42. Tao, T. *Biopolymers*, **1969**, *8*, 609.

43. Flom, S. R.; Fendler, J. H. *J. Phys. Chem.* **1988**, *92*, 5908.

44. Knutston, J. R.; Beechem, J. M.; Brand, L. *Chem. Phys. Lett.* **1983**, *102*, 501.

45. Beechem, J. M.; Ameloot, M.; Brand, L. *Chem. Phys. Lett.* **1985**, *120*, 466.

46. Hanson, D. C.; Ygeurabide, J.; Schumaker, V. N. *Biochemistry* **1981**, *20*, 6842.

47. Ricke, J.; Amsler, K.; Binkert, Th. *Biopolymers* **1983**, *22*, 1301.

48. Martin, C. E.; Foyt, D. C. *Biochemistry* **1978**, *17*, 3587.

49. Munro, I.; Pecht, I.; Stryer, L. *Proc. Natl. Acad. Sci. USA* **1979**, *76*, 55.

50. Stein, A. D.; Peterson, K. A.; Fayer, M. D. *J. Chem. Phys.* **1990**, *92*, 5622.

51. Stein, A. D.; Hoffman, D. A.; Frank, C. W.; Fayer, M. D. *J. Chem. Phys.* **1992**, *96*, 3269.

52. Millar, D. P.; Robbins, R. J.; Zewail, A. H. *J. Chem. Phys.* **1982**, *76*, 2080.

53. Fleming, G. R.; Morris, J. M.; Robinson, G. W. *Chem. Phys.* **1976**, *17*, 91.

54. Cramer, L. E.; Spears, K. G. *J. Am. Chem. Soc.* **1978**, *100*, 221.

55. Lipari, G.; Szabo, A. *J. Am. Chem. Soc.* **1982**, *104*, 4559; Chang, M. C.; Cross, A. J.; Fleming, G. R. *J. Biomol. Struct. Dyn.* **1983**, *1*, 299; Petrich, J. W.; Longworth, J. W.; Fleming, G. R. *Biochemistry* **1987**, *26*, 2711.

56. Taylor, C. A.; El-Bayoumi, M. A.; Kasha, M. *Proc. Natl. Acad. Sci. USA* **1969**, *63*, 253.

57. Ingham, K. C.; Abu-Elgheit, M.; El-Bayoumi, M. A. *J. Am. Chem. Soc.* **1971**, *93*, 5023.

58. Ingham, K. C.; El-Bayoumi, M. A. *J. Am. Chem. Soc.* **1974**, *96*, 1674.

59. Hetherington, W. M., III; Micheels, R. M.; Eisenthal, K. B. *Chem. Phys. Lett.* **1979**, *66*, 230.

60. Share, P. E.; Sarisky, M. J; Pereira, M. A; Repinec, S. T.; Hochstrasser, R. M. *J. Lumin.* **1991**, *48/49*, 204.

61. Avouris, P.; Yang, L. L.; El-Bayoumi, M. A. *Photochem. Photobiol.* **1976**, *24*, 211.

62. McMorrow, D.; Aartsma, T. J. *Chem. Phys. Lett.* **1986**, *125*, 581.

63. Konijnenberg, J.; Huizer, A. H.; and Varma, C. A. G. O. *J. Chem. Soc. Faraday Trans. 2.* **1988**, *84*, 1163.

64. Moog, R. S.; Maroncelli, M. *J. Phys. Chem.* **1991**, *95*, 10359.

65. Collins, S. T. *J. Phys. Chem.* **1983**, *87*, 3202.

66. Still, W. C.; Kahn, M.; Mitra, A. *J. Org. Chem.* **1978**, *43*, 2923.

67. Kim, S. K.; Bernstein, E. R. *J. Phys. Chem.* **1990**, *94*, 3531.

68. Parker, C. A. *Photoluminescence of Solutions*; Elsevier: Amsterdam, 1968.

69. Jarzeba, W; Walker, G. C.; Johnson, A. E.; Kahlow, M. A.; Barbara, P. F. *J. Phys. Chem.* **1988**, *92*, 7039; Barbara, P. F.; Jarzeba, W. *Adv. Photochem.* **1990**, *15*, 1.

70. Maroncelli, M.; Fleming, G. R. *J. Chem. Phys.* **1987**, *86*, 6221.

71. Viswanath, D. S.; Natarajan, G. *Data Book on the Viscosity of Liquids*; Hemisphere Publishing: New York, 1989.

72. This assumption is based on the analogy with the effect of isotopic substitution on the fluorescence quantum yield of derivatives of tryptophan and indole, where photoionization and intersystem crossing are significant nonradiative decay pathways [29]: $1 \lesssim \phi_F (D_2O)/\phi_F (H_2O) \lesssim 2$. Robbins, R. J.; Fleming, G. R.; Beddard, G. S.; Robinson, G. W.; Thistlethwaite, P. J.; Woolfe, G. J. *J. Am. Chem. Soc.* **1980**, *102*, 6271; Kirby, E. P.; Steiner, R. F. *J. Phys. Chem.* **1970**, *74*, 4880. See also the data for indole in Table I.

73. Siebrand, W. *J. Chem. Phys.* **1967**, *46*, 440; *47*, 2411; Siebrand, W.; Williams, D. F. *J. Chem. Phys.* **1968**, *49*, 1860; Avouris, P.; Gelbart, W. M.; El-Sayed, M. A. *Chem. Rev.* **1977**, *77*, 793.

74. Birks, J. B. *Photophysics of Aromatic Molecules*; Wiley-Interscience: London, 1970, Chapter 7.

75. Waluk, J.; Pakula, B.; Komorowski, S. J. *J. Photochem.* **1987**, *39*, 49.

76. Weller, A. *Progr. Reaction Kinetics* **1961**, *1*, 187.

77. Vander Donckt, E. *Progr. Reaction Kinetics* **1970**, *5*, 273.

78. Laws, W. R.; Brand, L. *J. Phys. Chem.* **1979**, *83*, 795.

79. Ireland, J. F.; Wyatt, P. A. H. *Adv. Phys. Org. Chem.* **1976**, *12*, 643.

80. Flom, S. R.; Barbara, P. F. *J. Phys. Chem.* **1985**, *89*, 4489.

81. Inoue, H.; Hida, M.; Nakashima, N.; Yoshihara, K. *J. Phys. Chem.* **1982**, *86*, 3184.

82. Crooks, J. E. In *Comprehensive Chemical Kinetics*, Vol. 8. Eds. Bamford, C. H.; Tipper, C. F. H. (Elsevier, Amsterdam, 1977).

83. Arfken, G. *Mathematical Methods for Physicists*; Academic Press, Inc.: San Diego, 1985.

84. Chapman, C. F.; Maroncelli, M. *J. Phys. Chem.* Submitted.

85. Chou, P.-T.; Martinez, M. L.; Cooper, W. C.; Collins, S. T.; McMorrow, D. P.; Kasha, M. *J. Phys. Chem.* 1992, **96**, 5203.

86. Robison, M. M.; Robison, B. L. *J. Am. Chem. Soc.* **1955**, *77*, 6555.

87. Négrerie, M.; Gai, F.; Lambry, J.-C.; Martin, J.-L.; Petrich, J. W. In *Ultrafast Phenomena VIII*, Eds. Martin, J.-L.; Migus, A. (Springer, New York, 1992). In press.

88. Rich, R. L.; Chen, Y.; Gai, F.; Petrich, J. W. *J. Phys. Chem.* submitted.

89. Chen, Y.; Rich, R. L.; Gai, F.; Petrich, J. W. *J. Phys. Chem.* **1993**, *97*, 1770.

90. This viewpoint is in agreement with that in a similar report by Chou et al. [85]. Chapman and Maroncelli (*J. Phys. Chem.* 1992, **96**, 8430), however, propose that the entire 7-azaindole population in water undergoes excited-state tautomerization.

91. Schowen, K. B. J. in *Transition States of Biochemical Processes*, Eds. Gandour, R. D.; Schowen, R. L. (Plenum, New York, 1978), p. 225.

92. Wang, M.-S.; Gandour, R. D.; Rodgers, J.; Haslam, J. L.; Schowen, R. L. *Bioorg. Chem.* **1975**, *4*, 392.

93. Kresge, A. J. *Pure Appl. Chem.* **1964**, *8*, 243.

94. Albery, J. In *Proton-Transfer Reactions;* Caldin, E.; Gold, V., Eds.; Chapman and Hall: London, 1975; p. 263.

95. Belasco, J. G.; Albery, W. J.; Knowles, J. R. *J. Am. Chem. Soc.* **1983,** *105,* 2475.

96. Belasco, J. G.; Albery, W. J.; Knowles, J. R. *Biochemistry.* **1983,** *25*, 2552.

97. Albery, W. J. *J. Phys. Chem.* **1986**, *90,* 3774.

98. Hermes, J. D.; Roeske, C. A.; O'Leary, M. H.; Cleland, W. W. *Biochemistry.* **1982,** *21*, 5106.

99. Limbach, H.-H.; Henning, J.; Gerritzen, D.; Rumpel, H. *Faraday Discuss. Chem. Soc.* **1982,** *74*, 229.

100. Gerritzen, D.; Limbach, H.-H. *J. Am. Chem. Soc.* **1984**, *106*, 869.

10I. Rumpel, H.; Limbach, H.-H. *J. Am. Chem. Soc.* **1989,** *111*, 5429.

102. Meschede, L.; Limbach, H.-H. *J. Phys. Chem.* **1991,** *95,* 10267.

103. Eliason, R.; Kreevoy, M. M. *J. Am. Chem. Soc.* **1978**, *100,* 7037. Laughton, P. M.; Robertson, R. E. in *Solute-Solvent Interactions*, Coetzee, J. F.; Ritchie, C. D., Eds.; Marcel Dekker, New York; 1969. p. 399.

104. Négrerie, M.; Gai, F.; Lambry, J.-C.; Martin, J.-L.; Petrich, J. W. *J. Phys. Chem.* **1993**, *97*, 5046.

105. Gai, F.; Rich, R. L.; Petrich, J. W. *J. Am. Chem. Soc.* in press.

106. Wüthrich, K. *NMR of Proteins and Nucleic Acids* (Wiley, New York, 1986), Chapeter 2; Wüthrich, K.; Wagner, G. *J. Mol. Biol.* 1979, *130*, 1.

107. Bigeleisen, J. *J. Chem. Phys.* **1955**, *23*, 2264.

108. Dewar, M. J. S. *J. Am. Chem. Soc.* **1984**, *106,* 209.

109. Fersht, A. *Enzyme Structure and Function*; 2nd Edition; W. H. Freeman: New York, 1985.

110. Glasser, N.; Lami, H. *J. Chem. Phys.* **1981,** *74*, 6526.111. Demmer, D. R.; Leach, G. W.; Outhouse, E. A.; Hagar, J. W.; Wallace, S. C. *J. Phys. Chem.* **1990**, *94*, 582.

112. McMahon, L. P.; Colucci, W. J.; McLaughlin, M. L.; Barkley, M. D. *J. Am. Chem. Soc.* **1992,** *114*, 8442; Yu, H.-T.; Colucci, W. J.; McLaughlin, M. L.; Barkley, M. D. *J. Am. Chem. Soc.* **1992**, *114,* 8449.

113. Fuke, K.; Kaya, K. *J. Phys. Chem.* **1989**, *93*, 614.

114 Lakowicz, J. R.; Cherek, H.; Grycaynski, I.; Joshi, N.; Johnson, M. L. *Biophys. Chem.* **1987**, *28*, 35; James, D. R.; Ware, W. R. *Chem. Phys. Lett.* **1985**, *120*, 445; Siemiaruk, A.; Ware, W. R. *Chem. Phys. Lett.* **1987**, *140*, 277; Tanaka, F.; Mataga, N. *Biophys. J.* **1987**, *51*, 487; Livesey, A. K.; Brochon, J.-C. *Biophys. J.* **1987**, *52*, 693.

115 Senear, D. F.; Laue, T. M.; Ross, J. B. A.; Waxman, E.; Eaton, S.; Rusinova, E. *Biochemistry.* **1993**, *32*, 6179; Ross, J. B. A.; Senear, D. F.; Waxman, E.; Kombo, B. B.; Rusinova, E.; Huang, Y. T.; Laws, W. R.; Hasselbacher, C. A. *Proc. Natl. Acad. Sci. USA.* **1992**, *89*, 12023; Hogue, C. W. V.; Rasquinha, I.; Szabo, A. G.; MacManus, J. P. *FEBS Lett.* **1992**, *310*, 269; Kishi, T.; Tanaka, M.; Tanaka, J. *Bull. Chem. Soc. Jpn.* **1977**, *50*, 1267.

116. Chen, Y.; Gai, F.; Petrich, J. W. *J. Am. Chem. Soc.* **1993,** *115*, 10158.

117. Crooks, J. E. in *Comprehensive Chemical Kinetics* Vol. 8. Eds., Bamford, C. H.; Tipper, C. H. F. (Elsevier, Amsterdam, 1977), p. 197.

118. Schowen, K. B. J. in *Transition States of Biochemical Processes*, Eds. Gandour, R. D.; Schowen, R. L. (Plenum, New York, 1978), p. 225; Limbach, H.-H. in *Electron and Proton Transfer in Chemistry and Biology*, Eds. Müller, A.; Ratajczak, H.; Junge, W.; Diemann, E. (Elsevier, Amsterdam, 1992), p. 329.

119. Moog, R. S.; Maroncelli, M. *J. Phys. Chem.* **1991**, *95*, 10359; McMorrow, D.; Aartsma, T. J. *Chem. Phys. Lett.* **1986**, *125*, 581; Konijnenberg, J.; Huizer, A. H.; Varma, C. A. G. O. *J. Chem. Soc., Faraday Trans. 2* **1988,** *84*, 1163.

120. Miller, J. R.; Peeples, J. A.; Schmitt, M. J.; Closs, G. L. *J. Am. Chem. Soc.* **1982,** *104*, 6488.

121. See, for example, the following and references therein: Ulstrup, J. *Charge Transfer Processes in Condensed Media.* (Springer, Berlin, 1979); DeVault, D. *Quantum Mechanical Tunnelling in Biological Systems.* (Cambridge University Press, Cambridge, 1984).

122. Gudgin, E.; Lopez-Delgado, R.; Ware, W. R. *J. Phys. Chem.* **1983**, *87*, 1559.

123. Greenstein, J. P.; Winitz, M. *Chemistry of the Amino Acids*, Vol. 1. (Wiley, New York, 1961), Chapter 4 and p. 511.

124. Laughton, P. M.; Robertson, R. E. in *Solute-Solvent Interactions*, Coetzee, J. F.; Ritchie, C. D., Eds.; Marcel Dekker, New York; 1969. p. 399.

125. Wada, G.; Tamura, T.; Okina, M.; Nakamura, M. *Bull. Chem. Soc. Jpn.* **1982**, *55*, 3064.

126. Taylor, C. A.; El-Bayoumi, M. A.; Kasha, M. *Proc. Natl. Acad. Sci. U.S.A.* 1969, **63**, 253; Hetherington, W. M., III; Micheels, R. M.; Eisenthal, K. B. *Chem. Phys. Lett.* **1979**, *66*, 230.

127. Brucker, G. A. and Kelley, , *J. Phys. Chem.* **1987,** *97* 2856.

128. Strandjord, A. J. G. and Barbara, P. F. *J. Phys. Chem.* **1985**, *89*, 2355.

129. Barbara, P. F.; Walsh, P. K. and Brus, L. E. *J. Phys. Chem.* **1989**, *93,* 29.

130. McMorrow, D. and Kasha, M. *J. Phys. Chem. 88* (**1984**) 2235.

131. Schwartz, B. J.; Peteanu, L. A. and Harris, C. B. *J. Phys. Chem.* **1992** *96* 3591.

132. Yagil, G. *Tetrahedron* **1967**, *23*, 2855.

133. Britton, H. T. S.; Williams, W. G. *J. Chem. Soc.* **1935**, 796.

134. Adler, T. K.; Albert, A. *J. Chem. Soc.* **1960**, 1794.

135. Marcus, R. A.; *J. Chem. Phys.* **1956,** *24,* 966.

136. Marcus, R. A.; *J. Chem. Phys.* **1956**, *24*, 979.

137. Marcus, R. A.; *Ann. Rev. Phys. Chem.* **1964**, *15*, 155.

138. Closs, G. L.; Miller, J. R. *Science.* **1988**, *240*, 440.

139. Ulstrup, J.; Lecture Notes in Chemistry. Berlin; Springer-Verlag. 1979,419.

140. Frauenfelder, H.; Wolynes, P. G. *Science.* **1985,** *229*, 337.

141. Kramers, H. A.; *Physica* (Utrecht), **1940,** *7*, 284.

142. Kestner, N. R.; Logan, J.; Jortner, J. *J. Chem. Phys.* **1974**, *78,* 2148

143. Van Duyal, R. P.; Fischer, S. F.; *Chem. Phys.* **1974**, *5*, 183.

144. Newton, M. D. *Chem. Rev.* **1991**, *91*, 767.

145. Franzen, S.; Goldstein, R. F.; Boxer, S. G. *J. Chem. Phys.* **1993**, *97*, 3040.

146. Maroncelii, M.; Macinnis, J.; Fleming, G. R.; *Science.* **1989**, *243*, 1674.

147. Barbara, P. F.; Walker, G. C.; Smith, T. P. *Science.* **1992**, *256*, 975.

ACKNOWLEDGEMENTS

I am greatly indebted to my major professor, Jacob. W. Petrich, for his helpful guidance and discussions throughout my graduate studies. He has not only taught me many aspects of chemical sciences, but also demonstrated a model being a scientist to be going to success.

I would like to thank other members of my program of study committee, for their time and participation in my degree program: Professor Small, Professor Struve, Professor Cotton, and Professor Thornburg.

I wish to acknowledge all the members of the Petrich group for their friendship and assistance. Special thank should go to Feng Gai, who taught me laser operations and help me in many other aspects, to R. L. Rich for her kindness, care and support which made my staying in Ames more enjoyable.

Finally and importantly, I thank my parents, who have given me their constant support and encouragement throughout my education.